

The Finite Element Method

Fifth edition

Volume 1: The Basis

Professor O.C. Zienkiewicz, CBE, FRS, FREng is Professor Emeritus and Director of the Institute for Numerical Methods in Engineering at the University of Wales, Swansea, UK. He holds the UNESCO Chair of Numerical Methods in Engineering at the Technical University of Catalunya, Barcelona, Spain. He was the head of the Civil Engineering Department at the University of Wales Swansea between 1961 and 1989. He established that department as one of the primary centres of finite element research. In 1968 he became the Founder Editor of the *International Journal for Numerical Methods in Engineering* which still remains today the major journal in this field. The recipient of 24 honorary degrees and many medals, Professor Zienkiewicz is also a member of five academies – an honour he has received for his many contributions to the fundamental developments of the finite element method. In 1978, he became a Fellow of the Royal Society and the Royal Academy of Engineering. This was followed by his election as a foreign member to the U.S. Academy of Engineering (1981), the Polish Academy of Science (1985), the Chinese Academy of Sciences (1998), and the National Academy of Science, Italy (Accademia dei Lincei) (1999). He published the first edition of this book in 1967 and it remained the only book on the subject until 1971.

Professor R.L. Taylor has more than 35 years' experience in the modelling and simulation of structures and solid continua including two years in industry. In 1991 he was elected to membership in the U.S. National Academy of Engineering in recognition of his educational and research contributions to the field of computational mechanics. He was appointed as the T.Y. and Margaret Lin Professor of Engineering in 1992 and, in 1994, received the Berkeley Citation, the highest honour awarded by the University of California, Berkeley. In 1997, Professor Taylor was made a Fellow in the U.S. Association for Computational Mechanics and recently he was elected Fellow in the International Association of Computational Mechanics, and was awarded the USACM John von Neumann Medal. Professor Taylor has written several computer programs for finite element analysis of structural and non-structural systems, one of which, FEAP, is used world-wide in education and research environments. FEAP is now incorporated more fully into the book to address non-linear and finite deformation problems.

Front cover image: A Finite Element Model of the world land speed record (765.035 mph) car THRUST SSC. The analysis was done using the finite element method by K. Morgan, O. Hassan and N.P. Weatherill at the Institute for Numerical Methods in Engineering, University of Wales Swansea, UK. (see K. Morgan, O. Hassan and N.P. Weatherill, 'Why didn't the supersonic car fly?', *Mathematics Today, Bulletin of the Institute of Mathematics and Its Applications*, Vol. 35, No. 4, 110–114, Aug. 1999).

The Finite Element Method

Fifth edition

Volume 1: The Basis

O.C. Zienkiewicz, CBE, FRS, FEng

UNESCO Professor of Numerical Methods in Engineering
International Centre for Numerical Methods in Engineering, Barcelona
Emeritus Professor of Civil Engineering and Director of the Institute for
Numerical Methods in Engineering, University of Wales, Swansea

R.L. Taylor

Professor in the Graduate School
Department of Civil and Environmental Engineering
University of California at Berkeley
Berkeley, California

BUTTERWORTH
HEINEMANN

OXFORD AUCKLAND BOSTON JOHANNESBURG MELBOURNE NEW DELHI

Butterworth-Heinemann
Linacre House, Jordan Hill, Oxford OX2 8DP
225 Wildwood Avenue, Woburn, MA 01801-2041
A division of Reed Educational and Professional Publishing Ltd

 A member of the Reed Elsevier plc group

First published in 1967 by McGraw-Hill
Fifth edition published by Butterworth-Heinemann 2000

© O.C. Zienkiewicz and R.L. Taylor 2000

All rights reserved. No part of this publication may be reproduced in any material form (including photocopying or storing in any medium by electronic means and whether or not transiently or incidentally to some other use of this publication) without the written permission of the copyright holder except in accordance with the provisions of the Copyright, Designs and Patents Act 1988 or under the terms of a licence issued by the Copyright Licensing Agency Ltd, 90 Tottenham Court Road, London, England W1P 9HE. Applications for the copyright holder's written permission to reproduce any part of this publication should be addressed to the publishers

British Library Cataloguing in Publication Data

A catalogue record for this book is available from the British Library

Library of Congress Cataloguing in Publication Data

A catalogue record for this book is available from the Library of Congress

ISBN 0 7506 5049 4

**Published with the cooperation of CIMNE,
the International Centre for Numerical Methods in Engineering,
Barcelona, Spain (www.cimne.upc.es)**

Typeset by Academic & Technical Typesetting, Bristol
Printed and bound by MPG Books Ltd



FOR EVERY TITLE THAT WE PUBLISH, BUTTERWORTH-HEINEMANN
WILL PAY FOR BTCV TO PLANT AND CARE FOR A TREE.

Dedication

This book is dedicated to our wives Helen and Mary Lou and our families for their support and patience during the preparation of this book, and also to all of our students and colleagues who over the years have contributed to our knowledge of the finite element method. In particular we would like to mention Professor Eugenio Oñate and his group at CIMNE for their help, encouragement and support during the preparation process.

Contents

<i>Preface</i>	xv
1. Some preliminaries: the standard discrete system	1
1.1 Introduction	1
1.2 The structural element and the structural system	4
1.3 Assembly and analysis of a structure	8
1.4 The boundary conditions	9
1.5 Electrical and fluid networks	10
1.6 The general pattern	12
1.7 The standard discrete system	14
1.8 Transformation of coordinates	15
References	16
2. A direct approach to problems in elasticity	18
2.1 Introduction	18
2.2 Direct formulation of finite element characteristics	19
2.3 Generalization to the whole region	26
2.4 Displacement approach as a minimization of total potential energy	29
2.5 Convergence criteria	31
2.6 Discretization error and convergence rate	32
2.7 Displacement functions with discontinuity between elements	33
2.8 Bound on strain energy in a displacement formulation	34
2.9 Direct minimization	35
2.10 An example	35
2.11 Concluding remarks	37
References	37
3. Generalization of the finite element concepts. Galerkin-weighted residual and variational approaches	39
3.1 Introduction	39
3.2 Integral or 'weak' statements equivalent to the differential equations	42
3.3 Approximation to integral formulations	46
3.4 Virtual work as the 'weak form' of equilibrium equations for analysis of solids or fluids	53

3.5	Partial discretization	55
3.6	Convergence	58
3.7	What are ‘variational principles’?	60
3.8	‘Natural’ variational principles and their relation to governing differential equations	62
3.9	Establishment of natural variational principles for linear, self-adjoint differential equations	66
3.10	Maximum, minimum, or a saddle point?	69
3.11	Constrained variational principles. Lagrange multipliers and adjoint functions	70
3.12	Constrained variational principles. Penalty functions and the least square method	76
3.13	Concluding remarks	82
	References	84
4.	Plane stress and plane strain	87
4.1	Introduction	87
4.2	Element characteristics	87
4.3	Examples – an assessment of performance	97
4.4	Some practical applications	100
4.5	Special treatment of plane strain with an incompressible material	110
4.6	Concluding remark	111
	References	111
5.	Axisymmetric stress analysis	112
5.1	Introduction	112
5.2	Element characteristics	112
5.3	Some illustrative examples	121
5.4	Early practical applications	123
5.5	Non-symmetrical loading	124
5.6	Axisymmetry – plane strain and plane stress	124
	References	126
6.	Three-dimensional stress analysis	127
6.1	Introduction	127
6.2	Tetrahedral element characteristics	128
6.3	Composite elements with eight nodes	134
6.4	Examples and concluding remarks	135
	References	139
7.	Steady-state field problems – heat conduction, electric and magnetic potential, fluid flow, etc.	140
7.1	Introduction	140
7.2	The general quasi-harmonic equation	141
7.3	Finite element discretization	143
7.4	Some economic specializations	144
7.5	Examples – an assessment of accuracy	146
7.6	Some practical applications	149

7.7	Concluding remarks	161
	References	161
8.	'Standard' and 'hierarchical' element shape functions: some general families of C_0 continuity	164
8.1	Introduction	164
8.2	Standard and hierarchical concepts	165
8.3	Rectangular elements – some preliminary considerations	168
8.4	Completeness of polynomials	171
8.5	Rectangular elements – Lagrange family	172
8.6	Rectangular elements – 'serendipity' family	174
8.7	Elimination of internal variables before assembly – substructures	177
8.8	Triangular element family	179
8.9	Line elements	183
8.10	Rectangular prisms – Lagrange family	184
8.11	Rectangular prisms – 'serendipity' family	185
8.12	Tetrahedral elements	186
8.13	Other simple three-dimensional elements	190
8.14	Hierarchic polynomials in one dimension	190
8.15	Two- and three-dimensional, hierarchic, elements of the 'rectangle' or 'brick' type	193
8.16	Triangle and tetrahedron family	193
8.17	Global and local finite element approximation	196
8.18	Improvement of conditioning with hierarchic forms	197
8.19	Concluding remarks	198
	References	198
9.	Mapped elements and numerical integration – 'infinite' and 'singularity' elements	200
9.1	Introduction	200
9.2	Use of 'shape functions' in the establishment of coordinate transformations	203
9.3	Geometrical conformability of elements	206
9.4	Variation of the unknown function within distorted, curvilinear elements. Continuity requirements	206
9.5	Evaluation of element matrices (transformation in ξ, η, ζ coordinates)	208
9.6	Element matrices. Area and volume coordinates	211
9.7	Convergence of elements in curvilinear coordinates	213
9.8	Numerical integration – one-dimensional	217
9.9	Numerical integration – rectangular (2D) or right prism (3D) regions	219
9.10	Numerical integration – triangular or tetrahedral regions	221
9.11	Required order of numerical integration	223
9.12	Generation of finite element meshes by mapping. Blending functions	226
9.13	Infinite domains and infinite elements	229
9.14	Singular elements by mapping for fracture mechanics, etc.	234

9.15	A computational advantage of numerically integrated finite elements	236
9.16	Some practical examples of two-dimensional stress analysis	237
9.17	Three-dimensional stress analysis	238
9.18	Symmetry and repeatability	244
	References	246
10.	The patch test, reduced integration, and non-conforming elements	250
10.1	Introduction	250
10.2	Convergence requirements	251
10.3	The simple patch test (tests A and B) – a necessary condition for convergence	253
10.4	Generalized patch test (test C) and the single-element test	255
10.5	The generality of a numerical patch test	257
10.6	Higher order patch tests	257
10.7	Application of the patch test to plane elasticity elements with ‘standard’ and ‘reduced’ quadrature	258
10.8	Application of the patch test to an incompatible element	264
10.9	Generation of incompatible shape functions which satisfy the patch test	268
10.10	The weak patch test – example	270
10.11	Higher order patch test – assessment of robustness	271
10.12	Conclusion	273
	References	274
11.	Mixed formulation and constraints– complete field methods	276
11.1	Introduction	276
11.2	Discretization of mixed forms – some general remarks	278
11.3	Stability of mixed approximation. The patch test	280
11.4	Two-field mixed formulation in elasticity	284
11.5	Three-field mixed formulations in elasticity	291
11.6	An iterative method solution of mixed approximations	298
11.7	Complementary forms with direct constraint	301
11.8	Concluding remarks – mixed formulation or a test of element ‘robustness’	304
	References	304
12.	Incompressible materials, mixed methods and other procedures of solution	307
12.1	Introduction	307
12.2	Deviatoric stress and strain, pressure and volume change	307
12.3	Two-field incompressible elasticity ($u-p$ form)	308
12.4	Three-field nearly incompressible elasticity ($u-p-\epsilon_v$ form)	314
12.5	Reduced and selective integration and its equivalence to penalized mixed problems	318
12.6	A simple iterative solution process for mixed problems: Uzawa method	323

12.7	Stabilized methods for some mixed elements failing the incompressibility patch test	326
12.8	Concluding remarks	342
	References	343
13.	Mixed formulation and constraints – incomplete (hybrid) field methods, boundary/Trefftz methods	346
13.1	General	346
13.2	Interface traction link of two (or more) irreducible form subdomains	346
13.3	Interface traction link of two or more mixed form subdomains	349
13.4	Interface displacement ‘frame’	350
13.5	Linking of boundary (or Trefftz)-type solution by the ‘frame’ of specified displacements	355
13.6	Subdomains with ‘standard’ elements and global functions	360
13.7	Lagrange variables or discontinuous Galerkin methods?	361
13.8	Concluding remarks	361
	References	362
14.	Errors, recovery processes and error estimates	365
14.1	Definition of errors	365
14.2	Superconvergence and optimal sampling points	370
14.3	Recovery of gradients and stresses	375
14.4	Superconvergent patch recovery – SPR	377
14.5	Recovery by equilibration of patches – REP	383
14.6	Error estimates by recovery	385
14.7	Other error estimators – residual based methods	387
14.8	Asymptotic behaviour and robustness of error estimators – the Babuška patch test	392
14.9	Which errors should concern us?	398
	References	398
15.	Adaptive finite element refinement	401
15.1	Introduction	401
15.2	Some examples of adaptive h -refinement	404
15.3	p -refinement and hp -refinement	415
15.4	Concluding remarks	426
	References	426
16.	Point-based approximations; element-free Galerkin – and other meshless methods	429
16.1	Introduction	429
16.2	Function approximation	431
16.3	Moving least square approximations – restoration of continuity of approximation	438
16.4	Hierarchical enhancement of moving least square expansions	443
16.5	Point collocation – finite point methods	446

16.6	Galerkin weighting and finite volume methods	451
16.7	Use of hierarchic and special functions based on standard finite elements satisfying the partition of unity requirement	457
16.8	Closure	464
	References	464
17.	The time dimension – semi-discretization of field and dynamic problems and analytical solution procedures	468
17.1	Introduction	468
17.2	Direct formulation of time-dependent problems with spatial finite element subdivision	468
17.3	General classification	476
17.4	Free response – eigenvalues for second-order problems and dynamic vibration	477
17.5	Free response – eigenvalues for first-order problems and heat conduction, etc.	484
17.6	Free response – damped dynamic eigenvalues	484
17.7	Forced periodic response	485
17.8	Transient response by analytical procedures	486
17.9	Symmetry and repeatability	490
	References	491
18.	The time dimension – discrete approximation in time	493
18.1	Introduction	493
18.2	Simple time-step algorithms for the first-order equation	495
18.3	General single-step algorithms for first- and second-order equations	508
18.4	Multistep recurrence algorithms	522
18.5	Some remarks on general performance of numerical algorithms	530
18.6	Time discontinuous Galerkin approximation	536
18.7	Concluding remarks	538
	References	538
19.	Coupled systems	542
19.1	Coupled problems – definition and classification	542
19.2	Fluid–structure interaction (Class I problem)	545
19.3	Soil–pore fluid interaction (Class II problems)	558
19.4	Partitioned single-phase systems – implicit–explicit partitions (Class I problems)	565
19.5	Staggered solution processes	567
	References	572
20.	Computer procedures for finite element analysis	576
20.1	Introduction	576
20.2	Data input module	578
20.3	Memory management for array storage	588
20.4	Solution module – the command programming language	590
20.5	Computation of finite element solution modules	597

20.6	Solution of simultaneous linear algebraic equations	609
20.7	Extension and modification of computer program <i>FEAPpv</i>	618
	References	618
Appendix A:	Matrix algebra	620
Appendix B:	Tensor-indicial notation in the approximation of elasticity problems	626
Appendix C:	Basic equations of displacement analysis	635
Appendix D:	Some integration formulae for a triangle	636
Appendix E:	Some integration formulae for a tetrahedron	637
Appendix F:	Some vector algebra	638
Appendix G:	Integration by parts in two and three dimensions (Green's theorem)	643
Appendix H:	Solutions exact at nodes	645
Appendix I:	Matrix diagonalization or lumping	648
	Author index	655
	Subject index	663

Volume 2: Solid and structural mechanics

1. General problems in solid mechanics and non-linearity
 2. Solution of non-linear algebraic equations
 3. Inelastic materials
 4. Plate bending approximation: thin (Kirchhoff) plates and C_1 continuity requirements
 5. ‘Thick’ Reissner–Mindlin plates – irreducible and mixed formulations
 6. Shells as an assembly of flat elements
 7. Axisymmetric shells
 8. Shells as a special case of three-dimensional analysis – Reissner–Mindlin assumptions
 9. Semi-analytical finite element processes – use of orthogonal functions and ‘finite strip’ methods
 10. Geometrically non-linear problems – finite deformation
 11. Non-linear structural problems – large displacement and instability
 12. Pseudo-rigid and rigid–flexible bodies
 13. Computer procedures for finite element analysis
- Appendix A: Invariants of second-order tensors

Volume 3: Fluid dynamics

1. Introduction and the equations of fluid dynamics
 2. Convection dominated problems – finite element approximations
 3. A general algorithm for compressible and incompressible flows – the characteristic based split (CBS) algorithm
 4. Incompressible laminar flow – newtonian and non-newtonian fluids
 5. Free surfaces, buoyancy and turbulent incompressible flows
 6. Compressible high speed gas flow
 7. Shallow-water problems
 8. Waves
 9. Computer implementation of the CBS algorithm
- Appendix A. Non-conservative form of Navier–Stokes equations
- Appendix B. Discontinuous Galerkin methods in the solution of the convection–diffusion equation
- Appendix C. Edge-based finite element formulation
- Appendix D. Multi grid methods
- Appendix E. Boundary layer – inviscid flow coupling

Plane stress and plane strain

4.1 Introduction

Two-dimensional elastic problems were the first successful examples of the application of the finite element method.^{1,2} Indeed, we have already used this situation to illustrate the basis of the finite element formulation in Chapter 2 where the general relationships were derived. These basic relationships are given in Eqs (2.1)–(2.5) and (2.23) and (2.24), which for quick reference are summarized in Appendix C.

In this chapter the particular relationships for the plane stress and plane strain problem will be derived in more detail, and illustrated by suitable practical examples, a procedure that will be followed throughout the remainder of the book.

Only the simplest, triangular, element will be discussed in detail but the basic approach is general. More elaborate elements to be discussed in Chapters 8 and 9 could be introduced to the same problem in an identical manner.

The reader not familiar with the applicable basic definitions of elasticity is referred to elementary texts on the subject, in particular to the text by Timoshenko and Goodier,³ whose notation will be widely used here.

In both problems of plane stress and plane strain the displacement field is uniquely given by the u and v displacement in the directions of the cartesian, orthogonal x and y axes.

Again, in both, the only strains and stresses that have to be considered are the three components in the xy plane. In the case of *plane stress*, by definition, all other components of stress are zero and therefore give no contribution to internal work. In *plane strain* the stress in a direction perpendicular to the xy plane is not zero. However, by definition, the strain in that direction is zero, and therefore no contribution to internal work is made by this stress, which can in fact be explicitly evaluated from the three main stress components, if desired, at the end of all computations.

4.2 Element characteristics

4.2.1 Displacement functions

Figure 4.1 shows the typical triangular element considered, with nodes i, j, m

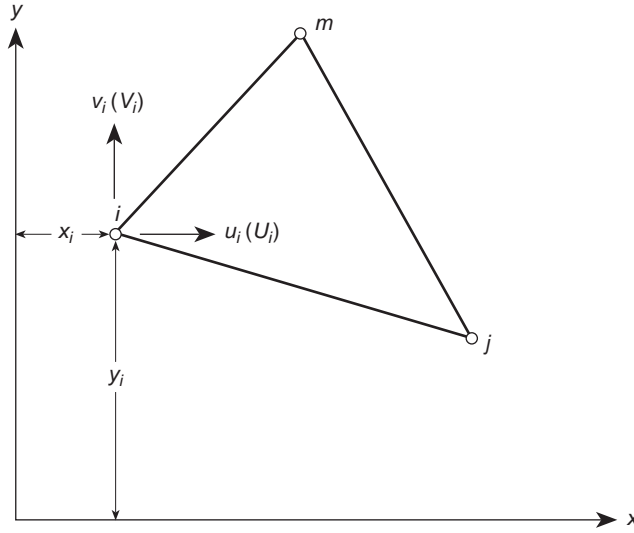


Fig. 4.1 An element of a continuum in plane stress or plane strain.

numbered in an anticlockwise order. The displacements of a node have two components

$$\mathbf{a}_i = \begin{Bmatrix} u_i \\ v_i \end{Bmatrix} \quad (4.1)$$

and the six components of element displacements are listed as a vector

$$\mathbf{a}^e = \begin{Bmatrix} \mathbf{a}_i \\ \mathbf{a}_j \\ \mathbf{a}_m \end{Bmatrix} \quad (4.2)$$

The displacements within an element have to be uniquely defined by these six values. The simplest representation is clearly given by two linear polynomials

$$\begin{aligned} u &= \alpha_1 + \alpha_2 x + \alpha_3 y \\ v &= \alpha_4 + \alpha_5 x + \alpha_6 y \end{aligned} \quad (4.3)$$

The six constants α can be evaluated easily by solving the two sets of three simultaneous equations which will arise if the nodal coordinates are inserted and the displacements equated to the appropriate nodal displacements. Writing, for example,

$$\begin{aligned} u_i &= \alpha_1 + \alpha_2 x_i + \alpha_3 y_i \\ u_j &= \alpha_1 + \alpha_2 x_j + \alpha_3 y_j \\ u_m &= \alpha_1 + \alpha_2 x_m + \alpha_3 y_m \end{aligned} \quad (4.4)$$

we can easily solve for α_1 , α_2 , and α_3 in terms of the nodal displacements u_i , u_j , u_m and obtain finally

$$u = \frac{1}{2\Delta} [(a_i + b_i x + c_i y)u_i + (a_j + b_j x + c_j y)u_j + (a_m + b_m x + c_m y)u_m] \quad (4.5a)$$

in which

$$\begin{aligned} a_i &= x_j y_m - x_m y_j \\ b_i &= y_j - y_m \\ c_i &= x_m - x_j \end{aligned} \quad (4.5b)$$

with the other coefficients obtained by a cycle permutation of subscripts in the order, i, j, m , and where[†]

$$2\Delta = \det \begin{vmatrix} 1 & x_i & y_i \\ 1 & x_j & y_j \\ 1 & x_m & y_m \end{vmatrix} = 2 \cdot (\text{area of triangle } ijm) \quad (4.5c)$$

As the equations for the vertical displacement v are similar we also have

$$v = \frac{1}{2\Delta} [(a_i + b_i x + c_i y)v_i + (a_j + b_j x + c_j y)v_j + (a_m + b_m x + c_m y)v_m] \quad (4.6)$$

Though not strictly necessary at this stage we can represent the above relations, Eqs (4.5a) and (4.6), in the standard form of Eq. (2.1):

$$\mathbf{u} = \begin{Bmatrix} u \\ v \end{Bmatrix} = \mathbf{N}\mathbf{a}^e = [\mathbf{I}N_i, \mathbf{I}N_j, \mathbf{I}N_m]\mathbf{a}^e \quad (4.7)$$

with \mathbf{I} a two by two identity matrix, and

$$N_i = \frac{a_i + b_i x + c_i y}{2\Delta}, \quad \text{etc.} \quad (4.8)$$

The chosen displacement function automatically guarantees continuity of displacement with adjacent elements because the displacements vary linearly along any side of the triangle and, with identical displacement imposed at the nodes, the same displacement will clearly exist all along an interface.

4.2.2 Strain (total)

The total strain at any point within the element can be defined by its three components which contribute to internal work. Thus

$$\boldsymbol{\varepsilon} = \begin{Bmatrix} \varepsilon_x \\ \varepsilon_y \\ \gamma_{xy} \end{Bmatrix} = \begin{bmatrix} \frac{\partial}{\partial x}, & 0 \\ 0, & \frac{\partial}{\partial y} \\ \frac{\partial}{\partial y}, & \frac{\partial}{\partial x} \end{bmatrix} \begin{Bmatrix} u \\ v \end{Bmatrix} = \mathbf{S}\mathbf{u} \quad (4.9)$$

[†] Note: If coordinates are taken from the centroid of the element then

$$x_i + x_j + x_m = y_i + y_j + y_m = 0 \quad \text{and} \quad a_i = 2\Delta/3 = a_j = a_m$$

See also Appendix D for a summary of integrals for a triangle.

Substituting Eq. (4.7) we have

$$\boldsymbol{\varepsilon} = \mathbf{B}\mathbf{a}^e = [\mathbf{B}_i, \mathbf{B}_j, \mathbf{B}_m] \begin{Bmatrix} \mathbf{a}_i \\ \mathbf{a}_j \\ \mathbf{a}_m \end{Bmatrix} \quad (4.10a)$$

with a typical matrix \mathbf{B}_i given by

$$\mathbf{B}_i = \mathbf{S}N_i = \begin{bmatrix} \frac{\partial N_i}{\partial x}, & 0 \\ 0, & \frac{\partial N_i}{\partial y} \\ \frac{\partial N_i}{\partial y}, & \frac{\partial N_i}{\partial x} \end{bmatrix} = \frac{1}{2\Delta} \begin{bmatrix} b_i, & 0 \\ 0, & c_i \\ c_i, & b_i \end{bmatrix} \quad (4.10b)$$

This defines matrix \mathbf{B} of Eq. (2.4) explicitly.

It will be noted that in this case the \mathbf{B} matrix is independent of the position within the element, and hence the strains are constant throughout it. Obviously, the criterion of constant strain mentioned in Chapter 2 is satisfied by the shape functions.

4.2.3 Elasticity matrix

The matrix \mathbf{D} of Eq. (2.5)

$$\boldsymbol{\sigma} = \begin{Bmatrix} \sigma_x \\ \sigma_y \\ \tau_{xy} \end{Bmatrix} = \mathbf{D} \left(\begin{Bmatrix} \varepsilon_x \\ \varepsilon_y \\ \gamma_{xy} \end{Bmatrix} - \boldsymbol{\varepsilon}_0 \right) \quad (4.11)$$

can be explicitly stated for any material (excluding here $\boldsymbol{\sigma}_0$ which is simply additive). To consider the special cases in two dimensions it is convenient to start from the form

$$\boldsymbol{\varepsilon} = \mathbf{D}^{-1} \boldsymbol{\sigma} + \boldsymbol{\varepsilon}_0$$

and impose the conditions of plane stress or plane strain.

Plane stress – isotropic material

For plane stress in an isotropic material we have by definition,

$$\begin{aligned} \varepsilon_x &= \frac{\sigma_x}{E} - \frac{\nu\sigma_y}{E} + \varepsilon_{x0} \\ \varepsilon_y &= -\frac{\nu\sigma_x}{E} + \frac{\sigma_y}{E} + \varepsilon_{y0} \\ \gamma_{xy} &= \frac{2(1+\nu)\tau_{xy}}{E} + \gamma_{xy0} \end{aligned} \quad (4.12)$$

Solving the above for the stresses, we obtain the matrix \mathbf{D} as

$$\mathbf{D} = \frac{E}{1-\nu^2} \begin{bmatrix} 1 & \nu & 0 \\ \nu & 1 & 0 \\ 0 & 0 & (1-\nu)/2 \end{bmatrix} \quad (4.13)$$

and the initial strains as

$$\boldsymbol{\varepsilon}_0 = \begin{Bmatrix} \varepsilon_{x0} \\ \varepsilon_{y0} \\ \gamma_{xy0} \end{Bmatrix} \quad (4.14)$$

in which E is the elastic modulus and ν is Poisson's ratio.

Plane strain – isotropic material

In this case a normal stress σ_z exists in addition to the other three stress components. Thus we now have

$$\begin{aligned} \varepsilon_x &= \frac{\sigma_x}{E} - \frac{\nu\sigma_y}{E} - \frac{\nu\sigma_z}{E} + \varepsilon_{x0} \\ \varepsilon_y &= -\frac{\nu\sigma_x}{E} + \frac{\sigma_y}{E} - \frac{\nu\sigma_z}{E} + \varepsilon_{y0} \\ \gamma_{xy} &= \frac{2(1+\nu)\tau_{xy}}{E} + \gamma_{xy0} \end{aligned} \quad (4.15)$$

and in addition

$$\varepsilon_z = -\frac{\nu\sigma_x}{E} - \frac{\nu\sigma_y}{E} + \frac{\sigma_z}{E} + \varepsilon_{z0} = 0$$

which yields

$$\sigma_z = \nu(\sigma_x + \sigma_y) - E\varepsilon_{z0}$$

On eliminating σ_z and solving for the three remaining stresses we obtain the matrix \mathbf{D} as

$$\mathbf{D} = \frac{E}{(1+\nu)(1-2\nu)} \begin{bmatrix} 1-\nu & \nu & 0 \\ \nu & 1-\nu & 0 \\ 0 & 0 & (1-2\nu)/2 \end{bmatrix} \quad (4.16)$$

and the initial strains

$$\boldsymbol{\varepsilon}_0 = \begin{Bmatrix} \varepsilon_{x0} + \nu\varepsilon_{z0} \\ \varepsilon_{y0} + \nu\varepsilon_{z0} \\ \gamma_{xy0} \end{Bmatrix} \quad (4.17)$$

Anisotropic materials

For a completely anisotropic material, 21 independent elastic constants are necessary to define completely the three-dimensional stress–strain relationship.^{4,5}

If two-dimensional analysis is to be applicable a symmetry of properties must exist, implying at most six independent constants in the \mathbf{D} matrix. Thus, it is always possible to write

$$\mathbf{D} = \begin{bmatrix} d_{11} & d_{12} & d_{13} \\ & d_{22} & d_{23} \\ \text{sym.} & & d_{33} \end{bmatrix} \quad (4.18)$$

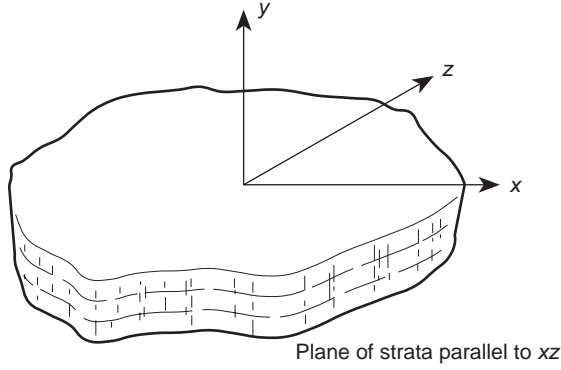


Fig. 4.2 A stratified (transversely isotropic) material.

to describe the most general two-dimensional behaviour. (The necessary symmetry of the \mathbf{D} matrix follows from the general equivalence of the Maxwell–Betti reciprocal theorem and is a consequence of invariant energy irrespective of the path taken to reach a given strain state.)

A case of particular interest in practice is that of a ‘stratified’ or transversely isotropic material in which a rotational symmetry of properties exists within the plane of the strata. Such a material possesses only five independent elastic constants.

The general stress–strain relations give in this case, following the notation of Lekhnitskii⁴ and taking now the y -axis as perpendicular to the strata (neglecting initial strain) (Fig. 4.2),

$$\begin{aligned}
 \varepsilon_x &= \frac{\sigma_x}{E_1} - \frac{\nu_2 \sigma_y}{E_2} - \frac{\nu_1 \sigma_z}{E_1} \\
 \varepsilon_y &= -\frac{\nu_2 \sigma_x}{E_2} + \frac{\sigma_y}{E_2} - \frac{\nu_2 \sigma_z}{E_2} \\
 \varepsilon_z &= -\frac{\nu_1 \sigma_x}{E_1} - \frac{\nu_2 \sigma_y}{E_2} + \frac{\sigma_z}{E_1} \\
 \gamma_{xz} &= \frac{2(1 + \nu_1)}{E_1} \tau_{xz} \\
 \gamma_{xy} &= \frac{1}{G_2} \tau_{xy} \\
 \gamma_{yz} &= \frac{1}{G_2} \tau_{yz}
 \end{aligned} \tag{4.19}$$

in which the constants E_1 , ν_1 (G_1 is dependent) are associated with the behaviour in the plane of the strata and E_2 , G_2 , ν_2 with a direction normal to the plane.

The \mathbf{D} matrix in two dimensions now becomes, taking $E_1/E_2 = n$ and $G_2/E_2 = m$,

$$\mathbf{D} = \frac{E_2}{1 - m\nu_2^2} \begin{bmatrix} n & m\nu_2 & 0 \\ m\nu_2 & 1 & 0 \\ 0 & 0 & m(1 - m\nu_2^2) \end{bmatrix} \tag{4.20}$$

for plane stress or

$$\mathbf{D} = \frac{E_2}{(1 + \nu_1)(1 - \nu_1 - 2\nu_2^2)} \times \begin{bmatrix} n(1 - \nu_2^2) & n\nu_2(1 + \nu_1) & 0 \\ n\nu_2(1 + \nu_1) & (1 - \nu_1^2) & 0 \\ 0 & 0 & m(1 + \nu_1)(1 - \nu_1 - 2\nu_2^2) \end{bmatrix} \quad (4.21)$$

for plane strain.

When, as in Fig. 4.3, the direction of the strata is inclined to the x -axis then to obtain the \mathbf{D} matrices in universal coordinates a transformation is necessary. Taking \mathbf{D}' as relating the stresses and strains in the inclined coordinate system (x', y') it is easy to show that

$$\mathbf{D} = \mathbf{T}\mathbf{D}'\mathbf{T}^T \quad (4.22)$$

where

$$\mathbf{T} = \begin{bmatrix} \cos^2 \beta & \sin^2 \beta & -2 \sin \beta \cos \beta \\ \sin^2 \beta & \cos^2 \beta & 2 \sin \beta \cos \beta \\ \sin \beta \cos \beta & -\sin \beta \cos \beta & \cos^2 \beta - \sin^2 \beta \end{bmatrix} \quad (4.23)$$

with β as defined in Fig. 4.3.

If the stress systems $\boldsymbol{\sigma}'$ and $\boldsymbol{\sigma}$ correspond to $\boldsymbol{\varepsilon}'$ and $\boldsymbol{\varepsilon}$ respectively then by equality of work

$$\boldsymbol{\sigma}'^T \boldsymbol{\varepsilon}' = \boldsymbol{\sigma}^T \boldsymbol{\varepsilon}$$

or

$$\boldsymbol{\varepsilon}'^T \mathbf{D}' \boldsymbol{\varepsilon}' = \boldsymbol{\varepsilon}^T \mathbf{D} \boldsymbol{\varepsilon}$$

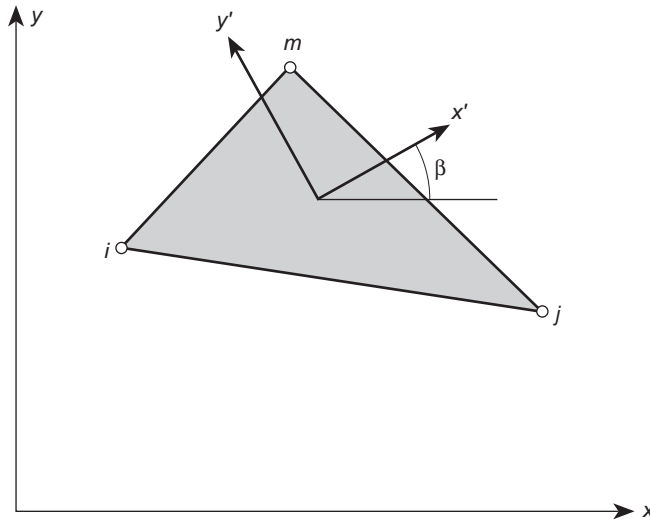


Fig. 4.3 An element of a stratified (transversely isotropic) material.

from which Eq. (4.22) follows on noting (see also Chapter 1)

$$\boldsymbol{\varepsilon}' = \mathbf{T}^T \boldsymbol{\varepsilon} \quad (4.24)$$

4.2.4 Initial strain (thermal strain)

'Initial' strains, i.e., strains which are independent of stress, may be due to many causes. Shrinkage, crystal growth, or, most frequently, temperature change will, in general, result in an initial strain vector:

$$\boldsymbol{\varepsilon}_0 = [\varepsilon_{x0} \quad \varepsilon_{y0} \quad \varepsilon_{z0} \quad \gamma_{xy0} \quad \gamma_{yz0} \quad \gamma_{zx0}]^T \quad (4.25)$$

Although this initial strain may, in general, depend on the position within the element, it will here be defined by average, constant values to be consistent with the constant strain conditions imposed by the prescribed displacement function.

For an isotropic material in an element subject to a temperature rise θ^e with a coefficient of thermal expansion α we will have

$$\boldsymbol{\varepsilon}_0 = \alpha \theta^e [1 \quad 1 \quad 1 \quad 0 \quad 0 \quad 0]^T \quad (4.26)$$

as no shear strains are caused by a thermal dilatation. Thus, for plane stress, Eq. (4.14) yields the initial strains given by

$$\boldsymbol{\varepsilon}_0 = \alpha \theta^e \begin{Bmatrix} 1 \\ 1 \\ 0 \end{Bmatrix} = \alpha \theta^e \mathbf{m} \quad (4.27)$$

In *plane strain* the σ_z stress perpendicular to the xy plane will develop due to the thermal expansion as shown above. Using Eq. (4.17) the initial thermal strains for this case are given by

$$\boldsymbol{\varepsilon}_0 = (1 + \nu) \alpha \theta^e \mathbf{m} \quad (4.28)$$

Anisotropic materials present special problems, since the coefficients of thermal expansion may vary with direction. In the general case the thermal strains are given by

$$\boldsymbol{\varepsilon}_0 = \boldsymbol{\alpha} \theta^e \quad (4.29)$$

where $\boldsymbol{\alpha}$ has properties similar to strain. Accordingly, it is always possible to find orthogonal directions for which $\boldsymbol{\alpha}$ is diagonal. If we let x' and y' denote the principal thermal directions of the material, the initial strain due to thermal expansion for a plane stress state becomes (assuming z' is a principal direction)

$$\boldsymbol{\varepsilon}' = \theta^e \begin{Bmatrix} \varepsilon_{x'0} \\ \varepsilon_{y'0} \\ \gamma_{x'y'0} \end{Bmatrix} = \theta^e \begin{Bmatrix} \alpha_1 \\ \alpha_2 \\ 0 \end{Bmatrix} \quad (4.30)$$

where α_1 and α_2 are the expansion coefficients referred to the x' and y' axes, respectively.

To obtain strain components in the x, y system it is necessary to use the strain transformation

$$\boldsymbol{\varepsilon}'_0 = \mathbf{T}^T \boldsymbol{\varepsilon}_0 \quad (4.31)$$

where \mathbf{T} is again given by Eq. (4.23). Thus, $\boldsymbol{\varepsilon}_0$ can be simply evaluated. It will be noted that the shear component of strain is no longer equal to zero in the x, y coordinates.

4.2.5 The stiffness matrix

The stiffness matrix of the element ijm is defined from the general relationship (2.13) with the coefficients

$$\mathbf{K}_{ij}^e = \int \mathbf{B}_i^T \mathbf{D} \mathbf{B}_j t \, dx \, dy \quad (4.32)$$

where t is the thickness of the element and the integration is taken over the area of the triangle. If the thickness of the element is assumed to be constant, an assumption convergent to the truth as the size of elements decreases, then, as neither of the matrices contains x or y we have simply

$$\mathbf{K}_{ij}^e = \mathbf{B}_i^T \mathbf{D} \mathbf{B}_j t \Delta \quad (4.33)$$

where Δ is the area of the triangle [already defined by Eq. (4.5)]. This form is now sufficiently explicit for computation with the actual matrix operations being left to the computer.

4.2.6 Nodal forces due to initial strain

These are given directly by the expression Eq. (2.13b) which, on performing the integration, becomes

$$(\mathbf{f}_i)_{\boldsymbol{\varepsilon}_0}^e = -\mathbf{B}_i^T \mathbf{D} \boldsymbol{\varepsilon}_0 t \Delta, \quad \text{etc.} \quad (4.34)$$

These 'initial strain' forces contribute to the nodes of an element in an unequal manner and require precise evaluation. Similar expressions are derived for initial stress forces.

4.2.7 Distributed body forces

In the general case of plane stress or strain each element of unit area in the xy plane is subject to forces

$$\mathbf{b} = \begin{Bmatrix} b_x \\ b_y \end{Bmatrix}$$

in the direction of the appropriate axes.

Again, by Eq. (2.13b), the contribution of such forces to those at each node is given by

$$\mathbf{f}_i^e = - \int N_i \begin{Bmatrix} b_x \\ b_y \end{Bmatrix} dx dy$$

or by Eq. (4.7),

$$\mathbf{f}_i^e = - \begin{Bmatrix} b_x \\ b_y \end{Bmatrix} \int N_i dx dy, \quad \text{etc.} \quad (4.35)$$

if the body forces b_x and b_y are constant. As N_i is not constant the integration has to be carried out explicitly. Some general integration formulae for a triangle are given in Appendix D.

In this special case the calculation will be simplified if the origin of coordinates is taken at the centroid of the element. Now

$$\int x dx dy = \int y dx dy = 0$$

and on using Eq. (4.8)

$$\mathbf{f}_i^e = - \begin{Bmatrix} b_x \\ b_y \end{Bmatrix} \int \frac{a_i dx dy}{2\Delta} = - \begin{Bmatrix} b_x \\ b_y \end{Bmatrix} \frac{a_i}{2} = - \begin{Bmatrix} b_x \\ b_y \end{Bmatrix} \frac{\Delta}{3} \quad (4.36)$$

by relations noted on page 89.

Explicitly, for the whole element

$$\mathbf{f}^e = \begin{Bmatrix} \mathbf{f}_i^e \\ \mathbf{f}_j^e \\ \mathbf{f}_m^e \end{Bmatrix} = - \begin{Bmatrix} b_x \\ b_y \\ b_x \\ b_y \\ b_x \\ b_y \end{Bmatrix} \frac{\Delta}{3} \quad (4.37)$$

which means simply that the total forces acting in the x and y directions due to the body forces are distributed to the nodes in three equal parts. This fact corresponds with physical intuition, and was often assumed implicitly.

4.2.8 Body force potential

In many cases the body forces are defined in terms of a body force potential ϕ as

$$b_x = - \frac{\partial \phi}{\partial x} \quad b_y = - \frac{\partial \phi}{\partial y} \quad (4.38)$$

and this potential, rather than the values of b_x and b_y , is known throughout the region and is specified at nodal points. If ϕ^e lists the three values of the potential associated with the nodes of the element, i.e.,

$$\phi^e = \begin{Bmatrix} \phi_i \\ \phi_j \\ \phi_m \end{Bmatrix} \quad (4.39)$$

and has to correspond with constant values of b_x and b_y , ϕ must vary linearly within the element. The ‘shape function’ of its variation will obviously be given by a procedure identical to that used in deriving Eqs (4.4)–(4.6), and yields

$$\phi = [N_i, N_j, N_m]\Phi^e \quad (4.40)$$

Thus,

$$b_x = -\frac{\partial\phi}{\partial x} = -[b_i, b_j, b_m]\frac{\Phi^e}{2\Delta}$$

and

$$b_y = -\frac{\partial\phi}{\partial y} = -[c_i, c_j, c_m]\frac{\Phi^e}{2\Delta} \quad (4.41)$$

The vector of nodal forces due to the body force potential will now replace Eq. (4.37) by

$$\mathbf{f}^e = \frac{1}{6} \begin{bmatrix} b_i & b_j & b_m \\ c_i & c_j & c_m \\ b_i & b_j & b_m \\ c_i & c_j & c_m \\ b_i & b_j & b_m \\ c_i & c_j & c_m \end{bmatrix} \Phi^e \quad (4.42)$$

4.2.9 Evaluation of stresses

The derived formulae enable the full stiffness matrix of the structure to be assembled, and a solution for displacements to be obtained.

The stress matrix given in general terms in Eq. (2.16) is obtained by the appropriate substitutions for each element.

The stresses are, by the basic assumption, constant within the element. It is usual to assign these to the centroid of the element, and in most of the examples in this chapter this procedure is followed. An alternative consists of obtaining stress values at the nodes by averaging the values in the adjacent elements. Some ‘weighting’ procedures have been used in this context on an empirical basis but their advantage appears small.

It is also usual to calculate the principal stresses and their directions for every element. In Chapter 14 we shall return to the problem of stress recovery and show that better procedures of stress recovery exist.^{6,7}

4.3 Examples – an assessment of performance

There is no doubt that the solution to plane elasticity problems as formulated in Sec. 4.2 is, in the limit of subdivision, an exact solution. Indeed at any stage of a

finite subdivision it is an approximate solution as is, say, a Fourier series solution with a limited number of terms.

As explained in Chapter 2, the total strain energy obtained during any stage of approximation will be below the true strain energy of the exact solution. In practice it will mean that the displacements, and hence also the stresses, will be underestimated by the approximation in its *general picture*. However, it must be emphasized that this is not necessarily true at every point of the continuum individually; hence the value of such a bound in practice is not great.

What is important for the engineer to know is the order of accuracy achievable in typical problems with a certain fineness of element subdivision. In any particular case the error can be assessed by comparison with known, exact, solutions or by a study of the convergence, using two or more stages of subdivision.

With the development of experience the engineer can assess *a priori* the order of approximation that will be involved in a specific problem tackled with a given element subdivision. Some of this experience will perhaps be conveyed by the examples considered in this book.

In the first place attention will be focused on some simple problems for which exact solutions are available.

4.3.1 Uniform stress field

If the exact solution is in fact that of a uniform stress field then, whatever the element subdivision, the finite element solution will coincide exactly with the exact one. This is an obvious corollary of the formulation; nevertheless it is useful as a first check of written computer programs.

4.3.2 Linearly varying stress field

Here, obviously, the basic assumption of constant stress within each element means that the solution will be approximate only. In Fig. 4.4 a simple example of a beam subject to constant bending moment is shown with a fairly coarse subdivision. It is readily seen that the axial (σ_y) stress given by the element 'straddles' the exact values and, in fact, if the constant stress values are associated with centroids of the elements and plotted, the best 'fit' line represents the exact stresses.

The horizontal and shear stress components differ again from the exact values (which are simply zero). Again, however, it will be noted that they oscillate by equal, small amounts around the exact values.

At internal nodes, if the average of the stresses of surrounding elements is taken it will be found that the exact stresses are very closely represented. The average at external faces is not, however, so good. The overall improvement in representing the stresses by nodal averages, as shown in Fig. 4.4, is often used in practice for contour plots. However, we shall show in Chapter 14 a method of recovery which gives much improved values at both interior and boundary points.

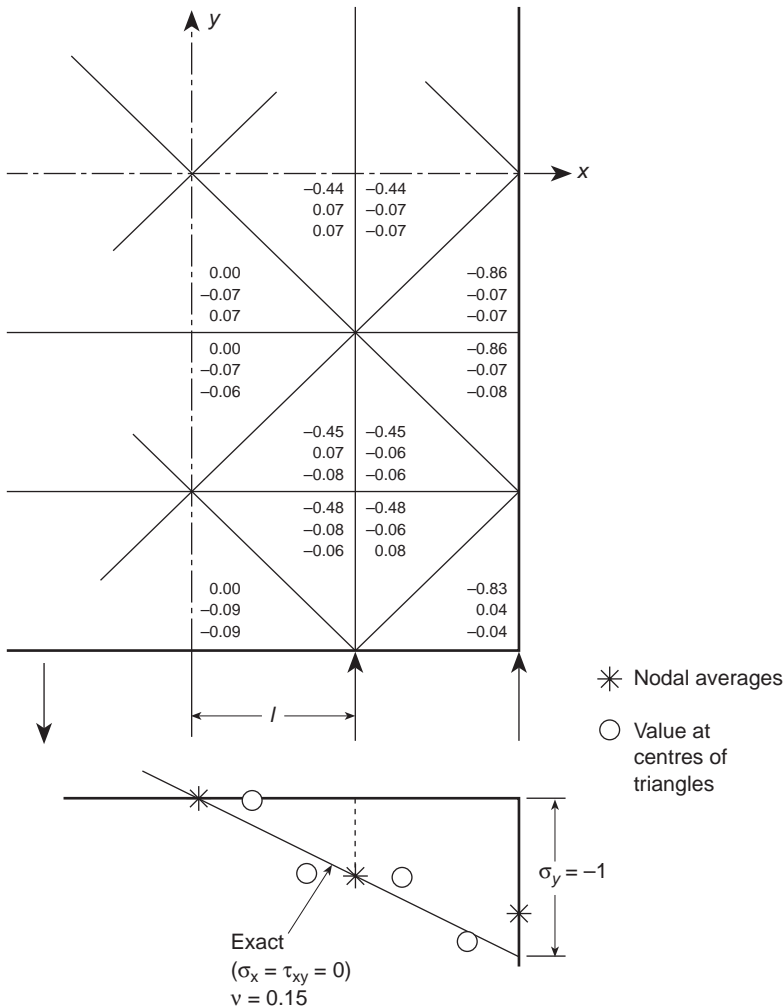


Fig. 4.4 Pure bending of a beam solved by a coarse subdivision into elements of triangular shape. (Values of σ_y , σ_x , and τ_{xy} listed in that order.)

4.3.3 Stress concentration

A more realistic test problem is shown in Figs 4.5 and 4.6. Here the flow of stress around a circular hole in an isotropic and in an anisotropic stratified material is considered when the stress conditions are uniform.⁸ A graded division into elements is used to allow a more detailed study in the region where high stress gradients are expected. The accuracy achievable can be assessed from Fig. 4.6 where some of the results are compared against exact solutions.^{3,9}

In later chapters we shall see that even more accurate answers can be obtained with the use of more elaborate elements; however, the principles of the analysis remain identical.

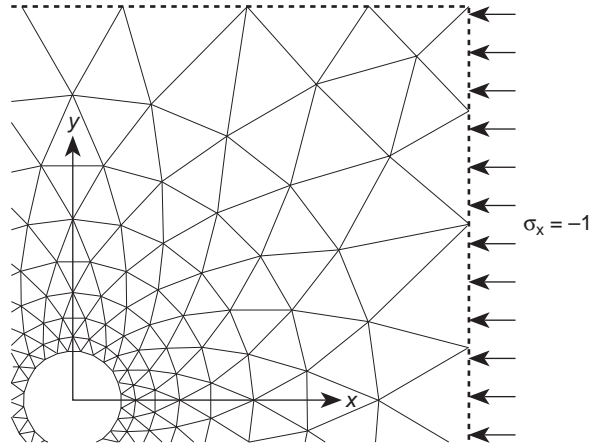


Fig. 4.5 A circular hole in a uniform stress field: (a) isotropic material; (b) stratified (orthotropic) material; $E_x = E_1 = 1$, $E_y = E_2 = 3$, $\nu_1 = 0.1$, $\nu_2 = 0$, $G_{xy} = 0.42$.

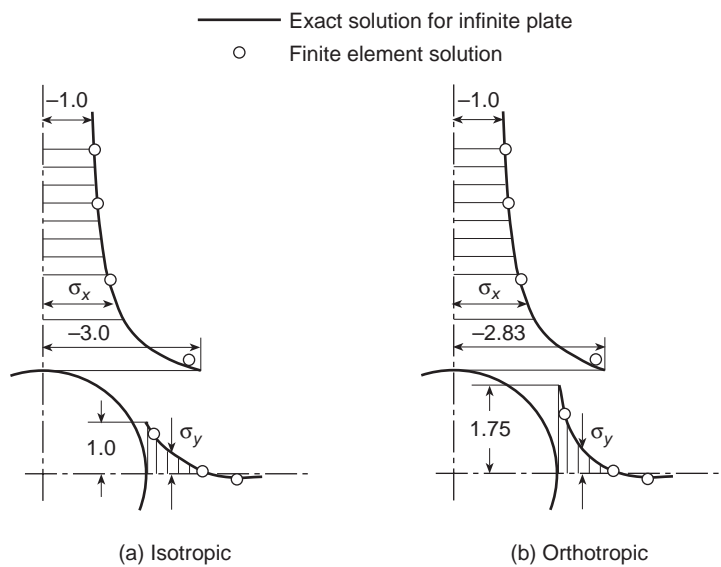


Fig. 4.6 Comparison of theoretical and finite element results for cases (a) and (b) of Fig. 4.5.

4.4 Some practical applications

Obviously, the practical applications of the method are limitless, and the finite element method has superseded experimental technique for plane problems because of its high accuracy, low cost, and versatility. The ease of treatment of material anisotropy, thermal stresses, or body force problems add to its advantages.

A few examples of actual early applications of the finite element method to complex problems of engineering practice will now be given.

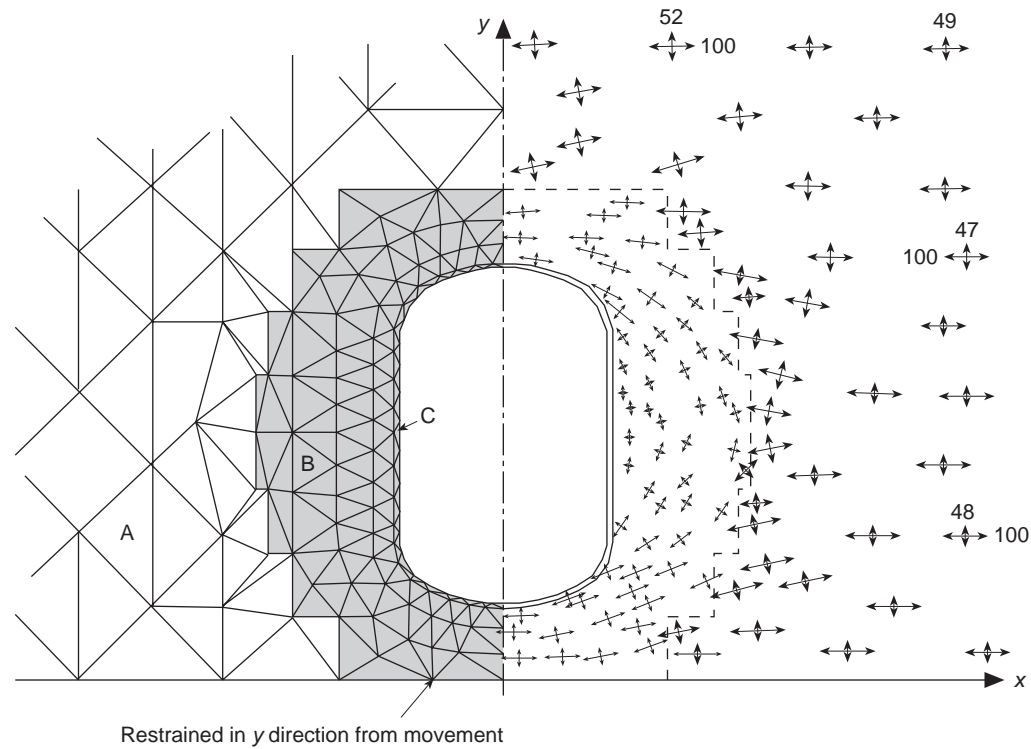


Fig. 4.7 A reinforced opening in a plate. Uniform stress field at a distance from opening $\sigma_x = 100$, $\sigma_y = 50$. Thickness of plate regions A, B, and C is in the ratio of 1 : 3 : 23.

4.4.1 Stress flow around a reinforced opening (Fig. 4.7)

In steel pressure vessels or aircraft structures, openings have to be introduced in the stressed skin. The penetrating duct itself provides some reinforcement round the edge and, in addition, the skin itself is increased in thickness to reduce the stresses due to concentration effects.

Analysis of such problems treated as cases of plane stress present no difficulties. The elements are chosen so as to follow the thickness variation, and appropriate values of this are assigned.

The narrow band of thick material near the edge can be represented either by special bar-type elements, or by very thin triangular elements of the usual type, to which appropriate thickness is assigned. The latter procedure was used in the problem shown in Fig. 4.7 which gives some of the resulting stresses near the opening itself. The fairly large extent of the region introduced in the analysis and the grading of the mesh should be noted.

4.4.2 An anisotropic valley subject to tectonic stress⁸ (Fig. 4.8)

A symmetrical valley subject to a uniform horizontal stress is considered. The material is stratified, and hence is 'transversely isotropic', and the direction of strata varies from point to point.

The stress plot shows the tensile region that develops. This phenomenon is of considerable interest to geologists and engineers concerned with rock mechanics. (See reference 10 for additional applications on this topic.)

4.4.3 A dam subject to external and internal water pressures^{11,12}

A buttress dam on a somewhat complex rock foundation is shown in Fig. 4.9 and analysed. This dam (completed in 1964) is of particular interest as it is the first to which the finite element method was applied during the design stage. The heterogeneous foundation region is subject to plane strain conditions while the dam itself is considered in a state of plane stress of variable thickness.

With external and gravity loading no special problems of analysis arise.

When pore pressures are considered, the situation, however, requires perhaps some explanation.

It is well known that in a porous material the water pressure is transmitted to the structure as a *body force* of magnitude

$$b_x = -\frac{\partial p}{\partial x} \quad b_y = -\frac{\partial p}{\partial y} \quad (4.43)$$

and that now the external pressure need not be considered.

The pore pressure p is, in fact, now a body force potential, as defined in Eq. (4.38). Figure 4.9 shows the element subdivision of the region and the outline of the dam. Figure 4.10(a) and (b) shows the stresses resulting from gravity (applied to the dam only) and due to water pressure assumed to be acting as an external load or, alternatively,

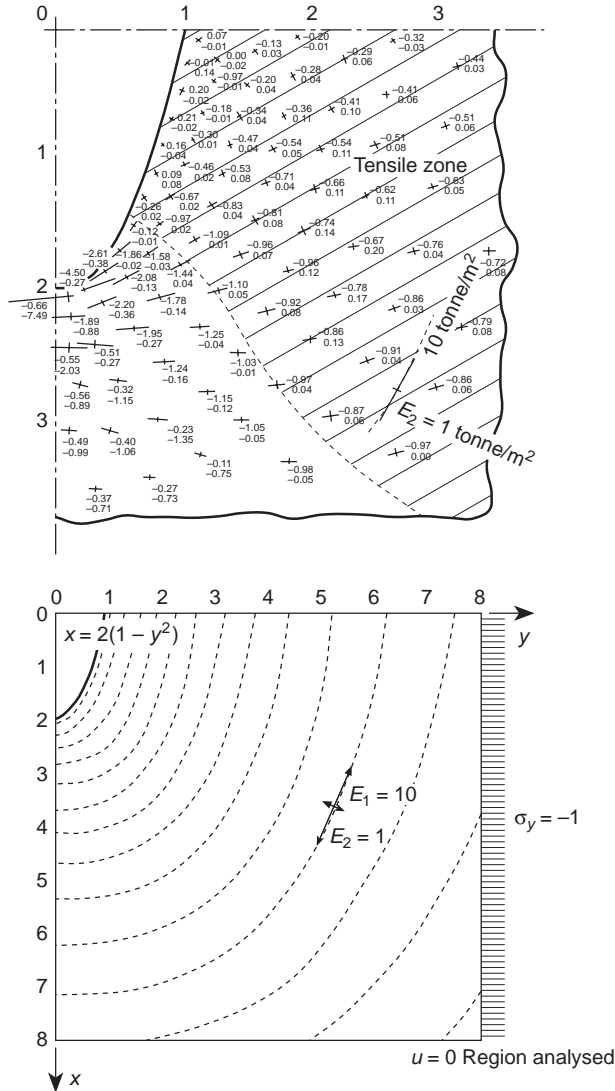


Fig. 4.8 A valley with curved strata subject to a horizontal tectonic stress (plane strain 170 nodes, 298 elements).

as an internal pore pressure. Both solutions indicate large tensile regions, but the increase of stresses due to the second assumption is important.

The stresses calculated here are the so-called ‘effective’ stresses. These represent the forces transmitted between the solid particles and are defined in terms of the *total* stresses σ and the pore pressures p by

$$\sigma' = \sigma + mp \quad \mathbf{m}^T = [1, 1, 0] \quad (4.44)$$

i.e., simply by removing the hydrostatic pressure component from the *total* stress.^{10,13}

The effective stress is of particular importance in the mechanics of porous media such as those that occur in the study of soils, rocks, or concrete. The basic assumption

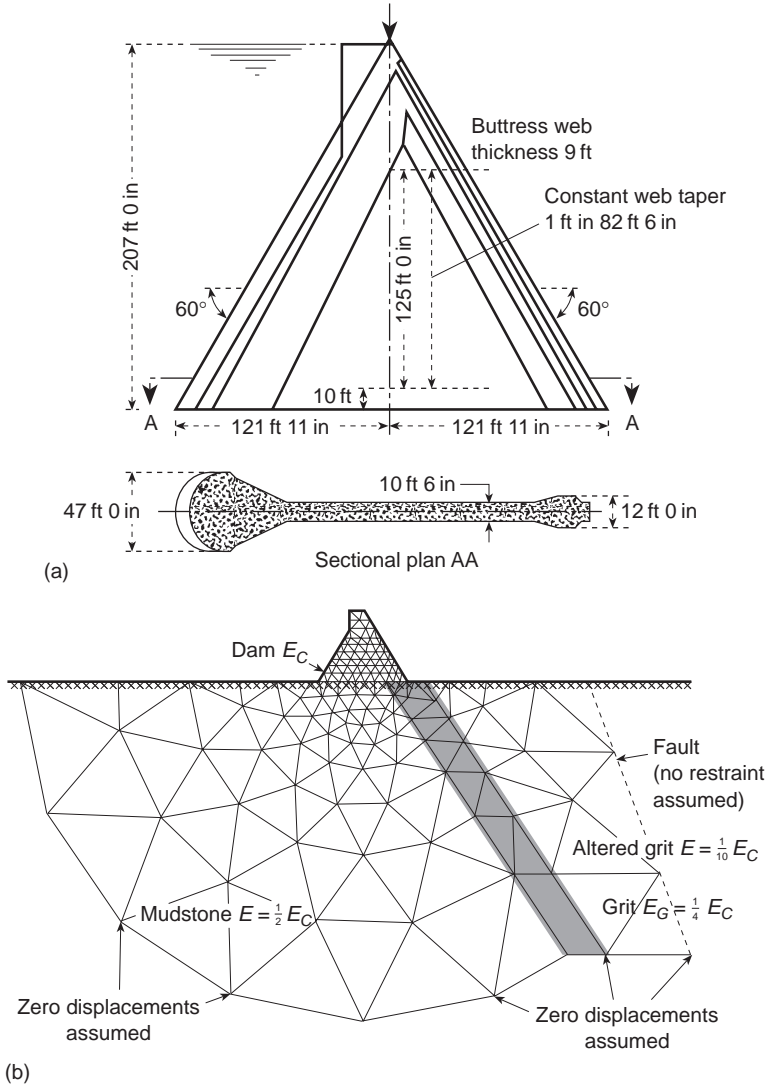


Fig. 4.9 Stress analysis of a buttress dam. A plane stress condition is assumed in the dam and plane strain in the foundation. (a) The buttress section analysed. (b) Extent of foundation considered and division into finite elements.

in deriving the body forces of Eq. (4.43) is that only the effective stress is of any importance in deforming the solid phase. This leads immediately to another possibility of formulation.¹⁴ If we examine the equilibrium conditions of Eq. (2.10) we note that this is written in terms of total stresses. Writing the constitutive relation, Eq. (2.5), in terms of effective stresses, i.e.,

$$\boldsymbol{\sigma}' = \mathbf{D}'(\boldsymbol{\varepsilon} - \boldsymbol{\varepsilon}_0) + \boldsymbol{\sigma}'_0 \quad (4.45)$$

and substituting into the equilibrium equation (2.10) we find that Eq. (2.12) is again obtained, with the stiffness matrix using the matrix \mathbf{D}' and the force terms of

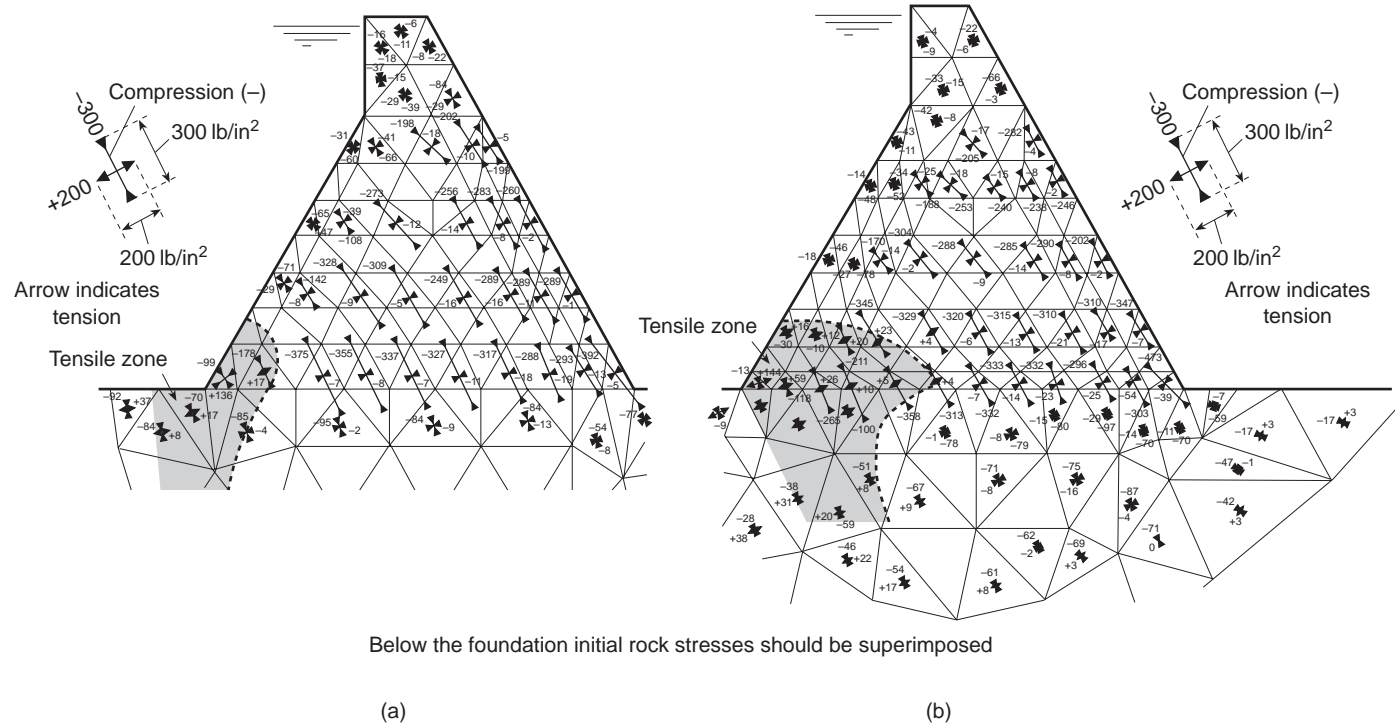


Fig. 4.10 Stress analysis of the buttress dam of Fig. 4.9. Principal stresses for gravity loads are combined with water pressures, which are assumed to act (a) as external loads, (b) as body forces due to pore pressure.

Eq. (2.13b) being augmented by an additional force

$$- \int_{V^e} \mathbf{B}^T \mathbf{m} p \, d(\text{vol}) \quad (4.46)$$

or, if p is interpolated by shape functions N'_i , the force becomes

$$- \int_{V^e} \mathbf{B}^T \mathbf{m} \mathbf{N}' \, d(\text{vol}) \bar{\mathbf{p}}^e \quad (4.47)$$

This alternative form of introducing pore pressure effects allows a discontinuous interpolation of p to be used [as in Eq. (4.46) no derivatives occur] and this is now frequently used in practice.

4.4.4 Cracking

The tensile stresses in the previous example will doubtless cause the rock to crack. If a stable situation can develop when such a crack spreads then the dam can be considered safe.

Cracks can be introduced very simply into the analysis by assigning zero elasticity values to chosen elements. An analysis with a wide cracked wedge is shown in Fig. 4.11, where it can be seen that with the extent of the crack assumed no tension within the dam body develops.

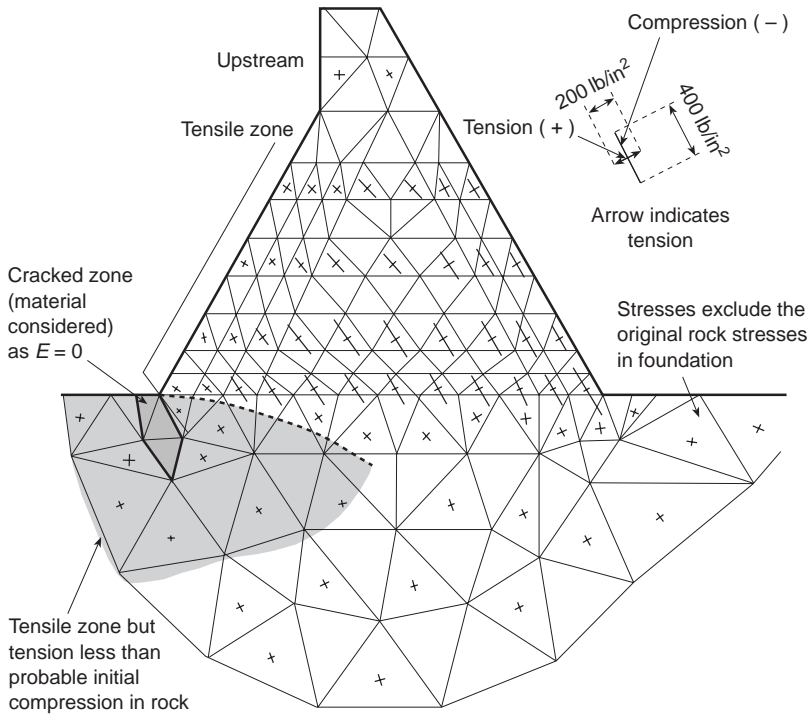


Fig. 4.11 Stresses in a buttress dam. The introduction of a 'crack' modifies the stress distribution [same loading as Fig. 4.10(b)].

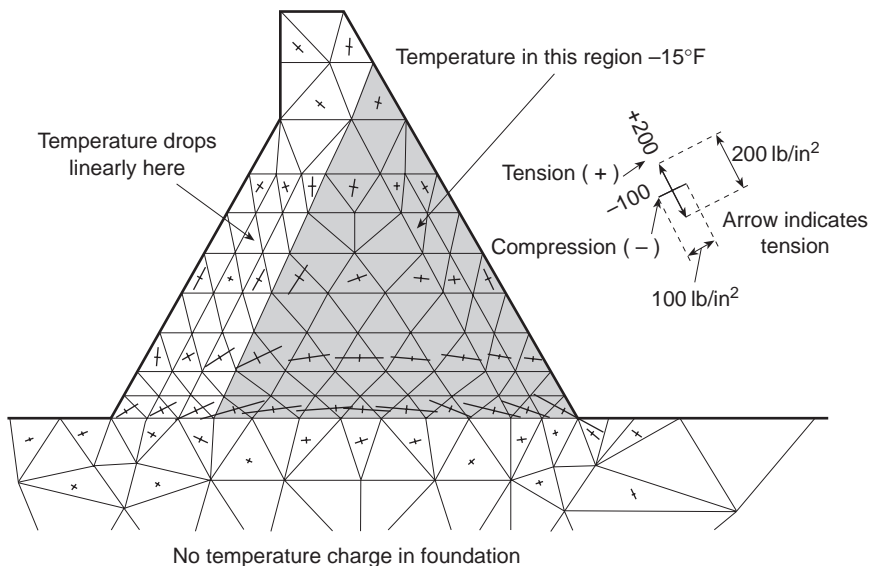


Fig. 4.12 Stress analysis of a buttress dam. Thermal stresses due to cooling of the shaded area by 15°F ($E = 3 \times 10^6 \text{ lb/in}^2$, $\alpha = 6 \times 10^{-6}/^{\circ}\text{F}$).

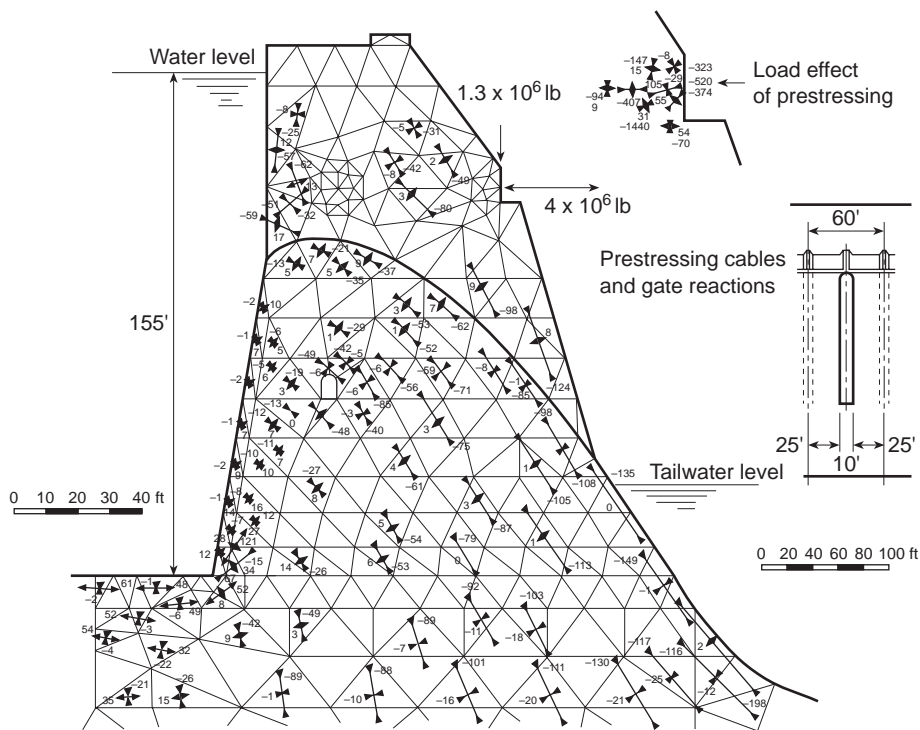


Fig. 4.13 A large barrage with piers and prestressing cables.

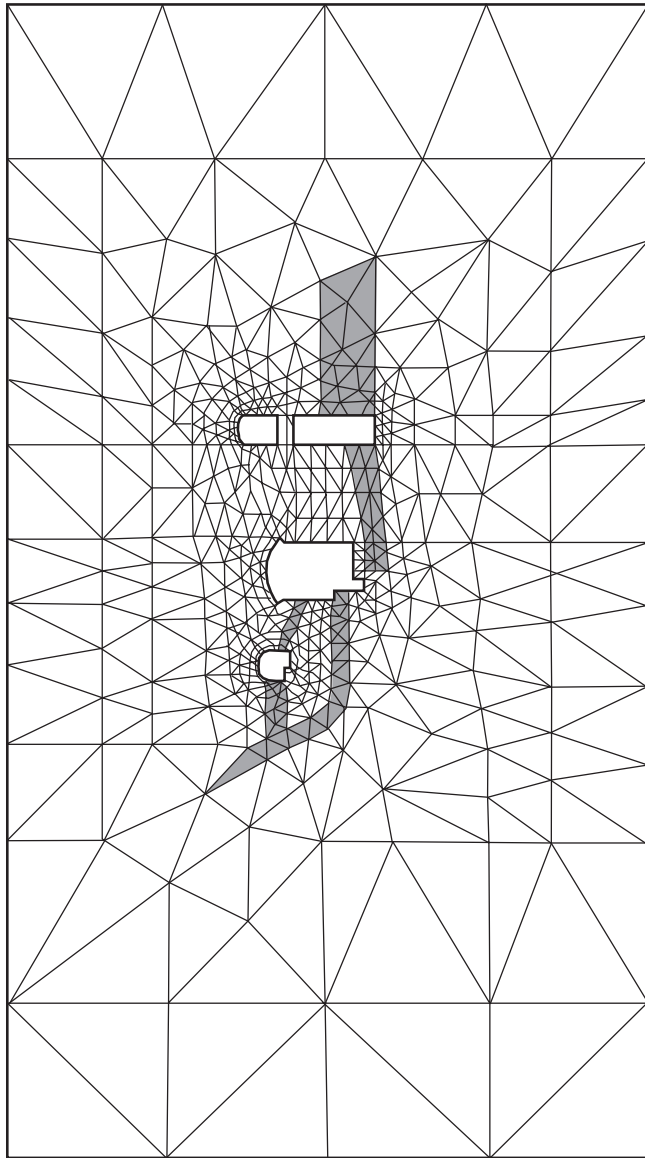


Fig. 4.14 An underground power station. Mesh used in analysis.

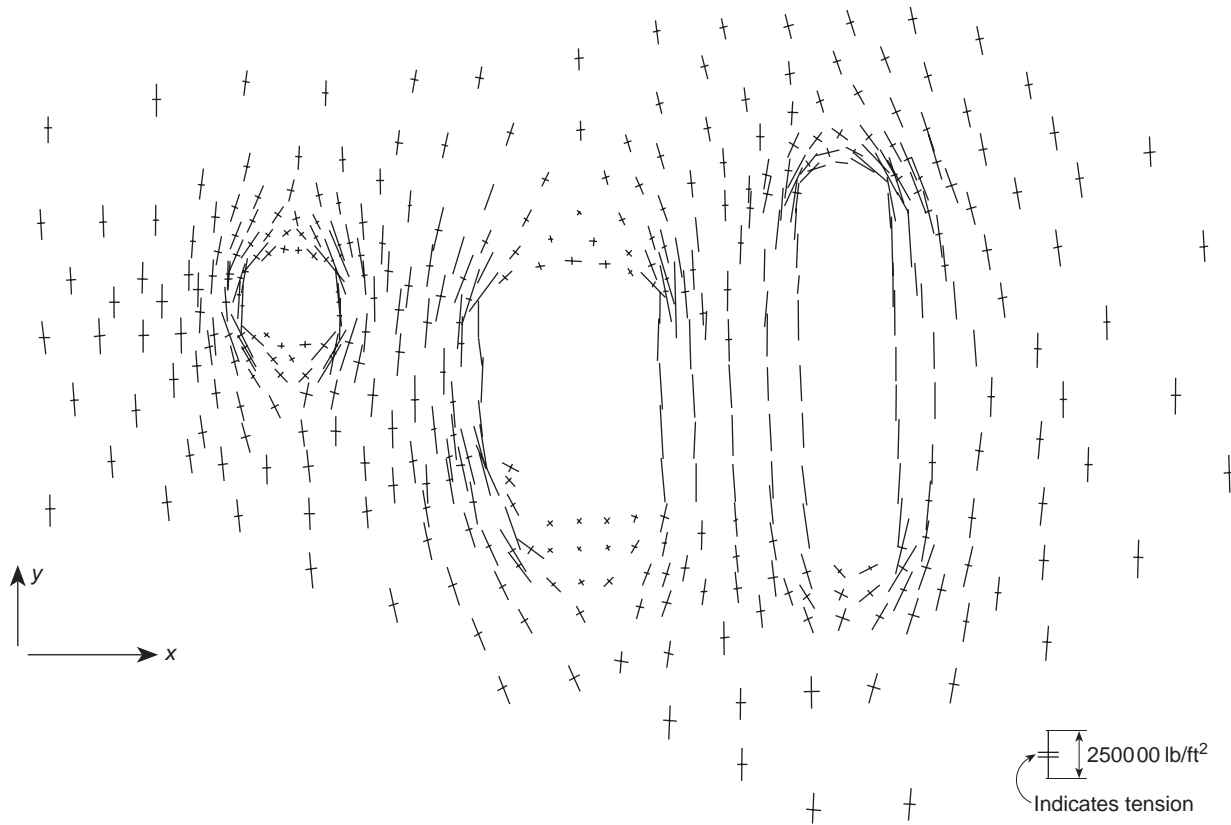


Fig. 4.15 An underground power station. Plot of principal stresses.

A more elaborate procedure for allowing crack propagation and resulting stress redistribution can be developed (see Volume 2).

4.4.5 Thermal stresses

As an example of thermal stress computation the same dam is shown under simple temperature distribution assumptions. Results of this analysis are given in Fig. 4.12.

4.4.6 Gravity dams

A buttress dam is a natural example for the application of finite element methods. Other types, such as gravity dams with or without piers and so on, can also be simply treated. Figure 4.13 shows an analysis of a large dam with piers and crest gates.

In this case the approximation of assuming a two-dimensional treatment in the vicinity of the abrupt change of section, i.e., where the piers join the main body of the dam, is clearly involved, but this leads to localized errors only.

It is important to note here how, in a single solution, the grading of element size is used to study concentration of stress at the cable anchorages, the general stress flow in the dam, and the foundation behaviour. The linear ratio of size of largest to smallest elements is of the order of 30 to 1 (the largest elements occurring in the foundation are not shown in the figure).

4.4.7 Underground power station

This last example, illustrated in Figs 4.14 and 4.15, shows an interesting application. Here principal stresses are plotted automatically. In this analysis many different components of σ_0 , the initial stress, were used due to uncertainty of knowledge about geological conditions. The rapid solution and plot of many results enabled the limits within which stresses vary to be found and an engineering decision arrived at. In this example, the exterior boundaries were taken far enough and ‘fixed’ ($u = v = 0$). However, a better treatment could be made using infinite elements as described in Sec. 9.13.

4.5 Special treatment of plane strain with an incompressible material

It will have been noted that the relationship (4.16) defining the elasticity matrix \mathbf{D} for an isotropic material breaks down when Poisson’s ratio reaches a value of 0.5 as the factor in parentheses becomes infinite. A simple way of side-stepping this difficulty is to use values of Poisson’s ratio approximating to 0.5 but not equal to it. Experience shows, however, that if this is done the solution deteriorates unless special formulations such as those discussed in Chapter 12 are used.

4.6 Concluding remark

In subsequent chapters, we shall introduce elements which give much greater accuracy for the same number of degrees of freedom in a particular problem. This has led to the belief that the simple triangle used here is completely superseded. In recent years, however, its very simplicity has led to its revival in practical use in combination with the error estimation and adaptive procedures discussed in Chapters 14 and 15.

References

1. M.J. Turner, R.W. Clough, H.C. Martin, and L.J. Topp. Stiffness and deflection analysis of complex structures. *J. Aero. Sci.*, **23**, 805–23, 1956.
2. R.W. Clough. The finite element in plane stress analysis. *Proc. 2nd ASCE Conf. on Electronic Computation*. Pittsburgh, Pa., Sept. 1960.
3. S. Timoshenko and J.N. Goodier. *Theory of Elasticity*. 2nd ed., McGraw-Hill, 1951.
4. S.G. Lekhnitskii. *Theory of Elasticity of an Anisotropic Elastic Body* (Translation from Russian by P. Fern). Holden Day, San Francisco, 1963.
5. R.F.S. Hearmon. *An Introduction to Applied Anisotropic Elasticity*. Oxford University Press, 1961.
6. O.C. Zienkiewicz and J.Z. Zhu. The superconvergent patch recovery (SPR) and adaptive finite element refinement. *Comp. Methods Appl. Mech. Eng.*, **101**, 207–24, 1992.
7. B. Boroomand and O.C. Zienkiewicz. Recovery by equilibrium patches (REP). *Internat. J. Num. Meth. Eng.*, **40**, 137–54, 1997.
8. O.C. Zienkiewicz, Y.K. Cheung, and K.G. Stagg. Stresses in anisotropic media with particular reference to problems of rock mechanics. *J. Strain Analysis*, **1**, 172–82, 1966.
9. G.N. Savin. *Stress Concentration Around Holes* (Translation from Russian). Pergamon Press, 1961.
10. O.C. Zienkiewicz, A.H.C. Chan, M. Pastor, B. Schrefler, and T. Shiomi. *Computational Geomechanics*. John Wiley and Sons, Chichester, 1999.
11. O.C. Zienkiewicz and Y.K. Cheung. Buttress dams on complex rock foundations. *Water Power*, **16**, 193, 1964.
12. O.C. Zienkiewicz and Y.K. Cheung. Stresses in buttress dams. *Water Power*, **17**, 69, 1965.
13. K. Terzhagi. *Theoretical Soil Mechanics*. Wiley, 1943.
14. O.C. Zienkiewicz, C. Humpheson, and R.W. Lewis. A unified approach to soil mechanics problems, including plasticity and visco-plasticity. *Int. Symp. on Numerical Methods in Soil and Rock Mechanics*. Karlsruhe, 1975. See also Chapter 4 of *Finite Elements in Geomechanics* (ed. G. Gudehus), pp. 151–78, Wiley, 1977.

'Standard' and 'hierarchical' element shape functions: some general families of C_0 continuity

8.1 Introduction

In Chapters 4, 5, and 6 the reader was shown in some detail how linear elasticity problems could be formulated and solved using very simple finite element forms. In Chapter 7 this process was repeated for the quasi-harmonic equation. Although the detailed algebra was concerned with shape functions which arose from triangular and tetrahedral shapes only it should by now be obvious that other element forms could equally well be used. Indeed, once the element and the corresponding shape functions are determined, subsequent operations follow a standard, well-defined path which could be entrusted to an algebraist not familiar with the physical aspects of the problem. It will be seen later that in fact it is possible to program a computer to deal with wide classes of problems by specifying the shape functions only. The choice of these is, however, a matter to which intelligence has to be applied and in which the human factor remains paramount. In this chapter some rules for the generation of several families of one-, two-, and three-dimensional elements will be presented.

In the problems of elasticity illustrated in Chapters 4, 5, and 6 the displacement variable was a vector with two or three components and the shape functions were written in matrix form. They were, however, derived for each component separately and in fact the matrix expressions in these were derived by multiplying a scalar function by an identity matrix [e.g., Eqs (4.7), (5.3), and (6.7)]. This scalar form was used directly in Chapter 7 for the quasi-harmonic equation. We shall therefore concentrate in this chapter on the scalar shape function forms, calling these simply N_i .

The shape functions used in the displacement formulation of elasticity problems were such that they satisfy the convergence criteria of Chapter 2:

- (a) the continuity of the *unknown only* had to occur between elements (i.e., slope continuity is not required), or, in mathematical language, C_0 continuity was needed;
- (b) the function has to allow any arbitrary linear form to be taken so that the constant strain (constant first derivative) criterion could be observed.

The shape functions described in this chapter will require the satisfaction of these two criteria. They will thus be applicable to all the problems of the preceding chapters

and also to other problems which require these conditions to be obeyed. Indeed they are applicable to any situation where the functional Π or $\delta\Pi$ (see Chapter 3) is defined by derivatives of first order only.

The element families discussed will progressively have an increasing number of degrees of freedom. The question may well be asked as to whether any economic or other advantage is gained by thus increasing the complexity of an element. The answer here is not an easy one although it can be stated as a general rule that as the order of an element increases so the total number of unknowns in a problem can be reduced for a given accuracy of representation. Economic advantage requires, however, a reduction of total computation and data preparation effort, and this does not follow automatically for a reduced number of total variables because, though equation-solving times may be reduced, the time required for element formulation increases.

However, an overwhelming economic advantage in the case of three-dimensional analysis has already been hinted at in Chapters 6 and 7 for three-dimensional analyses.

The same kind of advantage arises on occasion in other problems but in general the optimum element may have to be determined from case to case.

In Sec. 2.6 of Chapter 2 we have shown that the order of error in the approximation to the unknown function is $O(h^{p+1})$, where h is the element 'size' and p is the degree of the complete polynomial present in the expansion. Clearly, as the element shape functions increase in degree so will the order of error increase, and convergence to the exact solution becomes more rapid. While this says nothing about the magnitude of error at a particular subdivision, it is clear that we should seek element shape functions with the highest complete polynomial for a given number of degrees of freedom.

8.2 Standard and hierarchical concepts

The essence of the finite element method already stated in Chapters 2 and 3 is in approximating the unknown (displacement) by an expansion given in Eqs (2.1) and (3.3). For a scalar variable u this can be written as

$$u \approx \hat{u} = \sum_{i=1}^n N_i a_i = \mathbf{N} \mathbf{a} \quad (8.1)$$

where n is the total number of functions used and a_i are the unknown parameters to be determined.

We have explicitly chosen to identify such variables with the values of the unknown function at element nodes, thus making

$$u_i = a_i \quad (8.2)$$

The shape functions so defined will be referred to as 'standard' ones and are the basis of most finite element programs. If polynomial expansions are used and the element satisfies Criterion 1 of Chapter 2 (which specifies that rigid body displacements cause no strain), it is clear that a constant value of a_i specified at all nodes must result in a constant value of \hat{u} :

$$\hat{u} = \left(\sum_{i=1}^n N_i \right) u_0 = u_0 \quad (8.3)$$

when $a_i = u_0$. It follows that

$$\sum_{i=1}^n N_i = 1 \quad (8.4)$$

at all points of the domain. This important property is known as a *partition of unity*¹ which we will make extensive use of in Chapter 16. The first part of this chapter will deal with such *standard shape functions*.

A serious drawback exists, however, with 'standard' functions, since when element refinement is made totally new shape functions have to be generated and hence all calculations repeated. It would be of advantage to avoid this difficulty by considering the expression (8.1) as a *series* in which the shape function N_i does not depend on the number of nodes in the mesh n . This indeed is achieved with *hierarchic shape functions* to which the second part of this chapter is devoted.

The hierarchic concept is well illustrated by the one-dimensional (elastic bar) problem of Fig. 8.1. Here for simplicity elastic properties are taken as constant ($D = E$) and the body force b is assumed to vary in such a manner as to produce the exact solution shown on the figure (with zero displacements at both ends).

Two meshes are shown and a linear interpolation between nodal points assumed. For both standard and hierarchic forms the coarse mesh gives

$$K_{11}^c a_1^c = f_1 \quad (8.5)$$

For a fine mesh two additional nodes are added and with the standard shape function the equations requiring solution are

$$\begin{bmatrix} K_{11}^F & K_{12}^F & 0 \\ K_{21}^F & K_{22}^F & K_{23}^F \\ 0 & K_{32}^F & K_{33}^F \end{bmatrix} \begin{Bmatrix} a_1 \\ a_2 \\ a_3 \end{Bmatrix} = \begin{Bmatrix} f_1 \\ f_2 \\ f_3 \end{Bmatrix} \quad (8.6)$$

In this form the zero matrices have been automatically inserted due to element interconnection which is here obvious, and we note that as no coefficients are the same, the new equations have to be resolved. [Equation (2.13) shows how these coefficients are calculated and the reader is encouraged to work these out in detail.]

With the 'hierarchic' form using the shape functions shown, a similar form of equation arises and an identical approximation is achieved (being simply given by a series of straight segments). The *final* solution is identical but the meaning of the parameters a_i^* is now different, as shown in Fig. 8.1.

Quite generally,

$$K_{11}^F = K_{11}^c \quad (8.7)$$

as an identical shape function is used for the first variable. Further, in this particular case the off-diagonal coefficients are zero and the final equations become, for the fine mesh,

$$\begin{bmatrix} K_{11}^c & 0 & 0 \\ 0 & K_{22}^F & 0 \\ 0 & 0 & K_{33}^F \end{bmatrix} \begin{Bmatrix} a_1^* \\ a_2^* \\ a_3^* \end{Bmatrix} = \begin{Bmatrix} f_1 \\ f_2 \\ f_3 \end{Bmatrix} \quad (8.8)$$

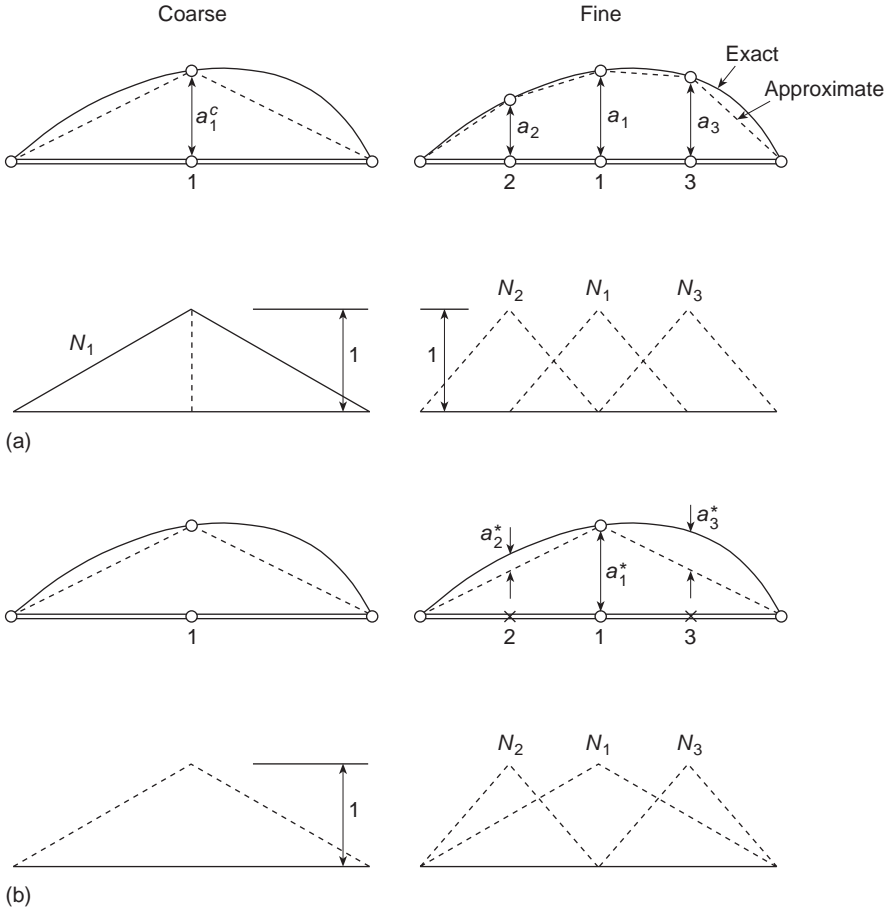


Fig. 8.1 A one-dimensional problem of stretching of a uniform elastic bar by prescribed body forces. (a) ‘Standard approximation. (b) Hierarchic approximation.

The ‘diagonality’ feature is only true in the one-dimensional problem, but in general it will be found that the matrices obtained using hierarchic shape functions are more nearly diagonal and hence imply better conditioning than those with standard shape functions.

Although the variables are now not subject to the obvious interpretation (as local displacement values), they can be easily transformed to those if desired. Though it is not usual to use hierarchic forms in linearly interpolated elements their derivation in polynomial form is simple and very advantageous.

The reader should note that with hierarchic forms it is convenient to consider the finer mesh as still using the same, coarse, elements but now adding additional refining functions.

Hierarchic forms provide a link with other approximate (orthogonal) series solutions. Many problems solved in classical literature by trigonometric, Fourier series, expansion are indeed particular examples of this approach.

In the following sections of this chapter we shall consider the development of shape functions for high order elements with many boundary and internal degree of freedoms. This development will generally be made on simple geometric forms and the reader may well question the wisdom of using increased accuracy for such simple shaped domains, having already observed the advantage of generalized finite element methods in fitting arbitrary domain shapes. This concern is well founded, but in the next chapter we shall show a general method to map high order elements into quite complex shapes.

Part 1 'Standard' shape functions

Two-dimensional elements

8.3 Rectangular elements – some preliminary considerations

Conceptually (especially if the reader is conditioned by education to thinking in the cartesian coordinate system) the simplest element form of a two-dimensional kind is that of a rectangle with sides parallel to the x and y axes. Consider, for instance, the rectangle shown in Fig. 8.2 with nodal points numbered 1 to 8, located as shown, and at which the values of an unknown function u (here representing, for instance, one of the components of displacement) form the element parameters. How can suitable C_0 continuous shape functions for this element be determined?

Let us first assume that u is expressed in polynomial form in x and y . To ensure interelement continuity of u along the top and bottom sides the variation must be linear. Two points at which the function is common between elements lying above or below exist, and as two values uniquely determine a linear function, its identity all along these sides is ensured with that given by adjacent elements. Use of this fact was already made in specifying linear expansions for a triangle.

Similarly, if a cubic variation along the vertical sides is assumed, continuity will be preserved there as four values determine a unique cubic polynomial. Conditions for satisfying the first criterion are now obtained.

To ensure the existence of constant values of the first derivative it is necessary that all the linear polynomial terms of the expansion be retained.

Finally, as eight points are to determine uniquely the variation of the function only eight coefficients of the expansion can be retained and thus we could write

$$u = \alpha_1 + \alpha_2 x + \alpha_3 y + \alpha_4 xy + \alpha_5 y^2 + \alpha_6 xy^2 + \alpha_7 y^3 + \alpha_8 xy^3 \quad (8.9)$$

The choice can in general be made unique by retaining the lowest possible expansion terms, though in this case apparently no such choice arises.† The reader will easily verify that all the requirements have now been satisfied.

† Retention of a higher order term of expansion, ignoring one of lower order, will usually lead to a poorer approximation though still retaining convergence,² providing the linear terms are always included.

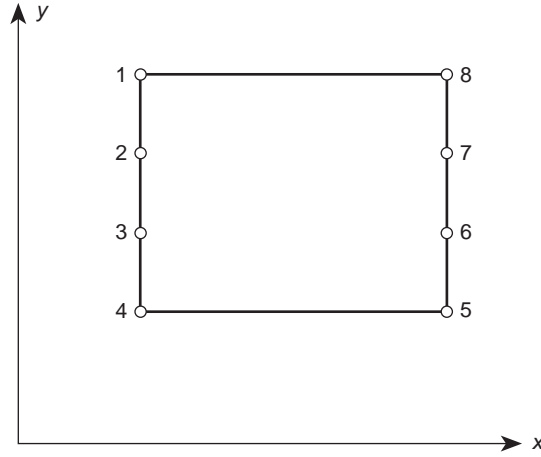


Fig. 8.2 A rectangular element.

Substituting coordinates of the various nodes a set of simultaneous equations will be obtained. This can be written in exactly the same manner as was done for a triangle in Eq. (4.4) as

$$\begin{Bmatrix} u_1 \\ \vdots \\ u_8 \end{Bmatrix} = \begin{bmatrix} 1 & x_1 & y_1 & x_1 y_1 & y_1^2 & x_1 y_1^2 & y_1^3 & x_1 y_1^3 \\ \cdot & \cdot & \cdot & \cdot & \cdot & \cdot & \cdot & \cdot \\ 1 & x_8 & y_8 & \cdot & \cdot & \cdot & \cdot & x_8 y_8^3 \end{bmatrix} \begin{Bmatrix} \alpha_1 \\ \vdots \\ \alpha_8 \end{Bmatrix} \quad (8.10)$$

or simply as

$$\mathbf{u}^e = \mathbf{C}\boldsymbol{\alpha} \quad (8.11)$$

Formally,

$$\boldsymbol{\alpha} = \mathbf{C}^{-1}\mathbf{u}^e \quad (8.12)$$

and we could write Eq. (8.9) as

$$u = \mathbf{P}\boldsymbol{\alpha} = \mathbf{P}\mathbf{C}^{-1}\mathbf{u}^e \quad (8.13)$$

in which

$$\mathbf{P} = [1, x, y, xy, y^2, xy^2, y^3, xy^3] \quad (8.14)$$

Thus the shape functions for the element defined by

$$u = \mathbf{N}\mathbf{u}^e = [N_1, N_2, \dots, N_8]\mathbf{u}^e \quad (8.15)$$

can be found as

$$\mathbf{N} = \mathbf{P}\mathbf{C}^{-1} \quad (8.16)$$

This process has, however, some considerable disadvantages. Occasionally an inverse of \mathbf{C} may not exist^{2,3} and *always* considerable algebraic difficulty is experienced in obtaining an expression for the inverse in general terms suitable for all element geometries. It is therefore worthwhile to consider whether shape functions $N_i(x, y)$ can be written down directly. Before doing this some general properties of these functions have to be mentioned.

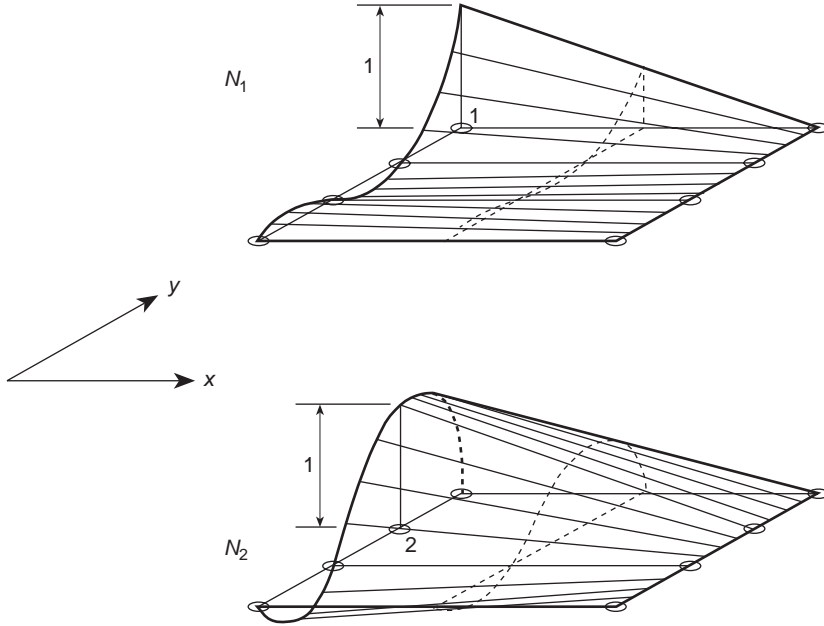


Fig. 8.3 Shape functions for elements of Fig. 8.2.

Inspection of the defining relation, Eq. (8.15), reveals immediately some important characteristics. Firstly, as this expression is valid for all components of \mathbf{u}^e ,

$$N_i(x_j, y_j) = \delta_{ij} = \begin{cases} 1; & i = j \\ 0; & i \neq j \end{cases}$$

where δ_{ij} is known as the Kronecker delta. Further, the basic type of variation along boundaries defined for continuity purposes (e.g., linear in x and cubic in y in the above example) must be retained. The typical form of the shape functions for the elements considered is illustrated isometrically for two typical nodes in Fig. 8.3. It is clear that these could have been written down directly as a product of a suitable linear function in x with a cubic function in y . The easy solution of this example is not always as obvious but given sufficient ingenuity, a direct derivation of shape functions is always preferable.

It will be convenient to use normalized coordinates in our further investigation. Such normalized coordinates are shown in Fig. 8.4 and are chosen so that their values are ± 1 on the faces of the rectangle:

$$\begin{aligned} \xi &= \frac{x - x_c}{a} & d\xi &= \frac{dx}{a} \\ \eta &= \frac{y - y_c}{b} & d\eta &= \frac{dy}{b} \end{aligned} \quad (8.17)$$

Once the shape functions are known in the normalized coordinates, translation into actual coordinates or transformation of the various expressions occurring, for instance, in the stiffness derivation is trivial.

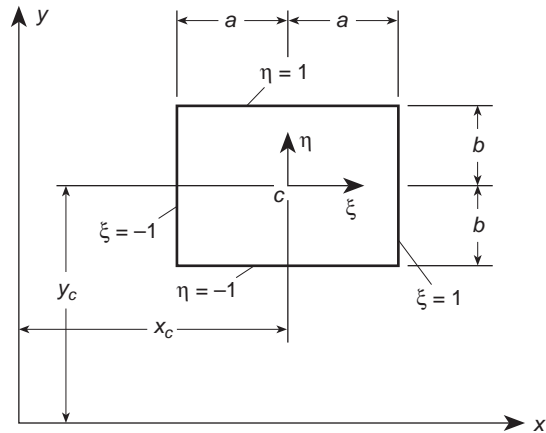


Fig. 8.4 Normalized coordinates for a rectangle.

8.4 Completeness of polynomials

The shape function derived in the previous section was of a rather special form [see Eq. (8.9)]. Only a linear variation with the coordinate x was permitted, while in y a full cubic was available. The complete polynomial contained in it was thus of order 1. In general use, a convergence order corresponding to a linear variation would occur despite an increase of the total number of variables. Only in situations where the linear variation in x corresponded closely to the exact solution would a higher order of convergence occur, and for this reason elements with such ‘preferential’ directions should be restricted to special use, e.g., in narrow beams or strips. In general, we shall seek element expansions which possess the highest order of a complete polynomial for a minimum of degrees of freedom. In this context it is useful to recall the Pascal triangle (Fig. 8.5) from which the number of terms

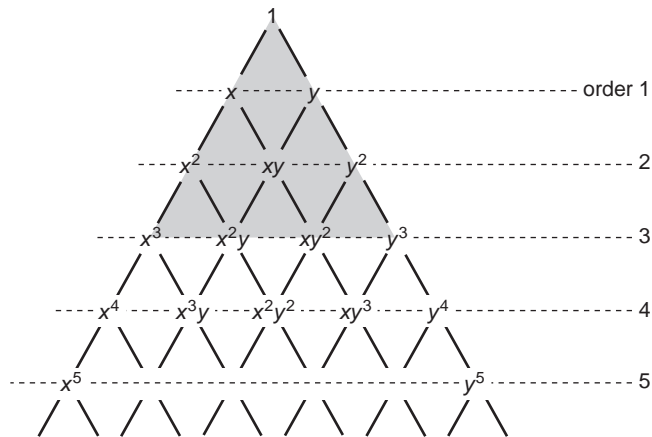


Fig. 8.5 The Pascal triangle. (Cubic expansion shaded – 10 terms).

occurring in a polynomial in two variables x, y can be readily ascertained. For instance, first-order polynomials require three terms, second-order require six terms, third-order require ten terms, etc.

8.5 Rectangular elements – Lagrange family^{4–6}

An easy and systematic method of generating shape functions of any order can be achieved by simple products of appropriate polynomials in the two coordinates. Consider the element shown in Fig. 8.6 in which a series of nodes, external and internal, is placed on a regular grid. It is required to determine a shape function for the point indicated by the heavy circle. Clearly the product of a fifth-order polynomial in ξ which has a value of unity at points of the second column of nodes and zero elsewhere and that of a fourth-order polynomial in η having unity on the coordinate corresponding to the top row of nodes and zero elsewhere satisfies all the interelement continuity conditions and gives unity at the nodal point concerned.

Polynomials in one coordinate having this property are known as Lagrange polynomials and can be written down directly as

$$l_k^n(\xi) = \frac{(\xi - \xi_0)(\xi - \xi_1) \cdots (\xi - \xi_{k-1})(\xi - \xi_{k+1}) \cdots (\xi - \xi_n)}{(\xi_k - \xi_0)(\xi_k - \xi_1) \cdots (\xi_k - \xi_{k-1})(\xi_k - \xi_{k+1}) \cdots (\xi_k - \xi_n)} \quad (8.18)$$

giving unity at ξ_k and passing through n points.

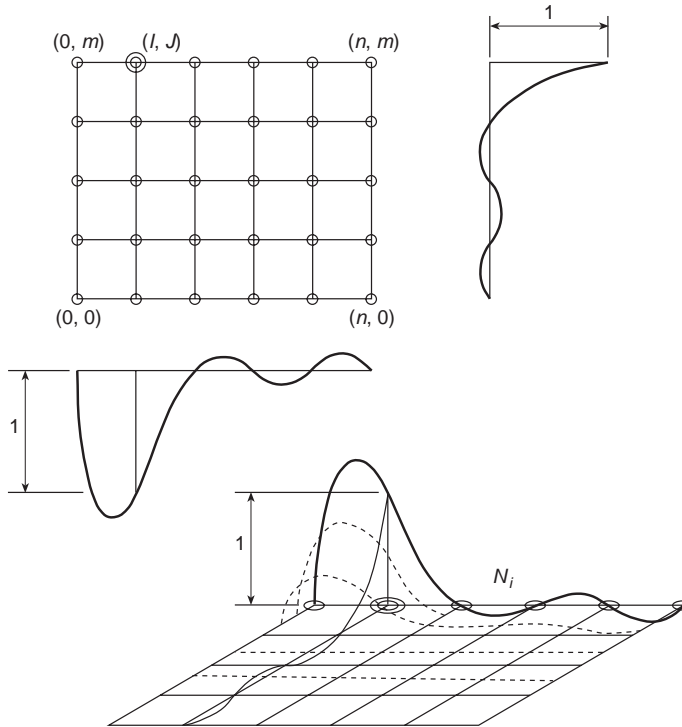


Fig. 8.6 A typical shape function for a Lagrangian element ($n = 5, m = 4, l = 1, J = 4$).

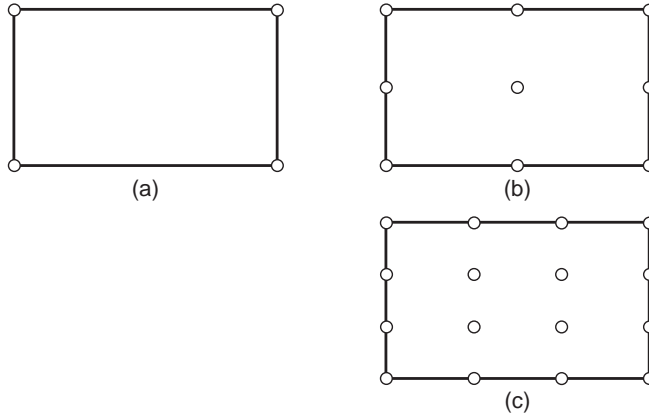


Fig. 8.7 Three elements of the Lagrange family: (a) linear, (b) quadratic, and (c) cubic.

Thus in two dimensions, if we label the node by its column and row number, I, J , we have

$$N_i \equiv N_{IJ} = l_I^n(\xi)l_J^m(\eta) \quad (8.19)$$

where n and m stand for the number of subdivisions in each direction.

Figure 8.7 shows a few members of this unlimited family where $m = n$.

Indeed, if we examine the polynomial terms present in a situation where $n = m$ we observe in Fig. 8.8, based on the Pascal triangle, that a large number of polynomial terms is present above those needed for a complete expansion.⁷ However, when mapping of shape functions is considered (Chapter 9) some advantages occur for this family.

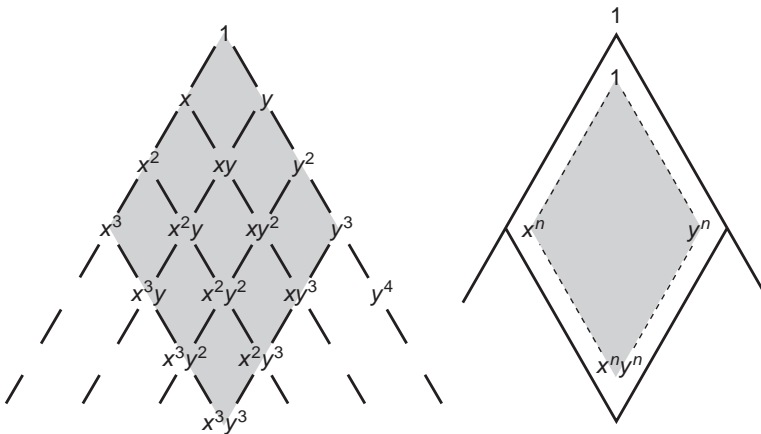


Fig. 8.8 Terms generated by a lagrangian expansion of order 3×3 (or $n \times n$). Complete polynomials of order 3 (or n).

8.6 Rectangular elements – 'serendipity' family^{4,5}

It is usually more efficient to make the functions dependent on nodal values placed on the element boundary. Consider, for instance, the first three elements of Fig. 8.9. In each a progressively increasing and equal number of nodes is placed on the element boundary. The variation of the function on the edges to ensure continuity is linear, parabolic, and cubic in increasing element order.

To achieve the shape function for the first element it is obvious that a product of linear lagrangian polynomials of the form

$$\frac{1}{4}(\xi + 1)(\eta + 1) \quad (8.20)$$

gives unity at the top right corners where $\xi = \eta = 1$ and zero at all the other corners. Further, a linear variation of the shape function of all sides exists and hence continuity is satisfied. Indeed this element is identical to the lagrangian one with $n = 1$.

Introducing new variables

$$\xi_0 = \xi\xi_i \quad \eta_0 = \eta\eta_i \quad (8.21)$$

in which ξ_i, η_i are the normalized coordinates at node i , the form

$$N_i = \frac{1}{4}(1 + \xi_0)(1 + \eta_0) \quad (8.22)$$

allows all shape functions to be written down in one expression.

As a linear combination of these shape functions yields any arbitrary linear variation of u , the second convergence criterion is satisfied.

The reader can verify that the following functions satisfy all the necessary criteria for quadratic and cubic members of the family.

'Quadratic' element

Corner nodes:

$$N_i = \frac{1}{4}(1 + \xi_0)(1 + \eta_0)(\xi_0 + \eta_0 - 1) \quad (8.23)$$

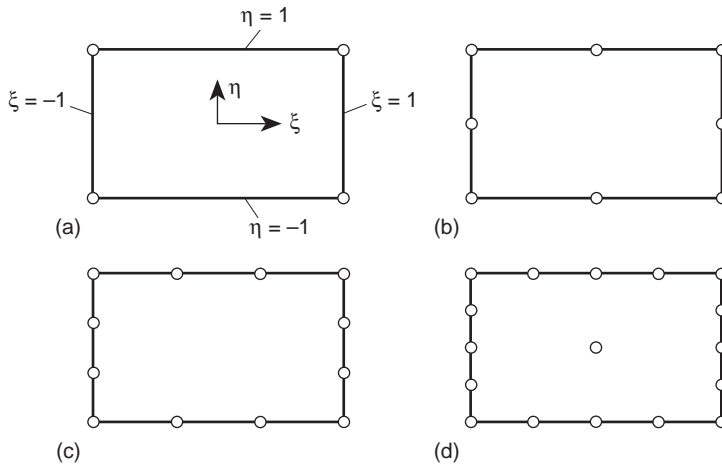


Fig. 8.9 Rectangles of boundary node (serendipity) family: (a) linear, (b) quadratic, (c) cubic, (d) quartic.

Mid-side nodes:

$$\xi_i = 0 \quad N_i = \frac{1}{2}(1 - \xi^2)(1 + \eta_0)$$

$$\eta_i = 0 \quad N_i = \frac{1}{2}(1 + \xi_0)(1 - \eta^2)$$

‘Cubic’ element

Corner nodes:

$$N_i = \frac{1}{32}(1 + \xi_0)(1 + \eta_0)[-10 + 9(\xi^2 + \eta^2)] \quad (8.24)$$

Mid-side nodes:

$$\xi_i = \pm 1 \quad \text{and} \quad \eta_i = \pm \frac{1}{3}$$

$$N_i = \frac{9}{32}(1 + \xi_0)(1 - \eta^2)(1 + 9\eta_0)$$

with the remaining mid-side node expression obtained by changing variables.

In the next, quartic, member⁸ of this family a central node is added so that all terms of a complete fourth-order expansion will be available. This central node adds a shape function $(1 - \xi^2)(1 - \eta^2)$ which is zero on all outer boundaries.

The above functions were originally derived by inspection, and progression to yet higher members is difficult and requires some ingenuity. It was therefore appropriate

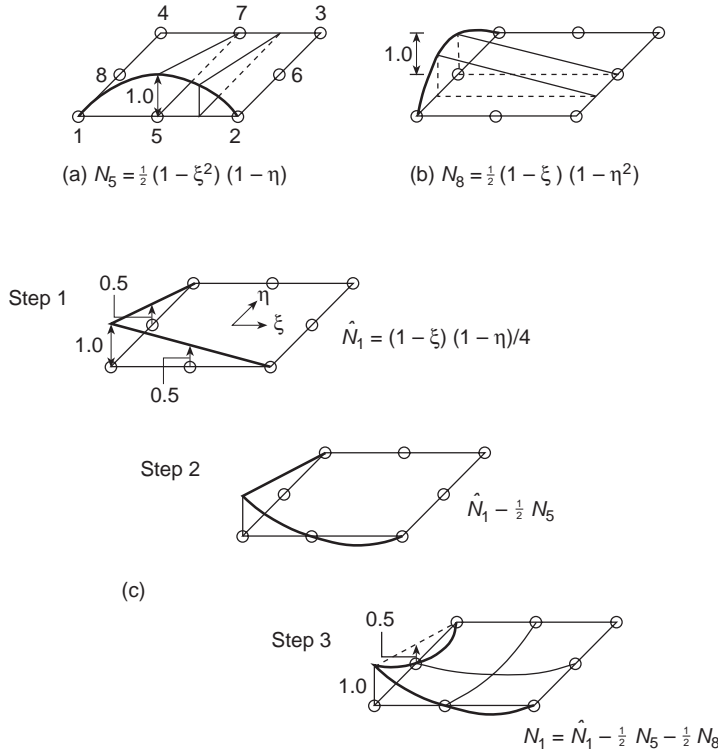


Fig. 8.10 Systematic generation of ‘serendipity’ shape functions.

to name this family 'serendipity' after the famous princes of Serendip noted for their chance discoveries (Horace Walpole, 1754).

However, a quite systematic way of generating the 'serendipity' shape functions can be devised, which becomes apparent from Fig. 8.10 where the generation of a quadratic shape function is presented.^{7,9}

As a starting point we observe that for *mid-side* nodes a lagrangian interpolation of a quadratic \times linear type suffices to determine N_i at nodes 5 to 8. N_5 and N_8 are shown at Fig. 8.10(a) and (b). For a *corner* node, such as Fig. 8.10(c), we start with a bilinear lagrangian family \hat{N}_1 and note immediately that while $\hat{N}_1 = 1$ at node 1, it is not zero at nodes 5 or 8 (step 1). Successive subtraction of $\frac{1}{2}N_5$ (step 2) and $\frac{1}{2}N_8$ (step 3) ensures that a zero value is obtained at these nodes. The reader can verify that the expressions obtained coincide with those of Eq. (8.23).

Indeed, it should now be obvious that for all higher order elements the *mid-side* and *corner shape* functions can be generated by an identical process. For the former a simple multiplication of *m*th-order and first-order lagrangian interpolations suffices. For the latter a combination of bilinear corner functions, together with appropriate fractions of mid-side shape functions to ensure zero at appropriate nodes, is necessary.

Similarly, it is quite easy to generate shape functions for elements with different numbers of nodes along each side by a systematic algorithm. This may be very

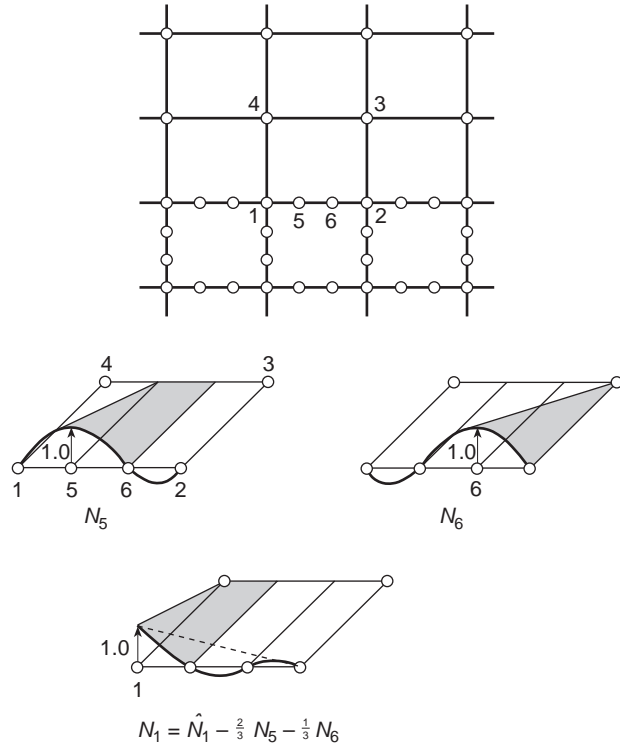


Fig. 8.11 Shape functions for a transition 'serendipity' element, cubic/linear.

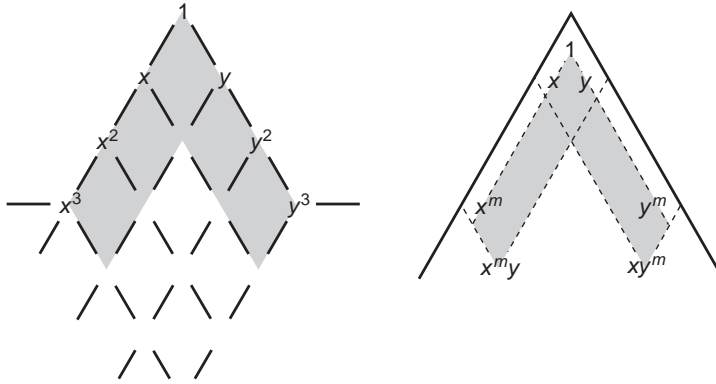


Fig. 8.12 Terms generated by edge shape functions in serendipity-type elements (3×3 and $m \times m$).

desirable if a transition between elements of different order is to be achieved, enabling a different order of accuracy in separate sections of a large problem to be studied. Figure 8.11 illustrates the necessary shape functions for a cubic/linear transition. Use of such special elements was first introduced in reference 9, but the simpler formulation used here is that of reference 7.

With the mode of generating shape functions for this class of elements available it is immediately obvious that fewer degrees of freedom are now necessary for a given complete polynomial expansion. Figure 8.12 shows this for a cubic element where only two surplus terms arise (as compared with six surplus terms in a lagrangian of the same degree).

It is immediately evident, however, that the functions generated by nodes placed only along the edges will not generate complete polynomials beyond cubic order. For higher order ones it is necessary to supplement the expansion by internal nodes (as was done in the quartic element of Fig. 8.9) or by the use of ‘nodeless’ variables which contain appropriate polynomial terms.

8.7 Elimination of internal variables before assembly – substructures

Internal nodes or nodeless internal parameters yield in the usual way the element properties (Chapter 2)

$$\frac{\partial \Pi^e}{\partial \mathbf{a}^e} = \mathbf{K}^e \mathbf{a}^e + \mathbf{f}^e \quad (8.25)$$

As \mathbf{a}^e can be subdivided into parts which are common with other elements, $\bar{\mathbf{a}}^e$, and others which occur in the particular element only, $\bar{\bar{\mathbf{a}}}^e$, we can immediately write

$$\frac{\partial \Pi}{\partial \bar{\bar{\mathbf{a}}}^e} = \frac{\partial \Pi^e}{\partial \bar{\bar{\mathbf{a}}}^e} = \mathbf{0}$$

and eliminate $\bar{\mathbf{a}}^e$ from further consideration. Writing Eq. (8.25) in a partitioned form we have

$$\frac{\partial \Pi^e}{\partial \mathbf{a}^e} = \left\{ \begin{array}{c} \frac{\partial \Pi^e}{\partial \bar{\mathbf{a}}^e} \\ \frac{\partial \Pi^e}{\partial \bar{\mathbf{a}}^e} \end{array} \right\} = \begin{bmatrix} \bar{\mathbf{K}}^e & \hat{\mathbf{K}}^e \\ \hat{\mathbf{K}}^{eT} & \bar{\mathbf{K}}^e \end{bmatrix} \left\{ \begin{array}{c} \bar{\mathbf{a}}^e \\ \bar{\mathbf{a}}^e \end{array} \right\} + \left\{ \begin{array}{c} \bar{\mathbf{f}}^e \\ \bar{\mathbf{f}}^e \end{array} \right\} = \left\{ \begin{array}{c} \frac{\partial \Pi^e}{\partial \mathbf{a}^e} \\ \mathbf{0} \end{array} \right\} \quad (8.26)$$

From the second set of equations given above we can write

$$\bar{\mathbf{a}}^e = -(\bar{\mathbf{K}}^e)^{-1}(\hat{\mathbf{K}}^{eT} \bar{\mathbf{a}}^e + \bar{\mathbf{f}}^e) \quad (8.27)$$

which on substitution yields

$$\frac{\partial \Pi^e}{\partial \mathbf{a}^e} = \mathbf{K}^{*e} \mathbf{a}^e + \mathbf{f}^{*e} \quad (8.28)$$

in which

$$\begin{aligned} \mathbf{K}^{*e} &= \bar{\mathbf{K}}^e - \hat{\mathbf{K}}^e (\bar{\mathbf{K}}^e)^{-1} \hat{\mathbf{K}}^{eT} \\ \mathbf{f}^{*e} &= \bar{\mathbf{f}}^e - \hat{\mathbf{K}}^e (\bar{\mathbf{K}}^e)^{-1} \bar{\mathbf{f}}^e \end{aligned} \quad (8.29)$$

Assembly of the total region then follows, by considering only the element boundary variables, thus giving a considerable saving in the equation-solving effort at the expense of a few additional manipulations carried out at the element stage.

Perhaps a structural interpretation of this elimination is desirable. What in fact is involved is the separation of a part of the structure from its surroundings and determination of its solution separately for any prescribed displacements at the inter-connecting boundaries. \mathbf{K}^{*e} is now simply the overall stiffness of the separated structure and \mathbf{f}^{*e} the equivalent set of nodal forces.

If the triangulation of Fig. 8.13 is interpreted as an assembly of pin-jointed bars the reader will recognize immediately the well-known device of 'substructures' used frequently in structural engineering.

Such a substructure is in fact simply a complex element from which the internal degrees of freedom have been eliminated.

Immediately a new possibility for devising more elaborate, and presumably more accurate, elements is presented.

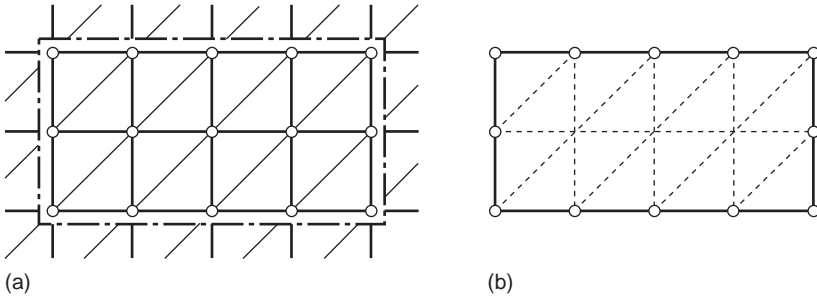


Fig. 8.13 Substructure of a complex element.

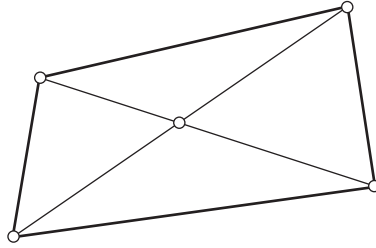


Fig. 8.14 A quadrilateral made up of four simple triangles.

Figure 8.13(a) can be interpreted as a continuum field subdivided into triangular elements. The substructure results in fact in one complex element shown in Fig. 8.13(b) with a number of boundary nodes.

The only difference from elements derived in previous sections is the fact that the unknown u is now not approximated internally by one set of smooth shape functions but by a series of piecewise approximations. This presumably results in a slightly poorer approximation but an economic advantage may arise if the total computation time for such an assembly is saved.

Substructuring is an important device in complex problems, particularly where a repetition of complicated components arises.

In simple, small-scale finite element analysis, much improved use of simple triangular elements was found by the use of simple subassemblies of the triangles (or indeed tetrahedra). For instance, a quadrilateral based on four triangles from which the central node is eliminated was found to give an economic advantage over direct use of simple triangles (Fig. 8.14). This and other subassemblies based on triangles are discussed in detail by Doherty *et al.*¹⁰

8.8 Triangular element family

The advantage of an arbitrary triangular shape in approximating to any boundary shape has been amply demonstrated in earlier chapters. Its apparent superiority here over rectangular shapes needs no further discussion. The question of generating more elaborate higher order elements needs to be further developed.

Consider a series of triangles generated on a pattern indicated in Fig. 8.15. The number of nodes in each member of the family is now such that a complete polynomial expansion, of the order needed for interelement compatibility, is ensured. This follows by comparison with the Pascal triangle of Fig. 8.5 in which we see the number of nodes coincides exactly with the number of polynomial terms required. This particular feature puts the triangle family in a special, privileged position, in which the inverse of the \mathbf{C} matrices of Eq. (8.11) will always exist.³ However, once again a direct generation of shape functions will be preferred – and indeed will be shown to be particularly easy.

Before proceeding further it is useful to define a special set of normalized co-ordinates for a triangle.

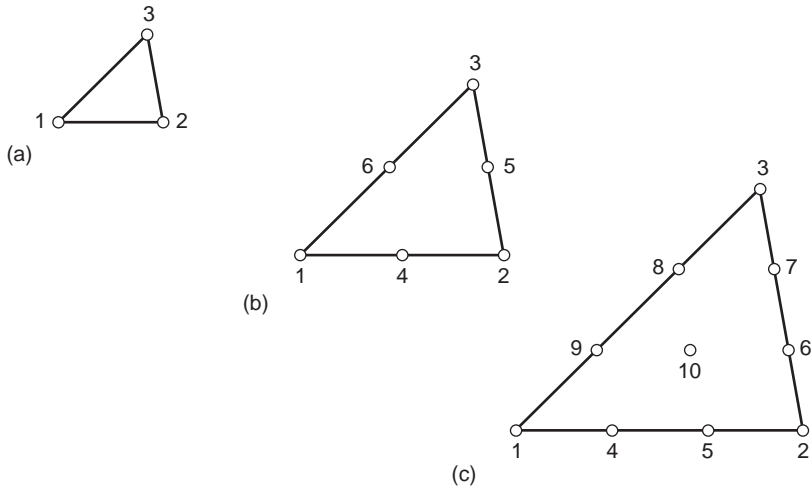


Fig. 8.15 Triangular element family: (a) linear, (b) quadratic, and (c) cubic.

8.8.1 Area coordinates

While cartesian directions parallel to the sides of a rectangle were a natural choice for that shape, in the triangle these are not convenient.

A new set of coordinates, L_1 , L_2 , and L_3 for a triangle 1, 2, 3 (Fig. 8.16), is defined by the following linear relation between these and the cartesian system:

$$\begin{aligned} x &= L_1 x_1 + L_2 x_2 + L_3 x_3 \\ y &= L_1 y_1 + L_2 y_2 + L_3 y_3 \\ 1 &= L_1 + L_2 + L_3 \end{aligned} \quad (8.30)$$

To every set, L_1 , L_2 , L_3 (which are not independent, but are related by the third equation), there corresponds a unique set of cartesian coordinates. At point 1, $L_1 = 1$ and $L_2 = L_3 = 0$, etc. A linear relation between the new and cartesian coordinates implies

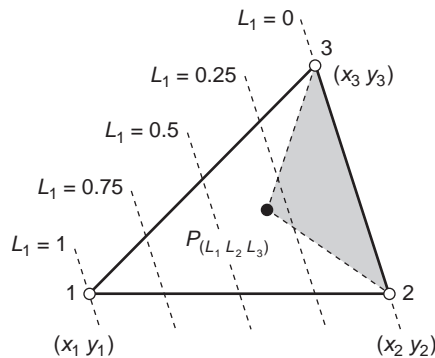


Fig. 8.16 Area coordinates.

that contours of L_1 are equally placed straight lines parallel to side 2–3 on which $L_1 = 0$, etc.

Indeed it is easy to see that an alternative definition of the coordinate L_1 of a point P is by a ratio of the area of the shaded triangle to that of the total triangle:

$$L_1 = \frac{\text{area } P23}{\text{area } 123} \quad (8.31)$$

Hence the name *area coordinates*.

Solving Eq. (8.30) gives

$$\begin{aligned} L_1 &= \frac{a_1 + b_1 x + c_1 y}{2\Delta} \\ L_2 &= \frac{a_2 + b_2 x + c_2 y}{2\Delta} \\ L_3 &= \frac{a_3 + b_3 x + c_3 y}{2\Delta} \end{aligned} \quad (8.32)$$

in which

$$\Delta = \frac{1}{2} \det \begin{vmatrix} 1 & x_1 & y_1 \\ 1 & x_2 & y_2 \\ 1 & x_3 & y_3 \end{vmatrix} = \text{area } 123 \quad (8.33)$$

and

$$a_1 = x_2 y_3 - x_3 y_2 \quad b_1 = y_2 - y_3 \quad c_1 = x_3 - x_2$$

etc., with cyclic rotation of indices 1, 2, and 3.

The identity of expressions with those derived in Chapter 4 [Eqs (4.5b) and (4.5c)] is worth noting.

8.8.2 Shape functions

For the first element of the series [Fig. 8.15(a)], the shape functions are simply the area coordinates. Thus

$$N_1 = L_1 \quad N_2 = L_2 \quad N_3 = L_3 \quad (8.34)$$

This is obvious as each individually gives unity at one node, zero at others, and varies linearly everywhere.

To derive shape functions for other elements a simple recurrence relation can be derived.³ However, it is very simple to write an arbitrary triangle of order M in a manner similar to that used for the lagrangian element of Sec. 8.5.

Denoting a typical node i by three numbers I , J , and K corresponding to the position of coordinates L_{1i} , L_{2i} , and L_{3i} we can write the shape function in terms of three lagrangian interpolations as [see Eq. (8.18)]

$$N_i = l_I^I(L_1) l_J^J(L_2) l_K^K(L_3) \quad (8.35)$$

In the above l_I^I , etc., are given by expression (8.18), with L_1 taking the place of ξ , etc.

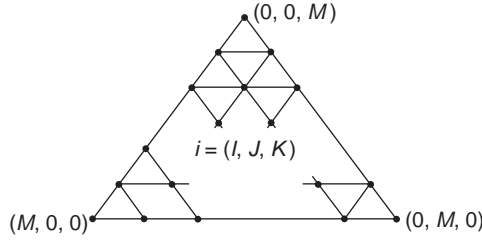


Fig. 8.17 A general triangular element.

It is easy to verify that the above expression gives

$$N_i = 1 \quad \text{at} \quad L_1 = L_{1I}, \quad L_2 = L_{2J}, \quad L_3 = L_{3K}$$

and zero at all other nodes.

The highest term occurring in the expansion is

$$L_1^I L_2^J L_3^K$$

and as

$$I + J + K \equiv M$$

for all points the polynomial is also of order M .

Expression (8.35) is valid for quite arbitrary distributions of nodes of the pattern given in Fig. 8.17 and simplifies if the spacing of the nodal lines is equal (i.e., $1/m$). The formula was first obtained by Argyris *et al.*¹¹ and formalized in a different manner by others.^{7,12}

The reader can verify the shape functions for the second- and third-order elements as given below and indeed derive ones of any higher order easily.

Quadratic triangle [Fig. 8.15(b)]

Corner nodes:

$$N_1 = (2L_1 - 1)L_1, \quad \text{etc.}$$

Mid-side nodes:

$$N_4 = 4L_1L_2, \quad \text{etc.}$$

Cubic triangle [Fig. 8.15(c)]

Corner nodes:

$$N_1 = \frac{1}{2}(3L_1 - 1)(3L_1 - 2)L_1, \quad \text{etc.} \quad (8.36)$$

Mid-side nodes:

$$N_4 = \frac{9}{2}L_1L_2(3L_1 - 1), \quad \text{etc.} \quad (8.37)$$

and for the internal node:

$$N_{10} = 27L_1L_2L_3$$

The last shape again is a ‘bubble’ function giving zero contribution along boundaries – and this will be found to be useful in many other contexts (see the mixed forms in Chapter 12).

The quadratic triangle was first derived by Veubeke¹³ and used later in the context of plane stress analysis by Argyris.¹⁴

When element matrices have to be evaluated it will follow that we are faced with integration of quantities defined in terms of area coordinates over the triangular region. It is useful to note in this context the following exact integration expression:

$$\iint_{\Delta} L_1^a L_2^b L_3^c dx dy = \frac{a! b! c!}{(a + b + c + 2)!} 2\Delta \quad (8.38)$$

One-dimensional elements

8.9 Line elements

So far in this book the continuum was considered generally in two or three dimensions. ‘One-dimensional’ members, being of a kind for which exact solutions are generally available, were treated only as trivial examples in Chapter 2 and in Sec. 8.2. In many practical two- or three-dimensional problems such elements do in fact appear in conjunction with the more usual continuum elements – and a unified treatment is desirable. In the context of elastic analysis these elements may represent lines of reinforcement (plane and three-dimensional problems) or sheets of thin lining material in axisymmetric bodies. In the context of field problems of the type discussed in Chapter 7 lines of drains in a porous medium of lesser conductivity can be envisaged.

Once the shape of such a function as displacement is chosen for an element of this kind, its properties can be determined, noting, however, that derived quantities such as strain, etc., have to be considered only in one dimension.

Figure 8.18 shows such an element sandwiched between two adjacent quadratic-type elements. Clearly for continuity of the function a quadratic variation of the

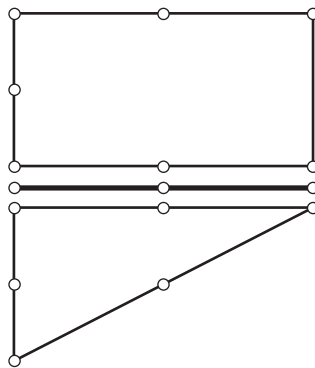


Fig. 8.18 A line element sandwiched between two-dimensional elements.

unknown with the one variable ξ is all that is required. Thus the shape functions are given directly by the Lagrange polynomial as defined in Eq. (8.18).

Three-dimensional elements

8.10 Rectangular prisms – Lagrange family

In a precisely analogous way to that given in previous sections equivalent elements of three-dimensional type can be described.

Now, for interelement continuity the simple rules given previously have to be modified. What is necessary to achieve is that along a whole face of an element the nodal values define a unique variation of the unknown function. With incomplete polynomials, this can be ensured only by inspection.

Shape function for such elements, illustrated in Fig. 8.19, will be generated by a direct product of three Lagrange polynomials. Extending the notation of Eq. (8.19) we now have

$$N_i \equiv N_{IJK} = l_I^n l_J^m l_K^p \quad (8.39)$$

for n , m , and p subdivisions along each side.

This element again is suggested by Zienkiewicz *et al.*⁵ and elaborated upon by Argyris *et al.*⁶ All the remarks about internal nodes and the properties of the formulation with mappings (to be described in the next chapter) are applicable here.

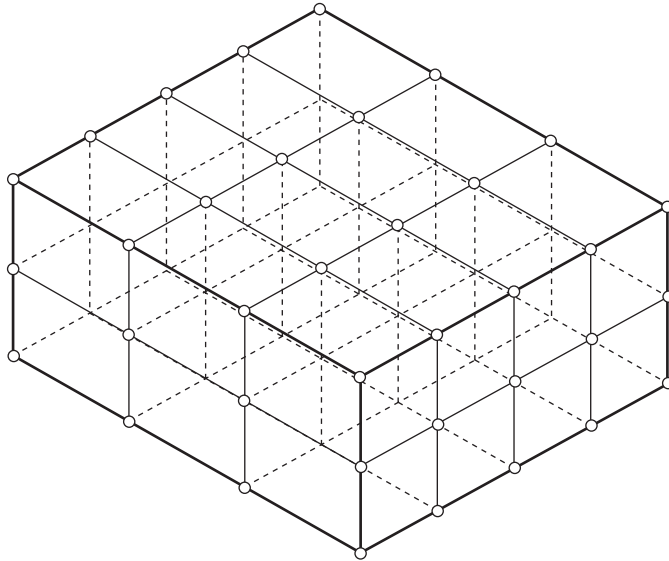


Fig. 8.19 Right prism of Lagrange family.

8.11 Rectangular prisms – ‘serendipity’ family^{4,9,15}

The family of elements shown in Fig. 8.20 is precisely equivalent to that of Fig. 8.9. Using now three normalized coordinates and otherwise following the terminology of Sec. 8.6 we have the following shape functions:

‘Linear’ element (8 nodes)

$$N_i = \frac{1}{8}(1 + \xi_0)(1 + \eta_0)(1 + \zeta_0) \quad (8.40)$$

which is identical with the linear lagrangian element.

‘Quadratic’ element (20 nodes)

Corner nodes:

$$N_i = \frac{1}{8}(1 + \xi_0)(1 + \eta_0)(1 + \zeta_0)(\xi_0 + \eta_0 + \zeta_0 - 2) \quad (8.41)$$

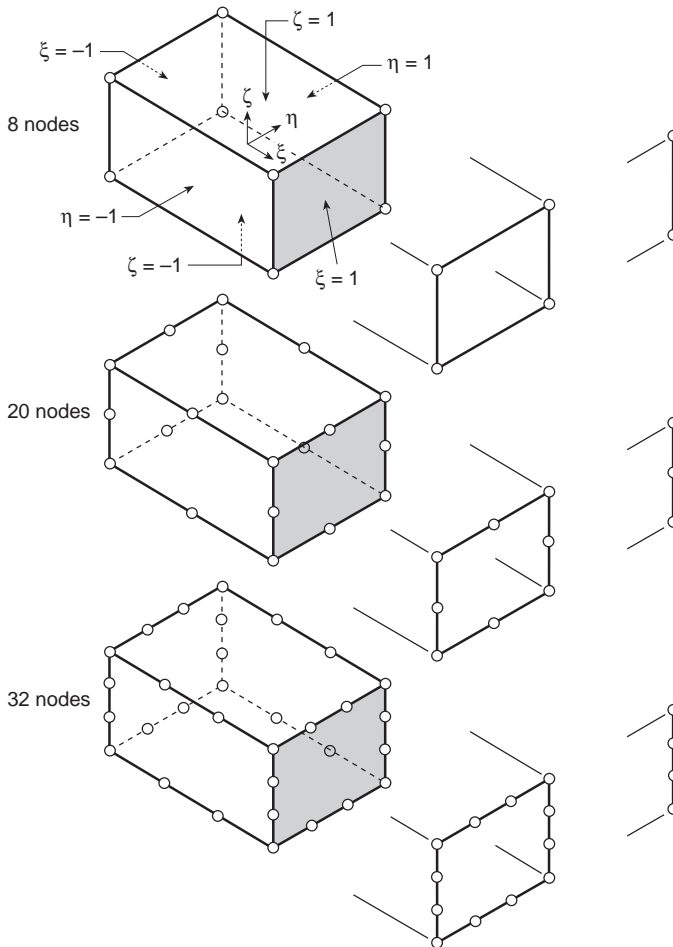


Fig. 8.20 Right prisms of boundary node (serendipity) family with corresponding sheet and line elements.

Typical mid-side node:

$$\begin{aligned}\xi_i &= 0 & \eta_i &= \pm 1 & \zeta_i &= \pm 1 \\ N_i &= \frac{1}{4}(1 - \xi^2)(1 + \eta_0)(1 + \zeta_0)\end{aligned}$$

'Cubic' elements (32 nodes)

Corner node:

$$N_i = \frac{1}{64}(1 + \xi_0)(1 + \eta_0)(1 + \zeta_0)[9(\xi^2 + \eta^2 + \zeta^2) - 19] \quad (8.42)$$

Typical mid-side node:

$$\begin{aligned}\xi_i &= \pm \frac{1}{3} & \eta_i &= \pm 1 & \zeta_i &= \pm 1 \\ N_i &= \frac{9}{64}(1 - \xi^2)(1 + 9\xi_0)(1 + \eta_0)(1 + \zeta_0)\end{aligned}$$

When $\zeta = 1 = \zeta_0$ the above expressions reduce to those of Eqs (8.22)–(8.24). Indeed such elements of three-dimensional type can be joined in a compatible manner to sheet or line elements of the appropriate type as shown in Fig. 8.20.

Once again the procedure for generating the shape functions follows that described in Figs 8.10 and 8.11 and once again elements with varying degrees of freedom along the edges can be derived following the same steps.

The equivalent of a Pascal triangle is now a tetrahedron and again we can observe the small number of surplus degrees of freedom – a situation of even greater magnitude than in two-dimensional analysis.

8.12 Tetrahedral elements

The tetrahedral family shown in Fig. 8.21 not surprisingly exhibits properties similar to those of the triangle family.

Firstly, once again complete polynomials in three coordinates are achieved at each stage. Secondly, as faces are divided in a manner identical with that of the previous triangles, the same order of polynomial in two coordinates in the plane of the face is achieved and element compatibility ensured. No surplus terms in the polynomial occur.

8.12.1 Volume coordinates

Once again special coordinates are introduced defined by (Fig. 8.22):

$$\begin{aligned}x &= L_1x_1 + L_2x_2 + L_3x_3 + L_4x_4 \\ y &= L_1y_1 + L_2y_2 + L_3y_3 + L_4y_4 \\ z &= L_1z_1 + L_2z_2 + L_3z_3 + L_4z_4 \\ 1 &= L_1 + L_2 + L_3 + L_4\end{aligned} \quad (8.43)$$

Solving Eq. (8.43) gives

$$L_1 = \frac{a_1 + b_1x + c_1y + d_1z}{6V} \quad \text{etc.}$$

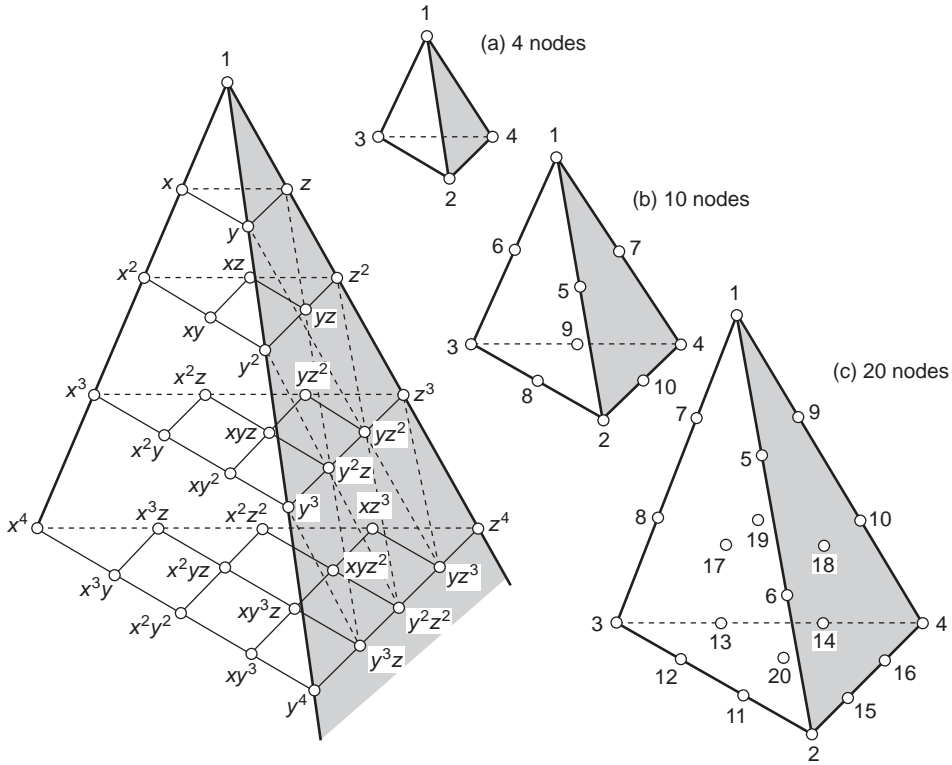


Fig. 8.21 The tetrahedron family: (a) linear, (b) quadratic, and (c) cubic.

where the constants can be identified from Chapter 6, Eq. (6.5). Again the physical nature of the coordinates can be identified as the ratio of volumes of tetrahedra based on an internal point P in the total volume, e.g., as shown in Fig. 8.22:

$$L_1 = \frac{\text{volume } P234}{\text{volume } 1234}, \quad \text{etc.} \quad (8.44)$$

8.12.2 Shape function

As the volume coordinates vary linearly with the cartesian ones from unity at one node to zero at the opposite face then shape functions for the linear element [Fig. 8.21(a)] are simply

$$N_1 = L_1 \quad N_2 = L_2, \quad \text{etc.} \quad (8.45)$$

Formulae for shape functions of higher order tetrahedra are derived in precisely the same manner as for the triangles by establishing appropriate Lagrange-type formulae similar to Eq. (8.35). Leaving this to the reader as a suitable exercise we quote the following:

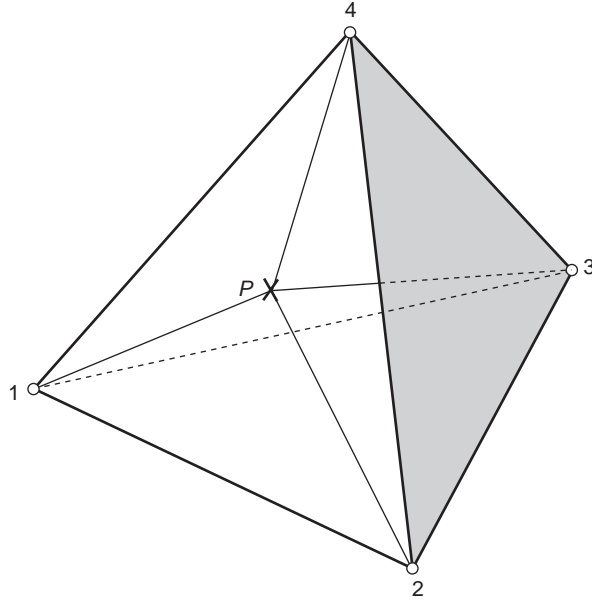


Fig. 8.22 Volume coordinates.

'Quadratic' tetrahedron [Fig. 8.21(b)]

For corner nodes:

$$N_1 = (2L_1 - 1)L_1, \quad \text{etc.} \quad (8.46)$$

For mid-edge nodes:

$$N_5 = 4L_1L_2, \quad \text{etc.}$$

'Cubic' tetrahedron

Corner nodes:

$$N_1 = \frac{1}{2}(3L_1 - 1)(3L_1 - 2)L_1, \quad \text{etc.} \quad (8.47)$$

Mid-edge nodes:

$$N_5 = \frac{9}{2}L_1L_2(3L_1 - 1), \quad \text{etc.}$$

Mid-face nodes:

$$N_{17} = 27L_1L_2L_3, \quad \text{etc.}$$

A useful integration formula may again be here quoted:

$$\iiint_{\text{vol}} L_1^a L_2^b L_3^c L_4^d dx dy dz = \frac{a! b! c! d!}{(a + b + c + d + 3)!} 6V \quad (8.48)$$

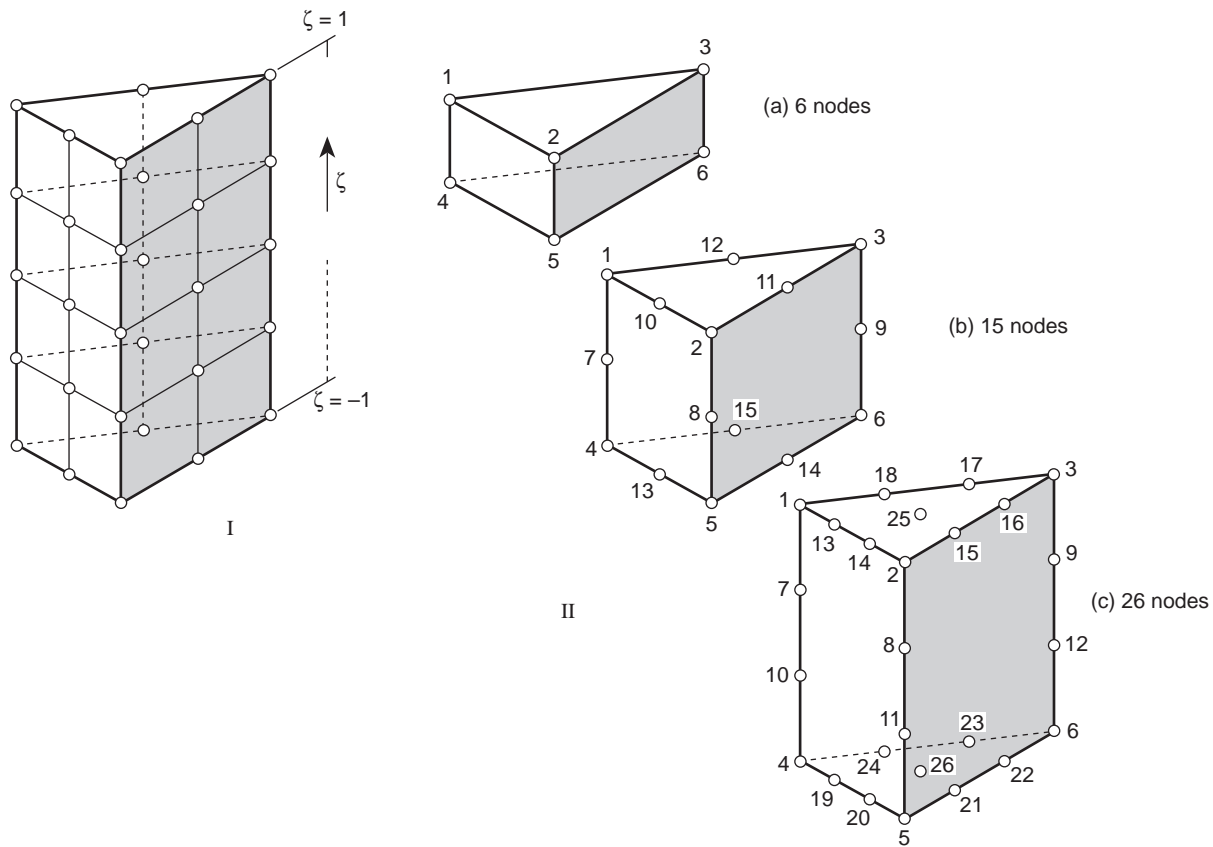


Fig. 8.23 Triangular prism elements (serendipity) family: (a) linear, (b) quadratic, and (c) cubic.

8.13 Other simple three-dimensional elements

The possibilities of simple shapes in three dimensions are greater, for obvious reasons, than in two dimensions. A quite useful series of elements can, for instance, be based on triangular prisms (Fig. 8.23). Here again variants of the product, Lagrange, approach or of the 'serendipity' type can be distinguished. The first element of both families is identical and indeed the shape functions for it are so obvious as not to need quoting.

For the 'quadratic' element illustrated in Fig. 8.23(b) the shape functions are

Corner nodes $L_1 = \zeta_1 = 1$:

$$N_1 = \frac{1}{2}L_1(2L_1 - 1)(1 + \zeta) - \frac{1}{2}L_1(1 - \zeta^2) \quad (8.49)$$

Mid-edge of triangles:

$$N_{10} = 2L_1L_2(1 + \zeta), \quad \text{etc.} \quad (8.50)$$

Mid-edge of rectangle:

$$N_7 = L_1(1 - \zeta^2), \quad \text{etc.}$$

Such elements are not purely esoteric but have a practical application as 'fillers' in conjunction with 20-noded serendipity elements.

Part 2 Hierarchical shape functions

8.14 Hierarchic polynomials in one dimension

The general ideas of hierarchic approximation were introduced in Sect. 8.2 in the context of simple, linear, elements. The idea of generating higher order hierarchic forms is again simple. We shall start from a one-dimensional expansion as this has been shown to provide a basis for the generation of two- and three-dimensional forms in previous sections.

To generate a polynomial of order p along an element side we do not need to introduce nodes but can instead use parameters without an obvious physical meaning. As shown in Fig. 8.24, we could use here a linear expansion specified by 'standard' functions N_0 and N_1 and add to this a series of polynomials always designed so as to have zero values at the ends of the range (i.e. points 0 and 1).

Thus for a quadratic approximation, we would write over the typical one-dimensional element, for instance,

$$\hat{u} = u_0N_0 + u_1N_1 + a_2N_2 \quad (8.51)$$

where

$$N_0 = -\frac{\xi - 1}{2} \quad N_1 = \frac{\xi + 1}{2} \quad N_2 = -(\xi - 1)(\xi + 1) \quad (8.52)$$

using in the above the normalized x -coordinate [viz. Eq. (8.17)].

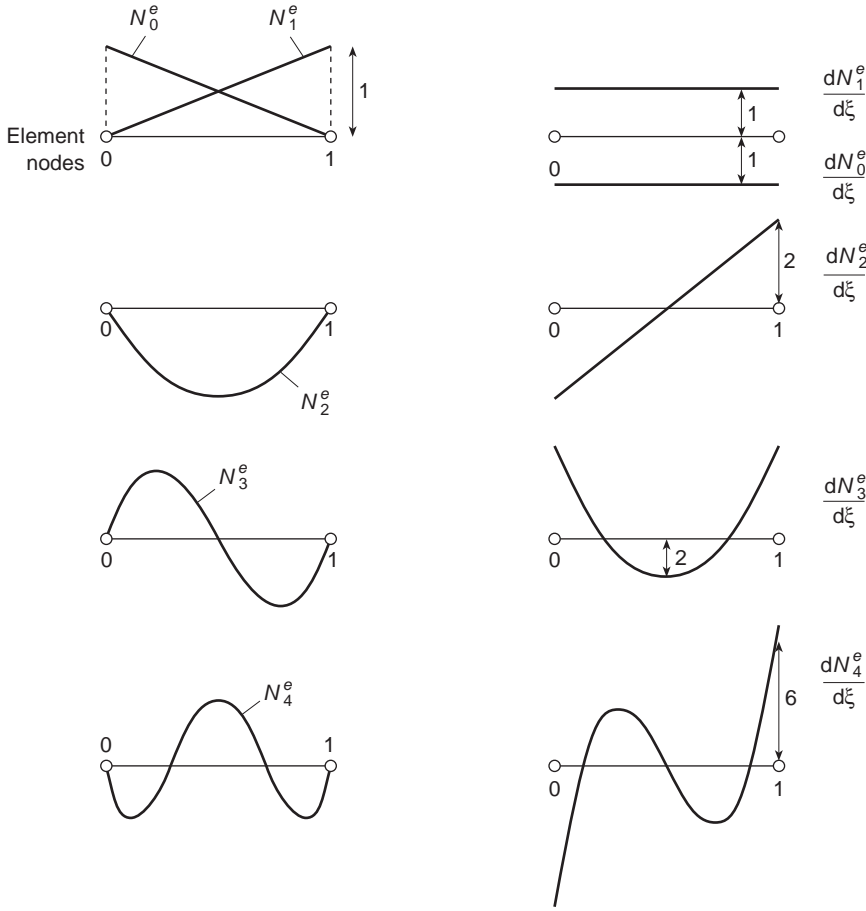


Fig. 8.24 Hierarchical element shape functions of nearly orthogonal form and their derivatives.

We note that the parameter a_2 does in fact have a meaning in this case as it is the magnitude of the departure from linearity of the approximation \hat{u} at the element centre, since N_2 has been chosen here to have the value of unity at that point.

In a similar manner, for a cubic element we simply have to add $a_3 N_3$ to the quadratic expansion of Eq. (8.51), where N_3 is any cubic of the form

$$N_3^e = \alpha_0 + \alpha_1 \xi + \alpha_2 \xi^2 + \alpha_3 \xi^3 \quad (8.53)$$

and which has zero values at $\xi = \pm 1$ (i.e., at nodes 0 and 1). Again an infinity of choices exists, and we could select a cubic of a simple form which has a zero value at the centre of the element and for which $dN_3/d\xi = 1$ at the same point. Immediately we can write

$$N_3^e = \xi(1 - \xi^2) \quad (8.54)$$

as the cubic function with the desired properties. Now the parameter a_3 denotes the departure of the slope at the centre of the element from that of the first approximation.

We note that we could proceed in a similar manner and define the fourth-order hierarchical element shape function as

$$N_4^e = \xi^2(1 - \xi^2) \quad (8.55)$$

but a physical identification of the parameter associated with this now becomes more difficult (even though it is not strictly necessary).

As we have already noted, the above set is not unique and many other possibilities exist. An alternative convenient form for the hierarchical functions is defined by

$$N_p^e(\xi) = \begin{cases} \frac{1}{p!}(\xi^p - 1) & p \text{ even} \\ \frac{1}{p!}(\xi^p - \xi) & p \text{ odd} \end{cases} \quad (8.56)$$

where p (≥ 2) is the degree of the introduced polynomial.¹⁶ This yields the set of shape functions:

$$\begin{aligned} N_2^e &= \frac{1}{2}(\xi^2 - 1) & N_3^e &= \frac{1}{6}(\xi^3 - \xi) \\ N_4^e &= \frac{1}{24}(\xi^4 - 1) & N_5^e &= \frac{1}{120}(\xi^5 - \xi) \quad \text{etc.} \end{aligned} \quad (8.57)$$

We observe that all derivatives of N_p^e of second or higher order have the value zero at $\xi = 0$, apart from $d^p N_p^e / d\xi^p$, which equals unity at that point, and hence, when shape functions of the form given by Eq. (8.57) are used, we can identify the parameters in the approximation as

$$a_p^e = \left. \frac{d^p u}{d\xi^p} \right|_{\xi=0} \quad p \geq 2 \quad (8.58)$$

This identification gives a general physical significance but is by no means necessary.

In two- and three-dimensional elements a simple identification of the hierarchic parameters on interfaces will automatically ensure C_0 continuity of the approximation.

As mentioned previously, an optimal form of hierarchical function is one that results in a diagonal equation system. This can on occasion be achieved, or at least approximated, quite closely.

In the elasticity problems which we have discussed in the preceding chapters the element matrix \mathbf{K}^e possesses terms of the form [using Eq. (8.17)]

$$K_{lm}^e = \int_{\Omega^e} k \frac{dN_l^e}{dx} \frac{dN_m^e}{dx} dx = \frac{1}{a} \int_{-1}^1 k \frac{dN_l^e}{d\xi} \frac{dN_m^e}{d\xi} d\xi \quad (8.59)$$

If shape function sets containing the appropriate polynomials can be found for which such integrals are zero for $l \neq m$, then orthogonality is achieved and the coupling between successive solutions disappears.

One set of polynomial functions which is known to possess this orthogonality property over the range $-1 \leq \xi \leq 1$ is the set of Legendre polynomials $P_p(\xi)$, and the shape functions could be defined in terms of integrals of these polynomials.⁹ Here we define the Legendre polynomial of degree p by

$$P_p(\xi) = \frac{1}{(p-1)!} \frac{1}{2^{p-1}} \frac{d^p}{d\xi^p} [(\xi^2 - 1)^p] \quad (8.60)$$

and integrate these polynomials to define

$$N_{p+1}^e = \int P_p(\xi) d\xi = \frac{1}{(p-1)! 2^{p-1}} \frac{d^{p-1}}{d\xi^{p-1}} [(\xi^2 - 1)^p] \quad (8.61)$$

Evaluation for each p in turn gives

$$N_2^e = \xi^2 - 1 \quad N_3^e = 2(\xi^3 - \xi) \quad \text{etc.}$$

These differ from the element shape functions given by Eq. (8.57) only by a multiplying constant up to N_3^e , but for $p \geq 3$ the differences become significant. The reader can easily verify the orthogonality of the derivatives of these functions, which is useful in computation. A plot of these functions and their derivatives is given in Fig. 8.24.

8.15 Two- and three-dimensional, hierarchic, elements of the 'rectangle' or 'brick' type

In deriving 'standard' finite element approximations we have shown that all shape functions for the Lagrange family could be obtained by a simple multiplication of one-dimensional ones and those for serendipity elements by a combination of such multiplications. The situation is even simpler for hierarchic elements. Here *all* the shape functions can be obtained by a simple multiplication process.

Thus, for instance, in Fig. 8.25 we show the shape functions for a lagrangian nine-noded element and the corresponding hierarchical functions. The latter not only have simpler shapes but are more easily calculated, being simple products of linear and quadratic terms of Eq. (8.56), (8.57), or (8.61). Using the last of these the three functions illustrated are simply

$$\begin{aligned} N_1 &= (1 - \xi)(1 + \eta)/4 \\ N_2 &= (1 - \xi)(1 - \eta^2)/2 \\ N_3 &= (1 - \xi^2)(1 - \eta^2) \end{aligned} \quad (8.62)$$

The distinction between lagrangian and serendipity forms now disappears as for the latter in the present case the last shape function (N_3) is simply omitted.

Indeed, it is now easy to introduce interpolation for elements of the type illustrated in Fig. 8.11 in which a different expansion is used along different sides. This essential characteristic of hierarchical elements is exploited in adaptive refinement (viz. Chapter 15) where new degrees of freedom (or polynomial order increase) is made only when required by the magnitude of the error.

8.16 Triangle and tetrahedron family^{16,17}

Once again the concepts of multiplication can be introduced in terms of area (volume) coordinates.

Returning to the triangle of Fig. 8.16 we note that along the side 1-2, L_3 is identically zero, and therefore we have

$$(L_1 + L_2)_{1-2} = 1 \quad (8.63)$$

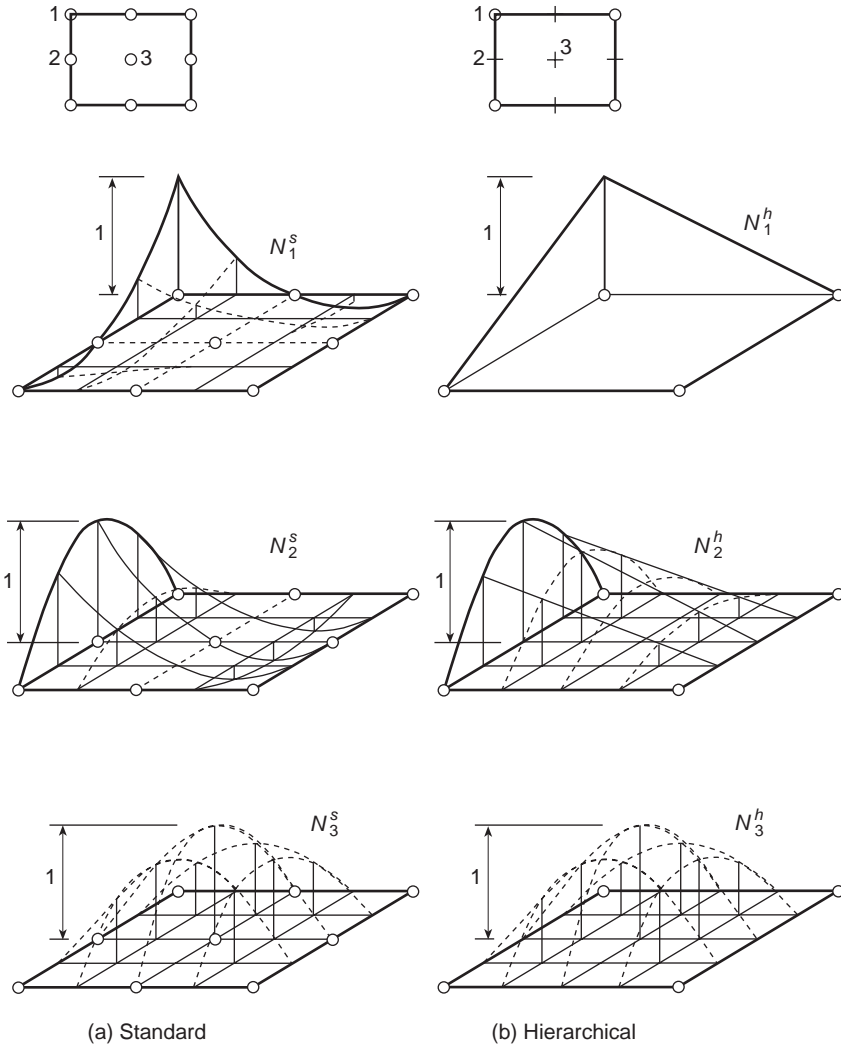


Fig. 8.25 Standard and hierarchic shape functions corresponding to a lagrangian, quadratic element.

If ξ , measured along side 1–2, is the usual non-dimensional local element coordinate of the type we have used in deriving hierarchical functions for one-dimensional elements, we can write

$$L_1|_{1-2} = \frac{1}{2}(1 - \xi) \quad L_2|_{1-2} = \frac{1}{2}(1 + \xi) \quad (8.64)$$

from which it follows that we have

$$\xi = (L_2 - L_1)|_{1-2} \quad (8.65)$$

This suggests that we could generate hierarchical shape functions over the triangle by generalizing the one-dimensional shape function forms produced earlier. For

example, using the expressions of Eq. (8.56), we associate with the side 1–2 the polynomial of degree p (≥ 2) defined by

$$N_{p(1-2)}^e = \begin{cases} \frac{1}{p!} [(L_2 - L_1)^p - (L_1 + L_2)^p] & p \text{ even} \\ \frac{1}{p!} [(L_2 - L_1)^p - (L_2 - L_1)(L_1 + L_2)^{p-1}] & p \text{ odd} \end{cases} \quad (8.66)$$

It follows from Eq. (8.64) that these shape functions are zero at nodes 1 and 2. In addition, it can easily be shown that $N_{p(1-2)}^e$ will be zero all along the sides 3–1 and 3–2 of the triangle, and so C_0 continuity of the approximation \hat{u} is assured.

It should be noted that in this case for $p \geq 3$ the number of hierarchical functions arising from the element sides in this manner is insufficient to define a complete polynomial of degree p , and internal hierarchical functions, which are identically zero on the boundaries, need to be introduced; for example, for $p = 3$ the function $L_1 L_2 L_3$ could be used, while for $p = 4$ the three additional functions $L_1^2 L_2 L_3$, $L_1 L_2^2 L_3$, $L_1 L_2 L_3^2$ could be adopted.

In Fig. 8.26 typical hierarchical linear, quadratic, and cubic trial functions for a triangular element are shown. Similar hierarchical shape functions could be generated

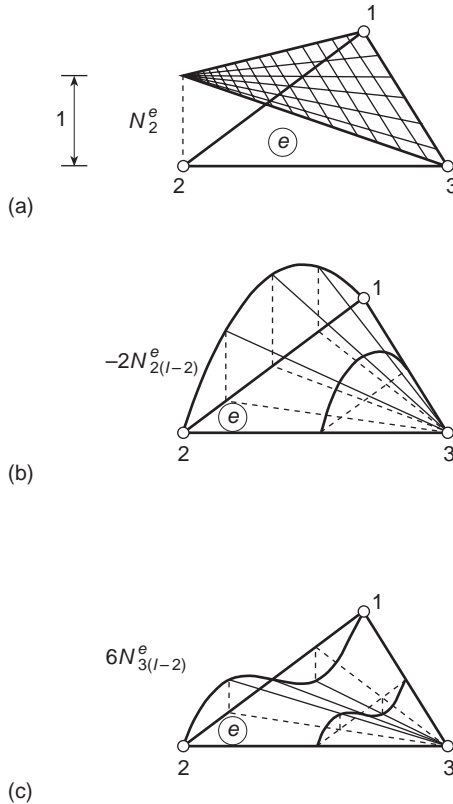


Fig. 8.26 Triangular elements and associated hierarchical shape functions of (a) linear, (b) quadratic, and (c) cubic form.

from the alternative set of one-dimensional shape functions defined in Eq. (8.61). Identical procedures are obvious in the context of tetrahedra.

8.17 Global and local finite element approximation

The very concept of hierarchic approximations (in which the shape functions are not affected by the refinement) means that it is possible to include in the expansion

$$u = \sum_{i=1}^n N_i a_i \quad (8.67)$$

functions N which are not local in nature. Such functions may, for instance, be the exact solutions of an analytical problem which in some way resembles the problem dealt with, but do not satisfy some boundary or inhomogeneity conditions. The 'finite element', local, expansions would here be a device for correcting this solution to satisfy the real conditions. This use of the global–local approximation was first suggested by Mote¹⁸ in a problem where the coefficients of this function were fixed. The example involved here is that of a rotating disc with cutouts (Fig. 8.27). The global, known, solution is the analytical one corresponding to a disc without cutout, and finite elements are added locally to modify the solution. Other examples of such 'fixed' solutions may well be those associated with point loads, where the use of the global approximation serves to eliminate the singularity modelled badly by the discretization.

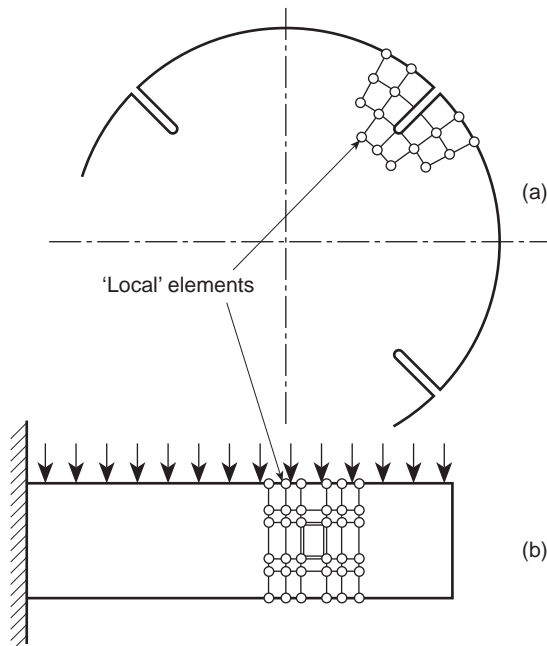


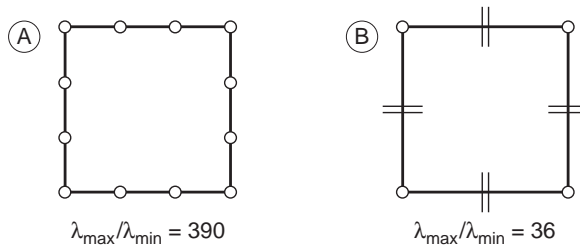
Fig. 8.27 Some possible uses of the local–global approximation: (a) rotating slotted disc, (b) perforated beam.

In some problems the singularity itself is unknown and the appropriate function can be added with an unknown coefficient.

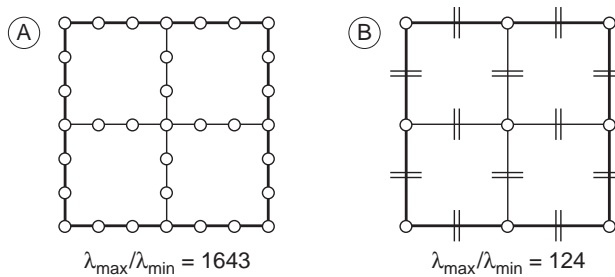
8.18 Improvement of conditioning with hierarchic forms

We have already mentioned that hierarchic element forms give a much improved equation conditioning for steady-state (static) problems due to their form which is more nearly diagonal. In Fig. 8.28 we show the ‘condition number’ (which is a measure of such diagonality and is defined in standard texts on linear algebra; see Appendix A) for a single cubic element and for an assembly of four cubic elements, using standard and hierarchic forms in their formulation. The improvement of the conditioning is a distinct advantage of such forms and allows the use of iterative solution techniques to be more easily adopted.¹⁹ Unfortunately much of this advantage disappears for transient analysis as the approximation must contain specific modes (see Chapter 17).

Single element (Reduction of condition number = 10.7)



Four element assembly (Reduction of condition number = 13.2)



Cubic order elements

- (A) Standard shape function
- (B) Hierarchic shape function

Fig. 8.28 Improvement of condition number (ratio of maximum to minimum eigenvalue of the stiffness matrix) by use of a hierarchic form (elasticity isotropic $\nu = 0.15$).

8.19 Concluding remarks

An unlimited selection of element types has been presented here to the reader – and indeed equally unlimited alternative possibilities exist.^{4,9} What of the use of such complex elements in practice? The triangular and tetrahedral elements are limited to situations where the real region is of a suitable shape which can be represented as an assembly of flat facets and all other elements are limited to situations represented by an assembly of right prisms. Such a limitation would be so severe that little practical purpose would have been served by the derivation of such shape functions unless some way could be found of distorting these elements to fit realistic curved boundaries. In fact, methods for doing this are available and will be described in the next chapter.

References

1. W. Rudin. *Principles of Mathematical Analysis*. 3rd ed, McGraw-Hill, 1976.
2. P.C. Dunne. Complete polynomial displacement fields for finite element methods. *Trans. Roy. Aero. Soc.* **72**, 245, 1968.
3. B.M. Irons, J.G. Ergatoudis, and O.C. Zienkiewicz. Comment on ref. 1. *Trans. Roy. Aero. Soc.* **72**, 709–11, 1968.
4. J.G. Ergatoudis, B.M. Irons, and O.C. Zienkiewicz. Curved, isoparametric, quadrilateral elements for finite element analysis. *Int. J. Solids Struct.* **4**, 31–42, 1968.
5. O.C. Zienkiewicz *et al.* Iso-parametric and associated elements families for two and three dimensional analysis. Chapter 13 of *Finite Element Methods in Stress Analysis* (eds I. Holand and K. Bell), Tech. Univ. of Norway, Tapir Press, Norway, Trondheim, 1969.
6. J.H. Argyris, K.E. Buck, H.M. Hilber, G. Mareczek, and D.W. Scharpf. Some new elements for matrix displacement methods. *2nd Conf. on Matrix Methods in Struct. Mech.* Air Force Inst. of Techn., Wright Patterson Base, Ohio, Oct. 1968.
7. R.L. Taylor. On completeness of shape functions for finite element analysis. *Int. J. Num. Meth. Eng.* **4**, 17–22, 1972.
8. F.C. Scott. A quartic, two dimensional isoparametric element. Undergraduate Project, Univ. of Wales, Swansea, 1968.
9. O.C. Zienkiewicz, B.M. Irons, J. Campbell, and F.C. Scott. Three dimensional stress analysis. *Int. Un. Th. Appl. Mech. Symposium on High Speed Computing in Elasticity*. Liège, 1970.
10. W.P. Doherty, E.L. Wilson, and R.L. Taylor. *Stress Analysis of Axisymmetric Solids Utilizing Higher-Order Quadrilateral Finite Elements*. Report 69–3, Structural Engineering Laboratory, Univ. of California, Berkeley, Jan. 1969.
11. J.H. Argyris, I. Fried, and D.W. Scharpf. The TET 20 and the TEA 8 elements for the matrix displacement method. *Aero. J.* **72**, 618–25, 1968.
12. P. Silvester. Higher order polynomial triangular finite elements for potential problems. *Int. J. Eng. Sci.* **7**, 849–61, 1969.
13. B. Fraeijs de Veubeke. Displacement and equilibrium models in the finite element method. Chapter 9 of *Stress Analysis* (eds O.C. Zienkiewicz and G.S. Holister), Wiley, 1965.
14. J.H. Argyris. Triangular elements with linearly varying strain for the matrix displacement method. *J. Roy. Aero. Soc. Tech. Note.* **69**, 711–13, Oct. 1965.

15. J.G. Ergatoudis, B.M. Irons, and O.C. Zienkiewicz. Three dimensional analysis of arch dams and their foundations. *Symposium on Arch Dams*. Inst. Civ. Eng., London, 1968.
16. A.G. Peano. Hierarchics of conforming finite elements for elasticity and plate bending. *Comp. Math. and Applications*. **2**, 3–4, 1976.
17. J.P. de S.R. Gago. *A posteri error analysis and adaptivity for the finite element method*. Ph.D thesis, University of Wales, Swansea, 1982.
18. C.D. Mote, Global–local finite element. *Int. J. Num. Meth. Eng.* **3**, 565–74, 1971.
19. O.C. Zienkiewicz, J.P. de S.R. Gago, and D.W. Kelly. The hierarchical concept in finite element analysis. *Computers and Structures*. **16**, 53–65, 1983.

Mapped elements and numerical integration – ‘infinite’ and ‘singularity’ elements

9.1 Introduction

In the previous chapter we have shown how some general families of finite elements can be obtained for C_0 interpolations. A progressively increasing number of nodes and hence improved accuracy characterizes each new member of the family and presumably the number of such elements required to obtain an adequate solution decreases rapidly. To ensure that a small number of elements can represent a relatively complex form of the type that is liable to occur in real, rather than academic, problems, simple rectangles and triangles no longer suffice. This chapter is therefore concerned with the subject of distorting such simple forms into others of more arbitrary shape.

Elements of the basic one-, two-, or three-dimensional types will be ‘mapped’ into distorted forms in the manner indicated in Figs 9.1 and 9.2.

In these figures it is shown that the ξ, η, ζ , or $L_1 L_2 L_3 L_4$ coordinates can be distorted to a new, curvilinear set when plotted in cartesian x, y, z space.

Not only can two-dimensional elements be distorted into others in two dimensions but the mapping of these can be taken into three dimensions as indicated by the flat sheet elements of Fig. 9.2 distorting into a three-dimensional space. This principle applies generally, providing a one-to-one correspondence between cartesian and curvilinear coordinates can be established, i.e., once the mapping relations of the type

$$\begin{Bmatrix} x \\ y \\ z \end{Bmatrix} = \begin{Bmatrix} f_x(\xi, \eta, \zeta) \\ f_y(\xi, \eta, \zeta) \\ f_z(\xi, \eta, \zeta) \end{Bmatrix} \quad \text{or} \quad \begin{Bmatrix} f_x(L_1, L_2, L_3, L_4) \\ f_y(L_1, L_2, L_3, L_4) \\ f_z(L_1, L_2, L_3, L_4) \end{Bmatrix} \quad (9.1)$$

can be established.

Once such coordinate relationships are known, shape functions can be specified in local coordinates and by suitable transformations the element properties established in the global coordinate system.

In what follows we shall first discuss the so-called isoparametric form of relationship (9.1) which has found a great deal of practical application. Full details of this formulation will be given, including the establishment of element matrices by numerical integration.

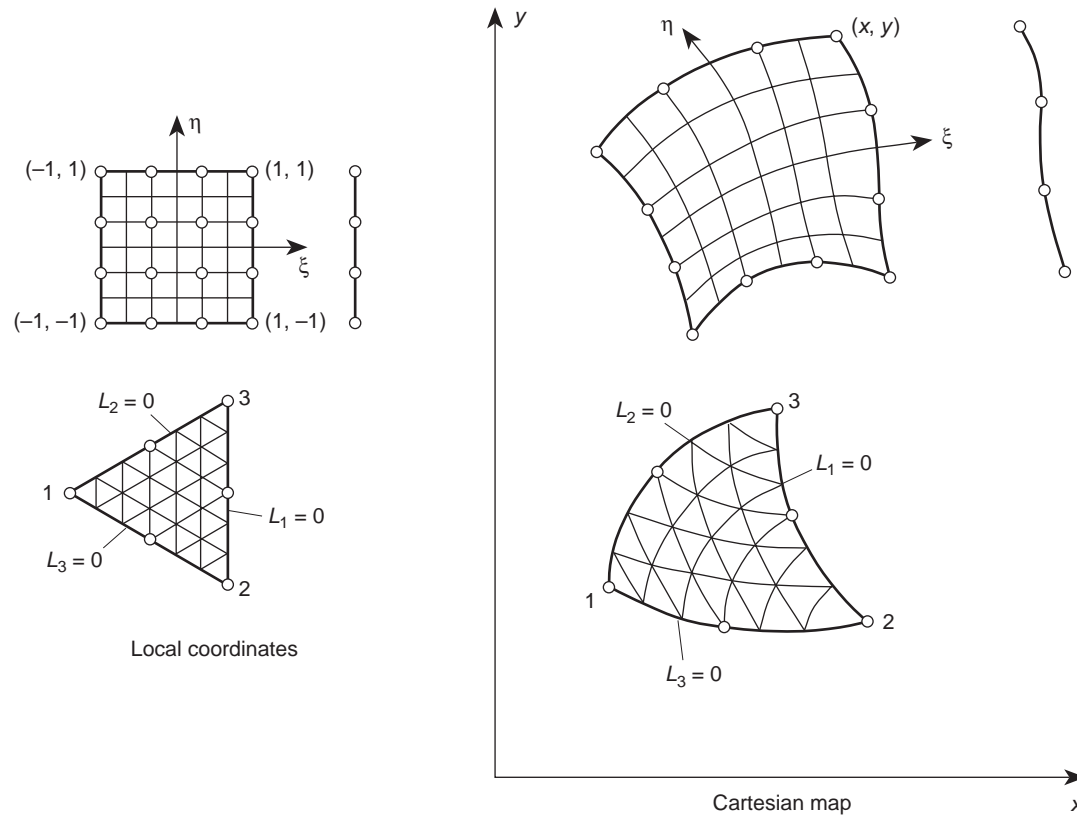


Fig. 9.1 Two-dimensional 'mapping' of some elements.

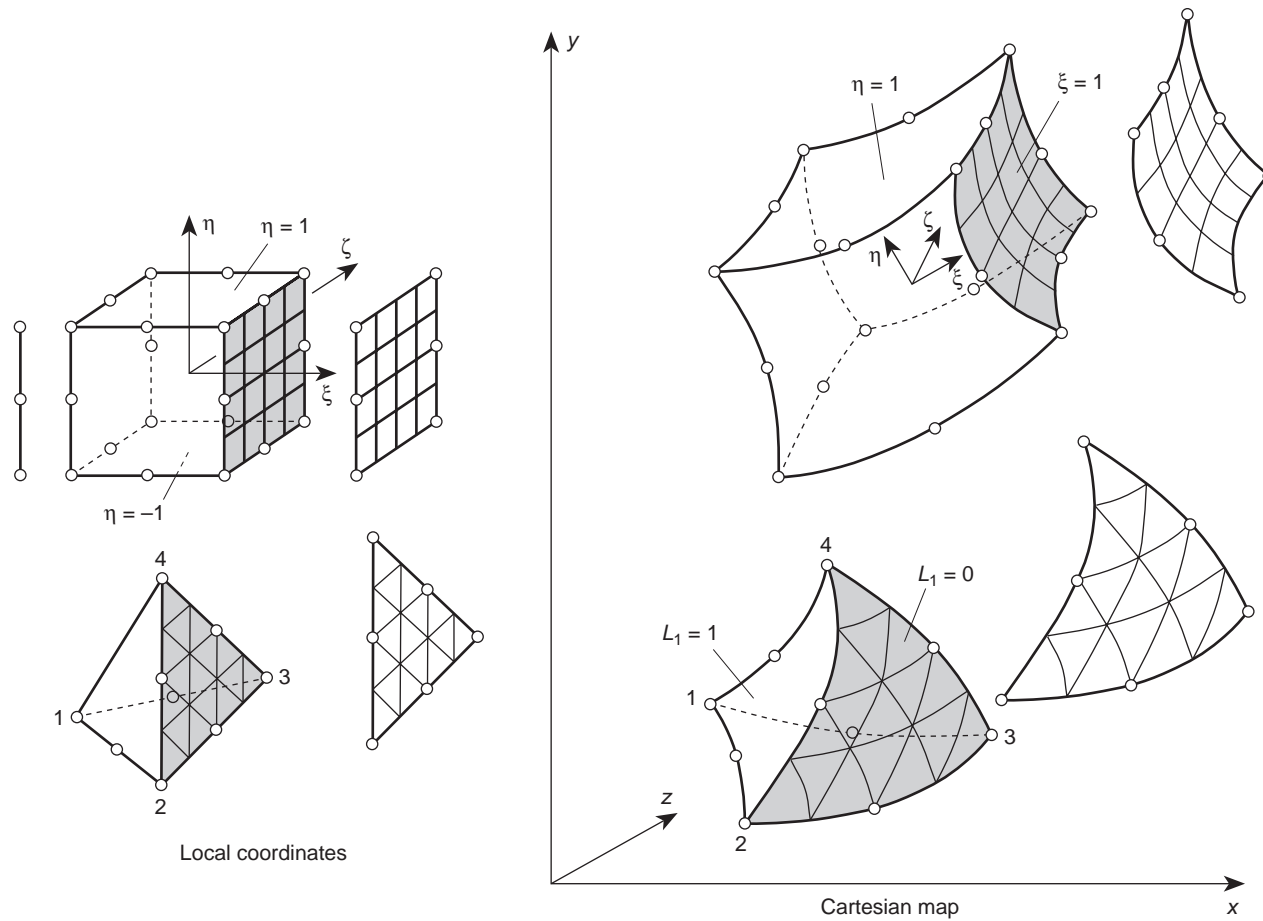


Fig. 9.2 Three-dimensional 'mapping' of some elements.

In the final section we shall show that many other coordinate transformations can be used effectively.

Parametric curvilinear coordinates

9.2 Use of 'shape functions' in the establishment of coordinate transformations

A most convenient method of establishing the coordinate transformations is to use the 'standard' type of C_0 shape functions we have already derived to represent the variation of the unknown function.

If we write, for instance, for each element

$$\begin{aligned} x &= N'_1 x_1 + N'_2 x_2 + \cdots = \mathbf{N}' \begin{Bmatrix} x_1 \\ x_2 \\ \vdots \end{Bmatrix} = \mathbf{N}' \mathbf{x} \\ y &= N'_1 y_1 + N'_2 y_2 + \cdots = \mathbf{N}' \begin{Bmatrix} y_1 \\ y_2 \\ \vdots \end{Bmatrix} = \mathbf{N}' \mathbf{y} \\ z &= N'_1 z_1 + N'_2 z_2 + \cdots = \mathbf{N}' \begin{Bmatrix} z_1 \\ z_2 \\ \vdots \end{Bmatrix} = \mathbf{N}' \mathbf{z} \end{aligned} \quad (9.2)$$

in which \mathbf{N}' are standard shape functions given in terms of the local coordinates, then a relationship of the required form is immediately available. Further, the points with coordinates x_1, y_1, z_1 , etc., will lie at appropriate points of the element boundary (as from the general definitions of the standard shape functions we know that these have a value of unity at the point in question and zero elsewhere). These points can establish nodes *a priori*.

To each set of local coordinates there will correspond a set of global cartesian coordinates and in general only one such set. We shall see, however, that a non-uniqueness may arise sometimes with violent distortion.

The concept of using such element shape functions for establishing curvilinear coordinates in the context of finite element analysis appears to have been first introduced by Taig.¹ In his first application basic linear quadrilateral relations were used. Irons^{2,3} generalized the idea for other elements.

Quite independently the exercises of devising various practical methods of generating curved surfaces for purposes of engineering design led to the establishment of similar definitions by Coons⁴ and Forrest,⁵ and indeed today the subjects of surface definitions and analysis are drawing closer together due to this activity.

In Fig. 9.3 an actual distortion of elements based on the cubic and quadratic members of the two-dimensional 'serendipity' family is shown. It is seen here that a one-to-one relationship exists between the local (ξ, η) and global (x, y) coordinates.

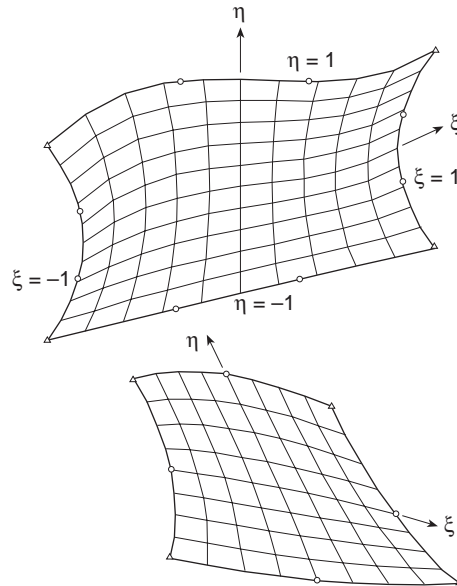


Fig. 9.3 Computer plots of curvilinear coordinates for cubic and parabolic elements (reasonable distortion).

If the fixed points are such that a violent distortion occurs then a non-uniqueness can occur in the manner indicated for two situations in Fig. 9.4. Here at internal points of the distorted element two or more local coordinates correspond to the same cartesian coordinate and in addition to some internal points being mapped outside the element. Care must be taken in practice to avoid such gross distortion.

Figure 9.5 shows two examples of a two-dimensional (ξ, η) element mapped into a three-dimensional (x, y, z) space.

We shall often refer to the basic element in undistorted, local, coordinates as a ‘parent’ element.

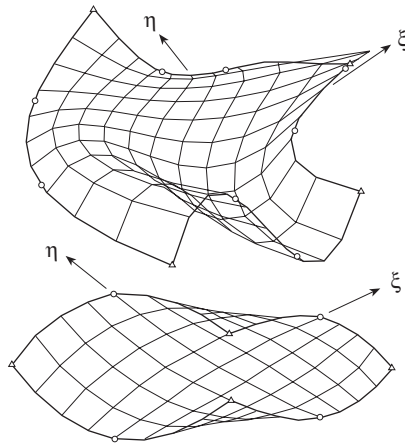


Fig. 9.4 Unreasonable element distortion leading to a non-unique mapping and ‘overspill’. Cubic and parabolic elements.

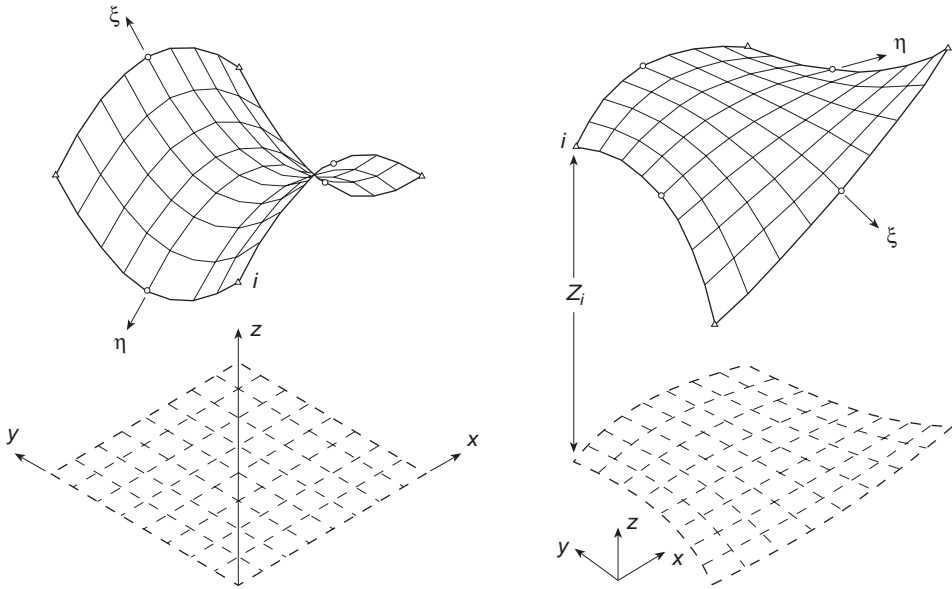


Fig. 9.5 Flat elements (of parabolic type) mapped into three-dimensions.

In Sec. 9.5 we shall define a quantity known as the jacobian determinant. The well-known condition for a *one-to-one* mapping (such as exists in Fig. 9.3 and does not in Fig. 9.4) is that the sign of this quantity should remain unchanged at all the points of the mapped element.

It can be shown that with a parametric transformation based on bilinear shape functions, the necessary condition is that no internal angle [such as α in Fig. 9.6(a)]

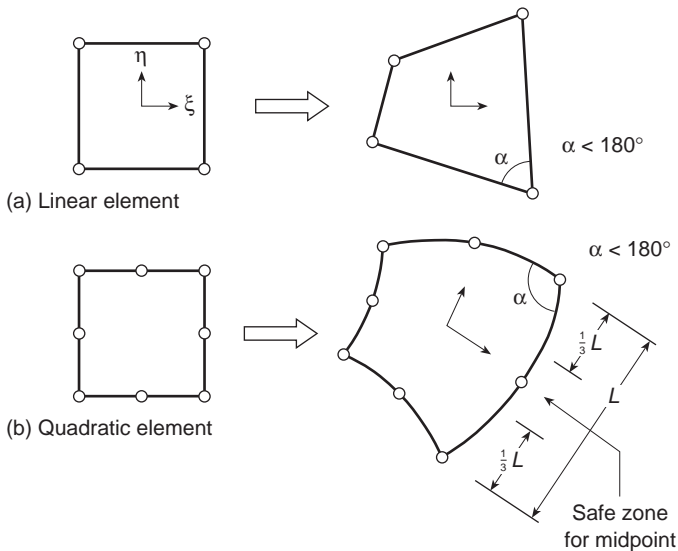


Fig. 9.6 Rules for uniqueness of mapping (a) and (b).

be greater than 180° .⁶ In transformations based on parabolic-type ‘serendipity’ functions, it is necessary in addition to this requirement to ensure that the mid-side nodes are in the ‘middle half’ of the distance between adjacent corners but a ‘middle third’ shown in Fig. 9.6 is safer. For cubic functions such general rules are impractical and numerical checks on the sign of the jacobian determinant are necessary. In practice a parabolic distortion is usually sufficient.

9.3 Geometrical conformability of elements

While it was shown that by the use of the shape function transformation each parent element maps uniquely a part of the real object, it is important that the subdivision of this into the new, curved, elements should leave no gaps. The possibility of such gaps is indicated in Fig. 9.7.

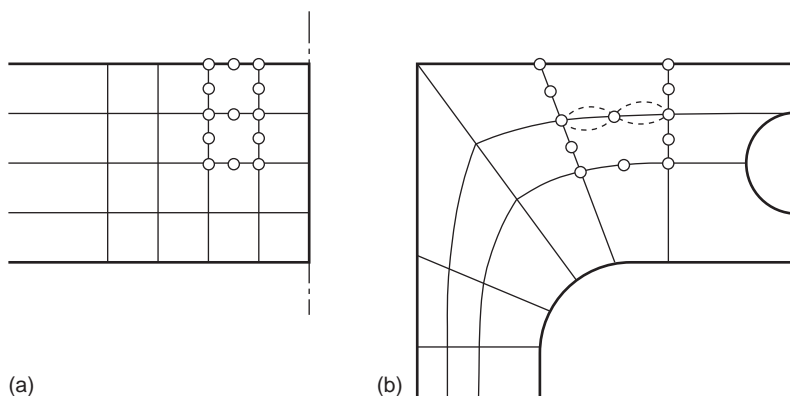


Fig. 9.7 Compatibility requirements in a real subdivision of space.

Theorem 1. *If two adjacent elements are generated from ‘parents’ in which the shape functions satisfy C_0 continuity requirements then the distorted elements will be contiguous (compatible).*

This theorem is obvious, as in such cases uniqueness of any function u required by continuity is simply replaced by that of uniqueness of the x , y , or z coordinate. As adjacent elements are given the same sets of coordinates at nodes, continuity is implied.

9.4 Variation of the unknown function within distorted, curvilinear elements. Continuity requirements

With the shape of the element now defined by the shape functions \mathbf{N}' the variation of the unknown, u , has to be specified before we can establish element properties. This is

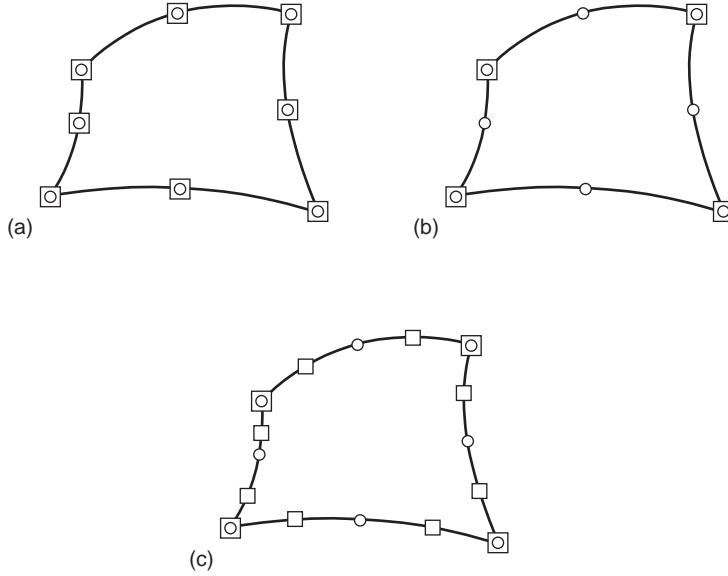


Fig. 9.8 Various element specifications: ○ point at which coordinate is specified; □ points at which the function parameter is specified. (a) Isoparametric, (b) superparametric, (c) subparametric.

most conveniently given in terms of local, curvilinear coordinates by the usual expression

$$u = \mathbf{N}\mathbf{a}^e \quad (9.3)$$

where \mathbf{a}^e lists the nodal values.

Theorem 2. *If the shape functions \mathbf{N} used in (9.3) are such that C_0 continuity of u is preserved in the parent coordinates then C_0 continuity requirements will be satisfied in distorted elements.*

The proof of this theorem follows the same lines as that in the previous section.

The nodal values may or may not be associated with the same nodes as used to specify the element geometry. For example, in Fig. 9.8 the points marked with a circle are used to define the element geometry. We could use the values of the function defined at nodes marked with a square to define the variation of the unknown.

In Fig. 9.8(a) the same points define the geometry and the finite element analysis points. If then

$$\mathbf{N} = \mathbf{N}' \quad (9.4)$$

i.e., the shape functions defining the geometry and the function are the same, the elements will be called *isoparametric*.

We could, however, use only the four corner points to define the variation of u [Fig. 9.8(b)]. We shall refer to such an element as *superparametric*, noting that the variation of geometry is more general than that of the actual unknown.

Similarly, if for instance we introduce more nodes to define u than are used to define the geometry, *subparametric* elements will result [Fig. 9.8(c)].

While for mapping it is convenient to use ‘standard’ forms of shape functions the interpolation of the unknown can, of course, use hierarchic forms defined in the previous chapter. Once again the definitions of sub- and superparametric variations are applicable.

Transformations

9.5 Evaluation of element matrices (transformation in ξ , η , ζ coordinates)

To perform finite element analysis the matrices defining element properties, e.g., stiffness, etc., have to be found. These will be of the form

$$\int_V \mathbf{G} dV \quad (9.5)$$

in which the matrix \mathbf{G} depends on \mathbf{N} or its derivatives with respect to *global coordinates*. As an example of this we have the stiffness matrix

$$\int_V \mathbf{B}^T \mathbf{D} \mathbf{B} dV \quad (9.6)$$

and associated body force vectors

$$\int_V \mathbf{N}^T \mathbf{b} dV \quad (9.7)$$

For each particular class of elastic problems the matrices of \mathbf{B} are given explicitly by their components [see the general form of Eqs (4.10), (5.6), and (6.11)]. Quoting the first of these, Eq. (4.10), valid for plane problems we have

$$\mathbf{B}_i = \begin{bmatrix} \frac{\partial N_i}{\partial x}, & 0 \\ 0, & \frac{\partial N_i}{\partial y} \\ \frac{\partial N_i}{\partial y}, & \frac{\partial N_i}{\partial x} \end{bmatrix} \quad (9.8)$$

In elasticity problems the matrix \mathbf{G} is thus a function of the first derivatives of \mathbf{N} and this situation will arise in many other classes of problem. In all, C_0 continuity is needed and, as we have already noted, this is readily satisfied by the functions of Chapter 8, written now in terms of curvilinear coordinates.

To evaluate such matrices we note that two transformations are necessary. In the first place, as N_i is defined in terms of local (curvilinear) coordinates, it is necessary to devise some means of expressing the global derivatives of the type occurring in Eq. (9.8) in terms of local derivatives.

In the second place the element of volume (or surface) over which the integration has to be carried out needs to be expressed in terms of the local coordinates with an appropriate change of limits of integration.

Consider, for instance, the set of local coordinates ξ, η, ζ and a corresponding set of global coordinates x, y, z . By the usual rules of partial differentiation we can write, for instance, the ξ derivative as

$$\frac{\partial N_i}{\partial \xi} = \frac{\partial N_i}{\partial x} \frac{\partial x}{\partial \xi} + \frac{\partial N_i}{\partial y} \frac{\partial y}{\partial \xi} + \frac{\partial N_i}{\partial z} \frac{\partial z}{\partial \xi} \quad (9.9)$$

Performing the same differentiation with respect to the other two coordinates and writing in matrix form we have

$$\begin{Bmatrix} \frac{\partial N_i}{\partial \xi} \\ \frac{\partial N_i}{\partial \eta} \\ \frac{\partial N_i}{\partial \zeta} \end{Bmatrix} = \begin{bmatrix} \frac{\partial x}{\partial \xi} & \frac{\partial y}{\partial \xi} & \frac{\partial z}{\partial \xi} \\ \frac{\partial x}{\partial \eta} & \frac{\partial y}{\partial \eta} & \frac{\partial z}{\partial \eta} \\ \frac{\partial x}{\partial \zeta} & \frac{\partial y}{\partial \zeta} & \frac{\partial z}{\partial \zeta} \end{bmatrix} \begin{Bmatrix} \frac{\partial N_i}{\partial x} \\ \frac{\partial N_i}{\partial y} \\ \frac{\partial N_i}{\partial z} \end{Bmatrix} = \mathbf{J} \begin{Bmatrix} \frac{\partial N_i}{\partial x} \\ \frac{\partial N_i}{\partial y} \\ \frac{\partial N_i}{\partial z} \end{Bmatrix} \quad (9.10)$$

In the above, the left-hand side can be evaluated as the functions N_i are specified in local coordinates. Further, as x, y, z are explicitly given by the relation defining the curvilinear coordinates [Eq. (9.2)], the matrix \mathbf{J} can be found explicitly in terms of the local coordinates. This matrix is known as the *jacobian matrix*.

To find now the global derivatives we invert \mathbf{J} and write

$$\begin{Bmatrix} \frac{\partial N_i}{\partial x} \\ \frac{\partial N_i}{\partial y} \\ \frac{\partial N_i}{\partial z} \end{Bmatrix} = \mathbf{J}^{-1} \begin{Bmatrix} \frac{\partial N_i}{\partial \xi} \\ \frac{\partial N_i}{\partial \eta} \\ \frac{\partial N_i}{\partial \zeta} \end{Bmatrix} \quad (9.11)$$

In terms of the shape function defining the coordinate transformation \mathbf{N}' (which as we have seen are only identical with the shape functions \mathbf{N} when the isoparametric formulation is used) we have

$$\mathbf{J} = \begin{bmatrix} \sum \frac{\partial N'_i}{\partial \xi} x_i & \sum \frac{\partial N'_i}{\partial \xi} y_i & \sum \frac{\partial N'_i}{\partial \xi} z_i \\ \sum \frac{\partial N'_i}{\partial \eta} x_i & \sum \frac{\partial N'_i}{\partial \eta} y_i & \sum \frac{\partial N'_i}{\partial \eta} z_i \\ \sum \frac{\partial N'_i}{\partial \zeta} x_i & \sum \frac{\partial N'_i}{\partial \zeta} y_i & \sum \frac{\partial N'_i}{\partial \zeta} z_i \end{bmatrix} = \begin{bmatrix} \frac{\partial N'_1}{\partial \xi} & \frac{\partial N'_2}{\partial \xi} & \dots \\ \frac{\partial N'_1}{\partial \eta} & \frac{\partial N'_2}{\partial \eta} & \dots \\ \frac{\partial N'_1}{\partial \zeta} & \frac{\partial N'_2}{\partial \zeta} & \dots \end{bmatrix} \begin{bmatrix} x_1 & y_1 & z_1 \\ x_2 & y_2 & z_2 \\ \vdots & \vdots & \vdots \end{bmatrix} \quad (9.12)$$

9.5.1 Volume integrals

To transform the variables and the region with respect to which the integration is made, a standard process will be used which involves the determinant of \mathbf{J} . Thus, for instance, a volume element becomes

$$dx dy dz = \det \mathbf{J} d\xi d\eta d\zeta \quad (9.13)$$

This type of transformation is valid irrespective of the number of coordinates used. For its justification the reader is referred to standard mathematical texts.† (See also Appendix F.)

Assuming that the inverse of \mathbf{J} can be found we now have reduced the evaluation of the element properties to that of finding integrals of the form of Eq. (9.5).

More explicitly we can write this as

$$\int_{-1}^1 \int_{-1}^1 \int_{-1}^1 \bar{\mathbf{G}}(\xi, \eta, \zeta) d\xi d\eta d\zeta \quad (9.14)$$

if the curvilinear coordinates are of the normalized type based on the right prism. Indeed the integration *is carried out within such a prism* and not in the complicated distorted shape, thus accounting for the simple integration limits. One- and two-dimensional problems will similarly result in integrals with respect to one or two coordinates within simple limits.

While the limits of integration are simple in the above case, unfortunately the explicit form of $\bar{\mathbf{G}}$ is not. Apart from the simplest elements, algebraic integration usually defies our mathematical skill, and numerical integration has to be used. This, as will be seen from later sections, is not a severe penalty and has the advantage that algebraic errors are more easily avoided and that general programs, not tied to a particular element, can be written for various classes of problems. Indeed in such numerical calculations the analytical inverses of \mathbf{J} are never explicitly found.

9.5.2 Surface integrals

In elasticity and other applications, surface integrals frequently occur. Typical here are the expressions for evaluating the contributions of surface tractions [see Chapter 2, Eq. (2.24b)]:

$$\mathbf{f} = - \int_A \mathbf{N}^T \bar{\mathbf{t}} dA$$

The element dA will generally lie on a surface where one of the coordinates (say ζ) is constant.

The most convenient process of dealing with the above is to consider dA as a vector oriented in the direction normal to the surface (see Appendix F). For three-dimensional problems we form the vector product

$$\mathbf{n} dA = d\mathbf{A} = \begin{Bmatrix} \frac{\partial x}{\partial \xi} \\ \frac{\partial y}{\partial \xi} \\ \frac{\partial z}{\partial \xi} \end{Bmatrix} \times \begin{Bmatrix} \frac{\partial x}{\partial \eta} \\ \frac{\partial y}{\partial \eta} \\ \frac{\partial z}{\partial \eta} \end{Bmatrix} d\xi d\eta$$

and on substitution integrate within the domain $-1 \leq \xi, \eta \leq 1$.

† The determinant of the jacobian matrix is known in the literature simply as ‘the jacobian’ and is often written as

$$\det \mathbf{J} \equiv \frac{\partial(x, y, z)}{\partial(\xi, \eta, \zeta)}$$

For two dimensions a line length dS arises and here the magnitude is simply

$$\mathbf{n} dS = d\mathbf{S} = \begin{Bmatrix} \frac{\partial x}{\partial \xi} \\ \frac{\partial y}{\partial \xi} \\ 0 \end{Bmatrix} \times \begin{Bmatrix} 0 \\ 0 \\ 1 \end{Bmatrix} d\xi = \begin{Bmatrix} \frac{\partial y}{\partial \xi} \\ -\frac{\partial x}{\partial \xi} \\ 0 \end{Bmatrix} d\xi$$

on constant η surfaces. This may now be reduced to two components for the two-dimensional problem.

9.6 Element matrices. Area and volume coordinates

The general relationship (9.2) for coordinate mapping and indeed all the following theorems are equally valid for any set of local coordinates and could relate the local L_1, L_2, \dots coordinates used for triangles and tetrahedra in the previous chapter, to the global cartesian ones.

Indeed most of the discussion of the previous chapter is valid if we simply rename the local coordinates suitably. However, two important differences arise.

The first concerns the fact that the local coordinates are not independent and in fact number one more than the cartesian system. The matrix \mathbf{J} would apparently therefore become rectangular and would not possess an inverse. The second is simply the difference of integration limits which have to correspond with a triangular or tetrahedral ‘parent’.

The simplest, though perhaps not the most elegant, way out of the first difficulty is to consider the last variable as a dependent one. Thus, for example, we can introduce formally, in the case of the tetrahedra,

$$\begin{aligned} \xi &= L_1 \\ \eta &= L_2 \\ \zeta &= L_3 \\ 1 - \xi - \eta - \zeta &= L_4 \end{aligned} \tag{9.15}$$

(by definition in the previous chapter) and thus preserve without change Eq. (9.9) and all the equations up to Eq. (9.14).

As the functions N_i are given in fact in terms of L_1, L_2 , etc., we must observe that

$$\frac{\partial N_i}{\partial \xi} = \frac{\partial N_i}{\partial L_1} \frac{\partial L_1}{\partial \xi} + \frac{\partial N_i}{\partial L_2} \frac{\partial L_2}{\partial \xi} + \frac{\partial N_i}{\partial L_3} \frac{\partial L_3}{\partial \xi} + \frac{\partial N_i}{\partial L_4} \frac{\partial L_4}{\partial \xi} \tag{9.16}$$

On using Eq. (9.15) this becomes simply

$$\frac{\partial N_i}{\partial \xi} = \frac{\partial N_i}{\partial L_1} - \frac{\partial N_i}{\partial L_4}$$

with the other derivatives obtainable by similar expressions.

The integration limits of Eq. (9.14) now change, however, to correspond with the tetrahedron limits, typically

$$\int_0^1 \int_0^{1-\zeta} \int_0^{1-\eta-\zeta} \bar{\mathbf{G}}(\xi, \eta, \zeta) d\xi d\eta d\zeta \quad (9.17)$$

The same procedure will clearly apply in the case of triangular coordinates.

It must be noted that once again the expression $\bar{\mathbf{G}}$ will necessitate numerical integration which, however, is carried out over the simple, undistorted, parent region whether this be triangular or tetrahedral.

An alternative to the above is to express the coordinates and constraint as

$$\begin{aligned} r_x &= x - x_1 N'_1 - x_2 N'_2 - x_3 N'_3 - \cdots = 0 \\ r_y &= y - y_1 N'_1 - y_2 N'_2 - y_3 N'_3 - \cdots = 0 \\ r_z &= z - z_1 N'_1 - z_2 N'_2 - z_3 N'_3 - \cdots = 0 \\ r_1 &= 1 - L_1 - L_2 - L_3 - L_4 = 0 \end{aligned} \quad (9.18)$$

where $N'_i = N'(L_1, L_2, L_3, L_4)$, etc. Now derivatives of the above with respect to x and y may be written directly as

$$\begin{aligned} \begin{bmatrix} \frac{\partial r_x}{\partial x} & \frac{\partial r_x}{\partial y} & \frac{\partial r_x}{\partial z} \\ \frac{\partial r_y}{\partial x} & \frac{\partial r_y}{\partial y} & \frac{\partial r_y}{\partial z} \\ \frac{\partial r_z}{\partial x} & \frac{\partial r_z}{\partial y} & \frac{\partial r_z}{\partial z} \\ \frac{\partial r_1}{\partial x} & \frac{\partial r_1}{\partial y} & \frac{\partial r_1}{\partial z} \end{bmatrix} &= \begin{bmatrix} 1 & 0 & 0 \\ 0 & 1 & 0 \\ 0 & 0 & 1 \\ 0 & 0 & 0 \end{bmatrix} - \begin{bmatrix} \sum x_k \frac{\partial N_k}{\partial L_1} & \sum x_k \frac{\partial N_k}{\partial L_2} & \sum x_k \frac{\partial N_k}{\partial L_3} & \sum x_k \frac{\partial N_k}{\partial L_4} \\ \sum y_k \frac{\partial N_k}{\partial L_1} & \sum y_k \frac{\partial N_k}{\partial L_2} & \sum y_k \frac{\partial N_k}{\partial L_3} & \sum y_k \frac{\partial N_k}{\partial L_4} \\ \sum z_k \frac{\partial N_k}{\partial L_1} & \sum z_k \frac{\partial N_k}{\partial L_2} & \sum z_k \frac{\partial N_k}{\partial L_3} & \sum z_k \frac{\partial N_k}{\partial L_4} \\ 1 & 1 & 1 & 1 \end{bmatrix} \\ &\times \begin{bmatrix} \frac{\partial L_1}{\partial x} & \frac{\partial L_1}{\partial y} & \frac{\partial L_1}{\partial z} \\ \frac{\partial L_2}{\partial x} & \frac{\partial L_2}{\partial y} & \frac{\partial L_2}{\partial z} \\ \frac{\partial L_3}{\partial x} & \frac{\partial L_3}{\partial y} & \frac{\partial L_3}{\partial z} \\ \frac{\partial L_4}{\partial x} & \frac{\partial L_4}{\partial y} & \frac{\partial L_4}{\partial z} \end{bmatrix} = \mathbf{0} \end{aligned} \quad (9.19)$$

The above may be solved for the partial derivatives of L_i with respect to the x, y, z coordinates and used directly with the chain rule written as

$$\frac{\partial N_i}{\partial x} = \frac{\partial N_i}{\partial L_1} \frac{\partial L_1}{\partial x} + \frac{\partial N_i}{\partial L_2} \frac{\partial L_2}{\partial x} + \frac{\partial N_i}{\partial L_3} \frac{\partial L_3}{\partial x} + \frac{\partial N_i}{\partial L_4} \frac{\partial L_4}{\partial x} \quad (19.20)$$

The above has advantages when the coordinates are written using mapping functions as the computation can still be more easily carried out. Also, the calculation of integrals will normally be performed numerically (as described in Sec. 9.10) where the points for integration are defined directly in terms of the volume coordinates.

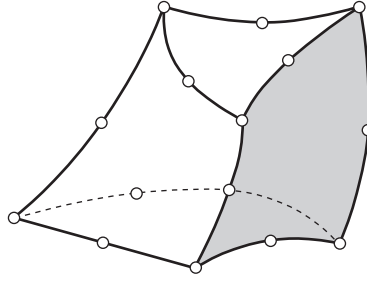


Fig. 9.9 A distorted triangular prism.

Finally it should be remarked that any of the elements given in the previous chapter are capable of being mapped. In some, such as the triangular prism, both area and rectangular coordinates are used (Fig. 9.9). The remarks regarding the dependence of coordinates apply once again with regard to the former but the processes of the present section should make procedures clear.

9.7 Convergence of elements in curvilinear coordinates

To consider the convergence aspects of the problem posed in curvilinear coordinates it is convenient to return to the starting point of the approximation where an energy functional Π , or an equivalent integral form (Galerkin problem statement), was defined by volume integrals essentially similar to those of Eq. (9.5), in which the integrand was a function of u and its first derivatives.

Thus, for instance, the variational principles of the energy kind discussed in Chapter 2 (or others of Chapter 3) could be stated for a scalar function u as

$$\Pi = \int_{\Omega} F\left(u, \frac{\partial u}{\partial x}, \frac{\partial u}{\partial y}, x, y\right) d\Omega + \int_{\Gamma} E(u, \dots) d\Gamma \quad (9.21)$$

The coordinate transformation changes the derivatives of any function by the jacobian relation (9.11). Thus

$$\begin{Bmatrix} \frac{\partial u}{\partial x} \\ \frac{\partial u}{\partial y} \end{Bmatrix} = \mathbf{J}^{-1}(\xi, \eta) \begin{Bmatrix} \frac{\partial u}{\partial \xi} \\ \frac{\partial u}{\partial \eta} \end{Bmatrix} \quad (9.22)$$

and the functional can be stated simply by a relationship of the form (9.21) with x, y , etc., replaced by ξ, η , etc., with the maximum order of differentiation unchanged.

It follows immediately that if the shape functions are chosen in curvilinear coordinate space so as to observe the usual rules of convergence (continuity and presence of complete first-order polynomials in these coordinates), then convergence will occur. Further, all the arguments concerning the order of convergence with the element size h still hold, providing the solution is related to the curvilinear coordinate system.

Indeed, all that has been said above is applicable to problems involving higher derivatives and to most unique coordinate transformations. It should be noted that

the patch test as conceived in the x, y, \dots coordinate system (see Chapters 2 and 10) is no longer simply applicable and in principle should be applied with polynomial fields imposed in the curvilinear coordinates. In the case of isoparametric (or subparametric) elements the situation is more advantageous. Here a linear (constant derivative x, y) field is always reproduced by the curvilinear coordinate expansion, and thus the lowest order patch test will be passed in the standard manner on such elements.

The proof of this is simple. Consider a standard isoparametric expansion

$$u = \sum_{i=1}^n N_i a_i \equiv \mathbf{N} \mathbf{a} \quad \mathbf{N} = \mathbf{N}(\xi, \eta, \zeta) \quad (9.23)$$

with coordinates of nodes defining the transformation as

$$x = \sum N_i x_i \quad y = \sum N_i y_i \quad z = \sum N_i z_i \quad (9.24)$$

The question is under what circumstances is it possible for expression (9.23) to define a linear expansion in cartesian coordinates:

$$\begin{aligned} u &= \alpha_1 + \alpha_2 x + \alpha_3 y + \alpha_4 z \\ &\equiv \alpha_1 + \alpha_2 \sum N_i x_i + \alpha_3 \sum N_i y_i + \alpha_4 \sum N_i z_i \end{aligned} \quad (9.25)$$

If we take

$$a_i = \alpha_1 + \alpha_2 x_i + \alpha_3 y_i + \alpha_4 z_i$$

and compare expression (9.23) with (9.25) we note that identity is obtained between these providing

$$\sum N_i = 1$$

As this is the usual requirement of standard element shape functions [see Eq. (8.4)] we can conclude that the following theorem is valid.

Theorem 3. *The constant derivative condition will be satisfied for all isoparametric elements.*

As subparametric elements can always be expressed as specific cases of an isoparametric transformation this theorem is obviously valid here also.

It is of interest to pursue the argument and to see under what circumstances higher polynomial expansions in cartesian coordinates can be achieved under various transformations. The simple linear case in which we ‘guessed’ the solution has now to be replaced by considering in detail the polynomial terms occurring in expressions such as (9.23) and (9.25) and establishing conditions for equating appropriate coefficients.

Consider a specific problem: the circumstances under which the bilinearly mapped quadrilateral of Fig. 9.10 can fully represent any quadratic cartesian expansion. We now have

$$x = \sum_1^4 N'_i x_i \quad y = \sum_1^4 N'_i y_i \quad (9.26)$$

and we wish to be able to reproduce

$$u = \alpha_1 + \alpha_2 x + \alpha_3 y + \alpha_4 x^2 + \alpha_5 xy + \alpha_6 y^2 \quad (9.27)$$

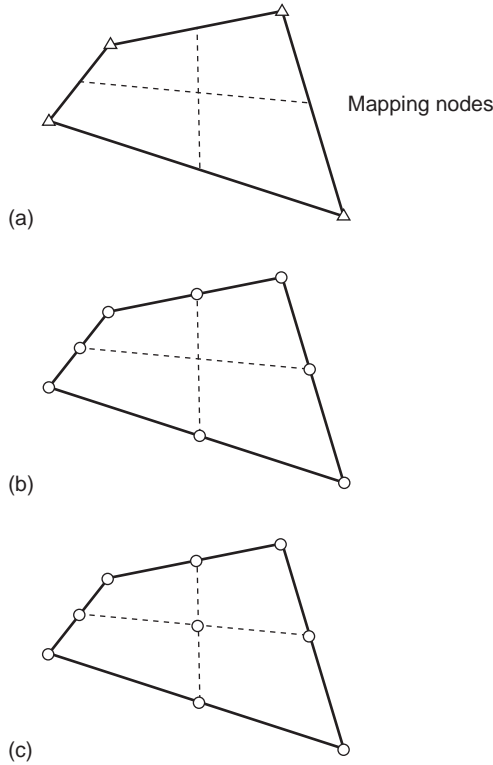


Fig. 9.10 Bilinear mapping of subparametric quadratic eight- and nine-noded element.

Noting that the bilinear form of N'_i contains terms such as 1, ξ , η and $\xi\eta$, the above can be written as

$$u = \beta_1 + \beta_2\xi + \beta_3\eta + \beta_4\xi^2 + \beta_5\xi\eta + \beta_6\eta^2 + \beta_7\xi\eta^2 + \beta_8\xi^2\eta + \beta_9\xi^2\eta^2 \quad (9.28)$$

where β_1 to β_9 depend on the values of α_1 to α_6 .

We shall now try to match the terms arising from the quadratic expansions of the serendipity and lagrangian kinds shown in Fig. 9.10(b) and (c):

$$u = \sum_{i=1}^8 N_i a_i \quad (9.29a)$$

$$u = \sum_{i=1}^9 N_i a_i \quad (9.29b)$$

where the appropriate terms are of the kind defined in the previous chapter.

For the eight-noded element (serendipity) [Fig. 9.10(b)] we can write (9.29a)) directly using polynomial coefficients b_i , $i = 1, \dots, 8$, in place of the nodal variables a_i (noting the terms occurring in the Pascal triangle) as

$$u = b_1 + b_2\xi + b_3\eta + b_4\xi^2 + b_5\xi\eta + b_6\eta^2 + b_7\xi\eta^2 + b_8\xi^2\eta \quad (9.30)$$

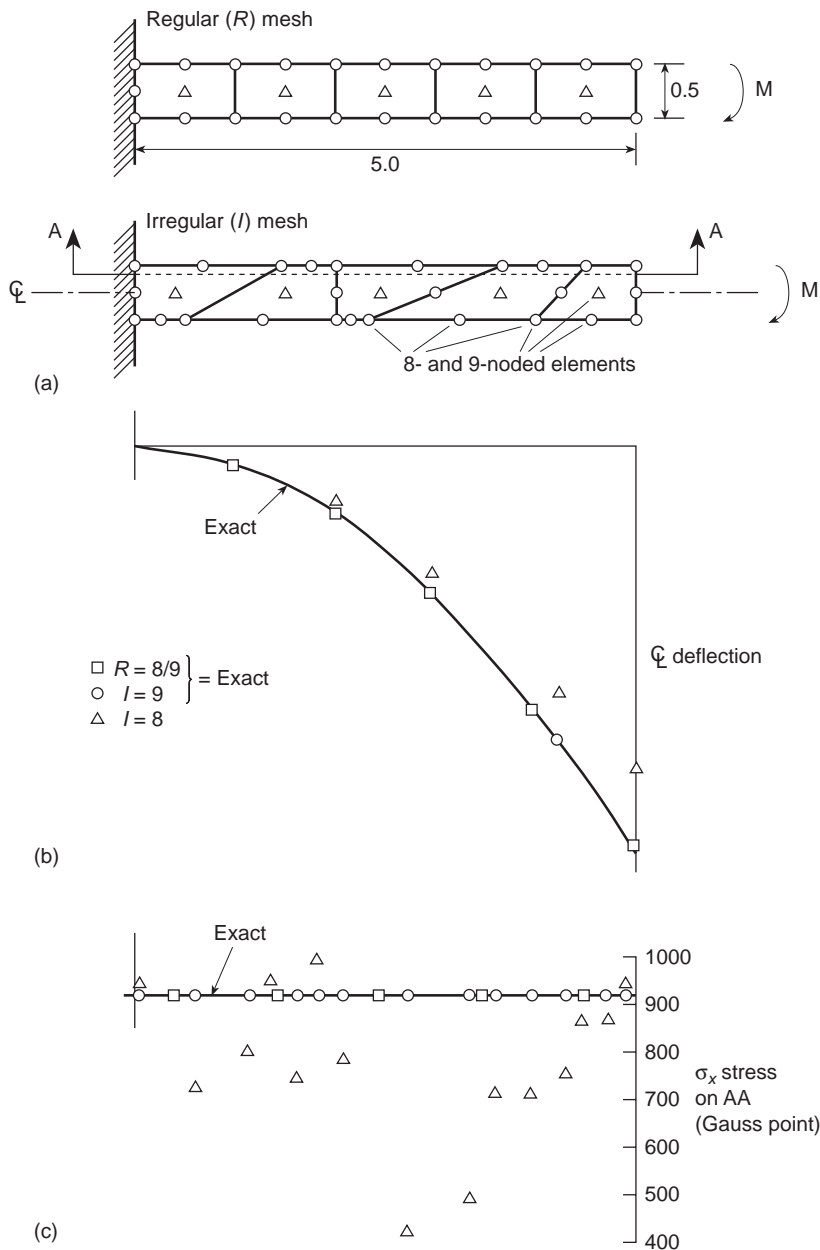


Fig. 9.11 Quadratic serendipity and Lagrange eight- and nine-noded elements in regular and distorted form. Elastic deflection of a beam under constant moment. Note the poor results of the eight-noded element.

It is immediately evident that for arbitrary values of β_1 to β_9 it is impossible to match the coefficients b_1 to b_8 due to the absence of the term $\xi^2\eta^2$ in Eq. (9.30). [However if higher order (quartic, etc.) expansions of the serendipity kind were used such matching would evidently be possible and we could conclude that for

linearly distorted elements the serendipity family of order four or greater will always represent quadratics.]

For the nine-noded, lagrangian, element [Fig. 9.10(c)] the expansion similar to (9.30) gives

$$u = b_1 + b_2\xi + b_3\eta + b_4\xi^2 + \cdots + b_8\xi^2\eta + b_9\xi^2\eta^2 \quad (9.31)$$

and the matching of the coefficients of Eqs (9.31) and (9.28) can be made directly.

We can conclude therefore that nine-noded elements represent better cartesian polynomials (when distorted linearly) and therefore are generally preferable in modelling smooth solutions. This matter was first presented by Wachspress but the simple proof presented above is due to Crochet.⁸ An example of this is given in Fig. 9.11 where we consider the results of a finite element calculation with eight- and nine-noded elements respectively used to reproduce a simple beam solution in which we know that the exact answers are quadratic. With no distortion both elements give exact results but when distorted only the nine-noded element does so, with the eight-noded element giving quite wild stress fluctuation.

Similar arguments will lead to the conclusion that in three dimensions again only the lagrangian 27-noded element is capable of reproducing fully the quadratic in cartesian coordinates when trilinearly distorted.

Lee and Bathe⁹ investigate the problem for cubic and quartic serendipity and lagrangian quadrilateral elements and show that under bilinear distortions the full order cartesian polynomial terms remain in Lagrange elements but not in serendipity ones. They also consider edge distortion and show that this polynomial order is always lost. Additional discussion of such problems is also given by Wachspress.⁷

9.8 Numerical integration – one-dimensional

In Chapter 5, dealing with a relatively simple problem of axisymmetric stress distribution and simple triangular elements, it was noted that exact integration of expressions for element matrices could be troublesome. Now for the more complex distorted elements numerical integration is essential.

Some principles of numerical integration will be summarized here together with tables of convenient numerical coefficients.

To find numerically the integral of a function of one variable we can proceed in one of several ways.¹⁰

9.8.1 Newton–Cotes quadrature†

In the most obvious procedure, points at which the function is to be found are determined *a priori* – usually at equal intervals – and a polynomial passed through the values of the function at these points and exactly integrated [Fig. 9.12(a)].

† ‘Quadrature’ is an alternative term to ‘numerical integration’.

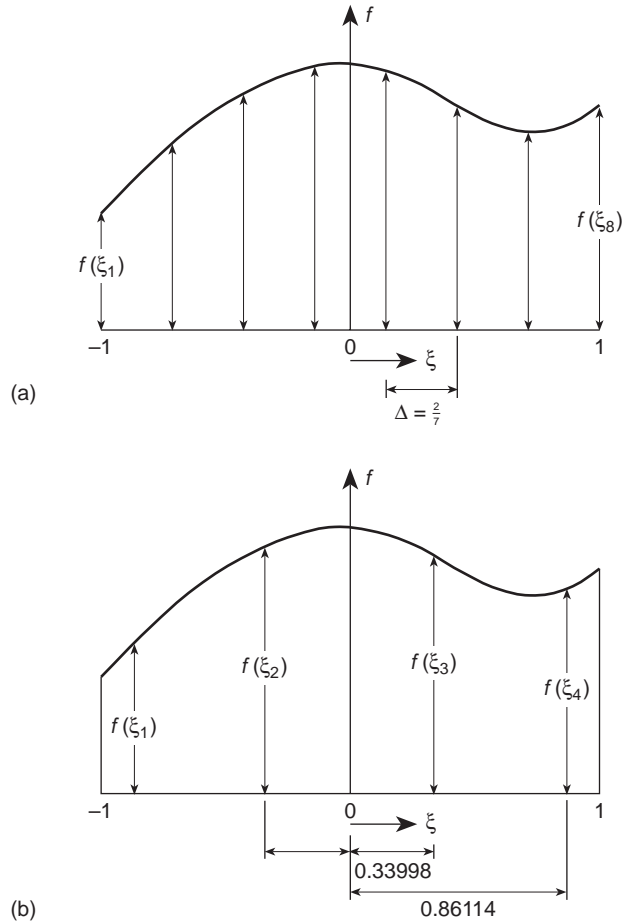


Fig. 9.12 (a) Newton–Cotes and (b) Gauss integrations. Each integrates exactly a seventh-order polynomial [i.e., error $O(h^8)$].

As n values of the function define a polynomial of degree $n - 1$, the errors will be of the order $O(h^n)$ where h is the element size. This leads to the well-known Newton–Cotes ‘quadrature’ formulae. The integrals can be written as

$$I = \int_{-1}^1 f(\xi) d\xi = \sum_1^n H_i f(\xi_i) \quad (9.32)$$

for the range of integration between -1 and $+1$ [Fig. 9.12(a)]. For example, if $n = 2$, we have the well-known trapezoidal rule:

$$I = f(-1) + f(1) \quad (9.33)$$

for $n = 3$, the Simpson ‘one-third’ rule:

$$I = \frac{1}{3} [f(-1) + 4f(0) + f(1)] \quad (9.34)$$

and for $n = 4$:

$$I = \frac{1}{4} [f(-1) + 3f(-\frac{1}{3}) + 3f(\frac{1}{3}) + f(1)] \quad (9.35)$$

Formulae for higher values of n are given in reference 10.

9.8.2 Gauss quadrature

If in place of specifying the position of sampling points *a priori* we allow these to be located at points to be determined so as to aim for best accuracy, then for a given number of sampling points increased accuracy can be obtained. Indeed, if we again consider

$$I = \int_{-1}^1 f(\xi) d\xi = \sum_1^n H_i f(\xi_i) \quad (9.36)$$

and again assume a polynomial expression, it is easy to see that for n sampling points we have $2n$ unknowns (H_i and ξ_i) and hence a polynomial of degree $2n - 1$ could be constructed and exactly integrated [Fig. 9.12(b)]. The error is thus of order $O(h^{2n})$.

The simultaneous equations involved are difficult to solve, but some mathematical manipulation will show that the solution can be obtained explicitly in terms of Legendre polynomials. Thus this particular process is frequently known as Gauss–Legendre quadrature.¹⁰

Table 9.1 shows the positions and weighting coefficients for gaussian integration.

For purposes of finite element analysis complex calculations are involved in determining the values of f , the function to be integrated. Thus the Gauss-type processes, requiring the least number of such evaluations, are ideally suited and from now on will be used exclusively.

Other expressions for integration of functions of the type

$$I = \int_{-1}^1 w(\xi) f(\xi) d\xi = \sum_1^n H_i f(\xi_i) \quad (9.37)$$

can be derived for prescribed forms of $w(\xi)$, again integrating up to a certain order of accuracy a polynomial expansion of $f(\xi)$.¹⁰

9.9 Numerical integration – rectangular (2D) or right prism (3D) regions

The most obvious way of obtaining the integral

$$I = \int_{-1}^1 \int_{-1}^1 f(\xi, \eta) d\xi d\eta \quad (9.38)$$

is to first evaluate the inner integral keeping η constant, i.e.,

$$\int_{-1}^1 f(\xi, \eta) d\xi = \sum_{j=1}^n H_j f(\xi_j, \eta) = \psi(\eta) \quad (9.39)$$

Table 9.1 Abscissae and weight coefficients of the gaussian quadrature formula $\int_{-1}^1 f(x) dx = \sum_{j=1}^n H_j f(a_j)$

$\pm a$	H
0	$n = 1$ 2.000 000 000 000 000
$1/\sqrt{3}$	$n = 2$ 1.000 000 000 000 000
$\sqrt{0.6}$	$n = 3$ 5/9
0.000 000 000 000 000	8/9
0.861 136 311 594 953	$n = 4$ 0.347 854 845 137 454
0.339 981 043 584 856	0.652 145 154 862 546
0.906 179 845 938 664	$n = 5$ 0.236 926 885 056 189
0.538 469 310 105 683	0.478 628 670 499 366
0.000 000 000 000 000	0.568 888 888 888 889
0.932 469 514 203 152	$n = 6$ 0.171 324 492 379 170
0.661 209 386 466 265	0.360 761 573 048 139
0.238 619 186 083 197	0.467 913 934 572 691
0.949 107 912 342 759	$n = 7$ 0.129 484 966 168 870
0.741 531 185 599 394	0.279 705 391 489 277
0.405 845 151 377 397	0.381 830 050 505 119
0.000 000 000 000 000	0.417 959 183 673 469
0.960 289 856 497 536	$n = 8$ 0.101 228 536 290 376
0.796 666 477 413 627	0.222 381 034 453 374
0.525 532 409 916 329	0.313 706 645 877 887
0.183 434 642 495 650	0.362 683 783 378 362
0.968 160 239 507 626	$n = 9$ 0.081 274 388 361 574
0.836 031 107 326 636	0.180 648 160 694 857
0.613 371 432 700 590	0.260 610 696 402 935
0.324 253 423 403 809	0.312 347 077 040 003
0.000 000 000 000 000	0.330 239 355 001 260
0.973 906 528 517 172	$n = 10$ 0.066 671 344 308 688
0.865 063 366 688 985	0.149 451 349 150 581
0.679 409 568 299 024	0.219 086 362 515 982
0.433 395 394 129 247	0.269 266 719 309 996
0.148 874 338 981 631	0.295 524 224 714 753

Evaluating the outer integral in a similar manner, we have

$$\begin{aligned}
 I &= \int_{-1}^1 \psi(\eta) d\eta = \sum_{i=1}^n H_i \psi(\eta_i) \\
 &= \sum_{i=1}^n H_i \sum_{j=1}^n H_j f(\xi_j, \eta_i) \\
 &= \sum_{i=1}^n \sum_{j=1}^n H_i H_j f(\xi_j, \eta_i)
 \end{aligned} \tag{9.40}$$

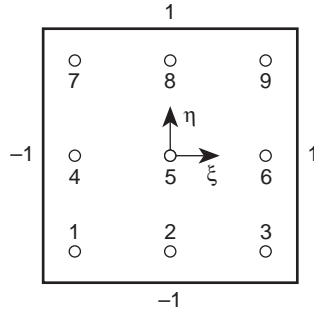


Fig. 9.13 Integrating points for $n = 3$ in a square region. (Exact for polynomial of fifth order in each direction).

For a right prism we have similarly

$$\begin{aligned}
 I &= \int_{-1}^1 \int_{-1}^1 \int_{-1}^1 f(\xi, \eta, \zeta) d\xi d\eta d\zeta \\
 &= \sum_{m=1}^n \sum_{j=1}^n \sum_{i=1}^n H_i H_j H_m f(\xi_i, \eta_j, \zeta_m)
 \end{aligned} \tag{9.41}$$

In the above, the number of integrating points in each direction was assumed to be the same. Clearly this is not necessary and on occasion it may be an advantage to use different numbers in each direction of integration.

It is of interest to note that in fact the double summation can be readily interpreted as a single one over $(n \times n)$ points for a rectangle (or n^3 points for a cube). Thus in Fig. 9.13 we show the nine sampling points that result in exact integrals of order 5 in each direction.

However, we could approach the problem directly and require an exact integration of a fifth-order polynomial in two dimensions. At any sampling point two coordinates and a value of f have to be determined in a weighting formula of type

$$I = \int_{-1}^1 \int_{-1}^1 f(\xi, \eta) d\xi d\eta = \sum_1^m w_i f(\xi_i, \eta_i) \tag{9.42}$$

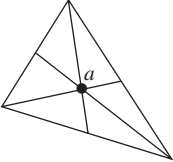
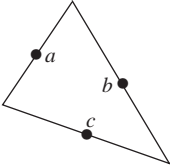
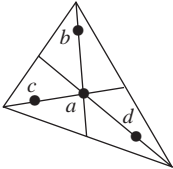
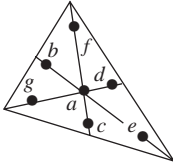
There it would appear that only seven points would suffice to obtain the same order of accuracy. Some formulae for three-dimensional bricks have been derived by Irons¹¹ and used successfully.¹²

9.10 Numerical integration – triangular or tetrahedral regions

For a triangle, in terms of the area coordinates the integrals are of the form

$$I = \int_0^1 \int_0^{1-L_1} f(L_1 L_2 L_3) dL_2 dL_1 \quad L_3 = 1 - L_1 - L_2 \tag{9.43}$$

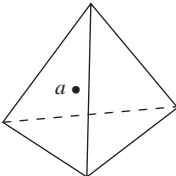
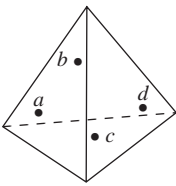
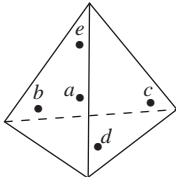
Table 9.2 Numerical integration formulae for triangles

Order	Figure	Error	Points	Triangular coordinates	Weights
Linear		$R = O(h^2)$	a	$\frac{1}{3}, \frac{1}{3}, \frac{1}{3}$	1
Quadratic		$R = O(h^3)$	a b c	$\frac{1}{2}, \frac{1}{2}, 0$ $0, \frac{1}{2}, \frac{1}{2}$ $\frac{1}{2}, 0, \frac{1}{2}$	$\frac{1}{3}$ $\frac{1}{3}$ $\frac{1}{3}$
Cubic		$R = O(h^4)$	a b c d	$\frac{1}{3}, \frac{1}{3}, \frac{1}{3}$ $0.6, 0.2, 0.2$ $0.2, 0.6, 0.2$ $0.2, 0.2, 0.6$	$-\frac{27}{48}$ $\frac{25}{48}$
Quintic		$R = O(h^6)$	a b c d e f g	$\frac{1}{3}, \frac{1}{3}, \frac{1}{3}$ $\alpha_1, \beta_1, \beta_1$ $\beta_1, \alpha_1, \beta_1$ $\beta_1, \beta_1, \alpha_1$ $\alpha_2, \beta_2, \beta_2$ $\beta_2, \alpha_2, \beta_2$ $\beta_2, \beta_2, \alpha_2$	0.225 000 000 0 0.132 394 152 7 0.125 939 180 5
with $\alpha_1 = 0.059\,715\,871\,7$ $\beta_1 = 0.470\,142\,064\,1$ $\alpha_2 = 0.797\,426\,985\,3$ $\beta_2 = 0.101\,286\,507\,3$					

Once again we could use n Gauss points and arrive at a summation expression of the type used in the previous section. However, the limits of integration now involve the variable itself and it is convenient to use alternative sampling points for the second integration by use of a special Gauss expression for integrals of the type given by Eq. (9.37) in which w is a linear function. These have been devised by Radau¹³ and used successfully in the finite element context.¹⁴ It is, however, much more desirable (and aesthetically pleasing) to use special formulae in which no bias is given to any of the natural coordinates L_i . Such formulae were first derived by Hammer *et al.*¹⁵ and Felippa¹⁶ and a series of necessary sampling points and weights is given in Table 9.2.¹⁷ (A more comprehensive list of higher formulae derived by Cowper is given on p. 184 of reference 17.)

A similar extension for tetrahedra can obviously be made. Table 9.3 presents some formulae based on reference 15.

Table 9.3 Numerical integration formulae for tetrahedra

No.	Order	Figure	Error	Points	Tetrahedral coordinates	Weights
1	Linear		$R = O(h^2)$	a	$\frac{1}{4}, \frac{1}{4}, \frac{1}{4}, \frac{1}{4}$	1
2	Quadratic		$R = O(h^3)$	a b c d	$\left. \begin{array}{l} \alpha, \beta, \beta, \beta \\ \beta, \alpha, \beta, \beta \\ \beta, \beta, \alpha, \beta \\ \beta, \beta, \beta, \alpha \end{array} \right\}$ $\alpha = 0.585\,410\,20$ $\beta = 0.138\,196\,60$	$\frac{1}{4}$
3	Cubic		$R = O(h^4)$	a b c d e	$\left. \begin{array}{l} \frac{1}{4}, \frac{1}{4}, \frac{1}{4}, \frac{1}{4} \\ \frac{1}{2}, \frac{1}{6}, \frac{1}{6}, \frac{1}{6} \\ \frac{1}{6}, \frac{1}{2}, \frac{1}{6}, \frac{1}{6} \\ \frac{1}{6}, \frac{1}{6}, \frac{1}{2}, \frac{1}{6} \\ \frac{1}{6}, \frac{1}{6}, \frac{1}{6}, \frac{1}{2} \end{array} \right\}$	$-\frac{4}{5}$ $\frac{9}{20}$

9.11 Required order of numerical integration

With numerical integration used in place of exact integration, an additional error is introduced into the calculation and the first impression is that this should be reduced as much as possible. Clearly the cost of numerical integration can be quite significant, and indeed in some early programs numerical formulation of element characteristics used a comparable amount of computer time as in the subsequent solution of the equations. It is of interest, therefore, to determine (a) the minimum integration requirement permitting convergence and (b) the integration requirements necessary to preserve the rate of convergence which would result if exact integration were used.

It will be found later (Chapters 10 and 12) that it is in fact often a positive disadvantage to use higher orders of integration than those actually needed under (b) as, for very good reasons, a 'cancellation of errors' due to discretization and due to inexact integration can occur.

9.11.1 Minimum order of integration for convergence

In problems where the energy functional (or equivalent Galerkin integral statements) defines the approximation we have already stated that convergence can occur providing any arbitrary constant value of the m th derivatives can be reproduced.

In the present case $m = 1$ and we thus require that in integrals of the form (9.5) a constant value of \mathbf{G} be correctly integrated. *Thus the volume of the element $\int_V dV$ needs to be evaluated correctly for convergence to occur.* In curvilinear coordinates we can thus argue that $\int_V \det |J| d\zeta d\eta d\xi$ has to be evaluated exactly.^{3,6}

9.11.2 Order of integration for no loss of convergence

In a general problem we have already found that the finite element approximate evaluation of energy (and indeed all the other integrals in a Galerkin-type approximation, see Chapter 3) was exact to the order $2(p - m)$, where p was the degree of the complete polynomial present and m the order of differentials occurring in the appropriate expressions.

Providing the integration is exact to order $2(p - m)$, or shows an error of $O(h^{2(p-m)+1})$, or less, then no loss of convergence order will occur.† If in curvilinear coordinates we take a curvilinear dimension h of an element, the same rule applies. For C_0 problems (i.e., $m = 1$) the integration formulae should be as follows:

$$\begin{aligned} p = 1, & \quad \text{linear elements} & O(h) \\ p = 2, & \quad \text{quadratic elements} & O(h^3) \\ p = 3, & \quad \text{cubic elements} & O(h^5) \end{aligned}$$

We shall make use of these results in practice, as will be seen later, but it should be noted that for a linear quadrilateral or triangle a single-point integration is adequate. For parabolic quadrilaterals (or bricks) 2×2 (or $2 \times 2 \times 2$), Gauss point integration is adequate and for parabolic triangles (or tetrahedra) three-point (and four-point) formulae of Tables 9.2 and 9.3 are needed.

The basic theorems of this section have been introduced and proved numerically in published work.¹⁸⁻²⁰

9.11.3 Matrix singularity due to numerical integration

The final outcome of a finite element approximation in linear problems is an equation system

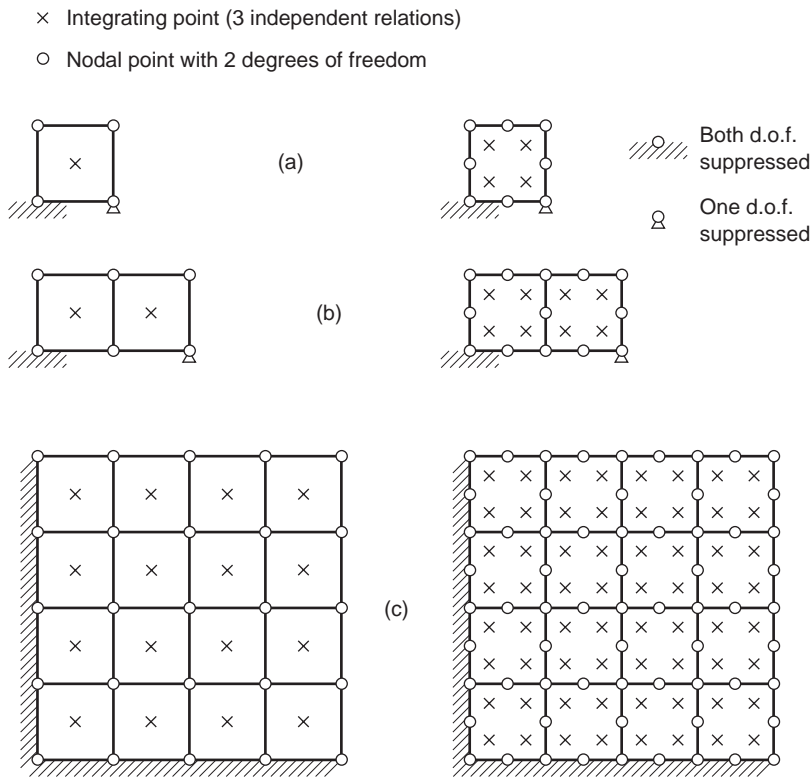
$$\mathbf{K}\mathbf{a} + \mathbf{f} = \mathbf{0} \tag{9.44}$$

in which the boundary conditions have been inserted and which should, on solution for the parameter \mathbf{a} , give an approximate solution for the physical situation. If a solution is unique, as is the case with well-posed physical problems, the equation matrix \mathbf{K} should be non-singular. We have *a priori* assumed that this was the case with exact integration and in general have not been disappointed. With numerical integration singularities may arise for low integration orders, and this may make such orders impractical. It is easy to show how, in some circumstances, a singularity of \mathbf{K} must

† For an energy principle use of quadrature may result in loss of a bound for $\Pi(\mathbf{a})$.

arise, but it is more difficult to prove that it will not. We shall, therefore, concentrate on the former case.

With numerical integration we replace the integrals by a weighted sum of independent linear relations between the nodal parameters **a**. These linear relations supply the only information from which the matrix **K** is constructed. *If the number of unknowns **a** exceeds the number of independent relations supplied at all the integrating points, then the matrix **K** must be singular.*



	Linear		Quadratic	
	Degree of freedom	Independent relation	Degree of freedom	Independent relation
(a)	$4 \times 2 - 3 = 5$	$1 \times 3 = 3$ singular	$2 \times 8 - 3 = 13$	$4 \times 3 = 12$ singular
(b)	$6 \times 2 - 3 = 9$	$2 \times 3 = 6$ singular	$13 \times 2 - 3 = 23$	$8 \times 3 = 24$
(c)	$25 \times 2 - 18 = 32$	$16 \times 3 = 48$	$48 \times 2 = 96$	$64 \times 3 = 192$

Fig. 9.14 Check on matrix singularity in two-dimensional elasticity problems (a), (b), and (c).

To illustrate this point we shall consider two-dimensional elasticity problems using linear and parabolic serendipity quadrilateral elements with one- and four-point quadratures respectively.

Here at each integrating point *three* independent ‘strain relations’ are used and the total number of independent relations equals $3 \times (\text{number of integration points})$. The number of unknowns **a** is simply $2 \times (\text{number of nodes})$ less restrained degrees of freedom.

In Fig. 9.14(a) and (b) we show a single element and an assembly of two elements supported by a minimum number of specified displacements eliminating rigid body motion. The simple calculation shows that only in the assembly of the quadratic elements is elimination of singularities possible, all the other cases remaining strictly singular.

In Fig. 9.14(c) a well-supported block of both kinds of elements is considered and here for both element types non-singular matrices may arise although local, near singularity may still lead to unsatisfactory results (see Chapter 10).

The reader may well consider the same assembly but supported again by the minimum restraint of three degrees of freedom. The assembly of linear elements with a single integrating point *will* be singular while the quadratic ones will, in fact, usually be well behaved.

For the reason just indicated, linear single-point integrated elements are used infrequently in static solutions, though they do find wide use in ‘explicit’ dynamics codes – but needing certain remedial additions (e.g., hourglass control^{21,22}) – while four-point quadrature is often used for quadratic serendipity elements.†

In Chapter 10 we shall return to the problem of convergence and will indicate dangers arising from local element singularities.

However, it is of interest to mention that in Chapter 12 we shall in fact *seek* matrix singularities for special purposes (e.g., incompressibility) using similar arguments.

9.12 Generation of finite element meshes by mapping. Blending functions

It would have been observed that it is an easy matter to obtain a coarse subdivision of the analysis domain with a small number of isoparametric elements. If second- or third-degree elements are used, the fit of these to quite complex boundaries is reasonable, as shown in Fig. 9.15(a) where four parabolic elements specify a sectorial region. This number of elements would be too small for analysis purposes *but a simple subdivision into finer elements* can be done automatically by, say, assigning new positions of nodes of the central points of the curvilinear coordinates and thus deriving a larger number of similar elements, as shown in Fig. 9.15(b). Indeed, automatic subdivision could be carried out further to generate a field of triangular elements. The process thus allows us, with a small amount of original *input data*, to derive a finite element mesh of any refinement desirable. In reference 23 this type of mesh generation is developed for two- and three-dimensional solids and surfaces and is reasonably

† Repeating the test for quadratic lagrangian elements indicates a singularity for 2×2 quadrature (see Chapter 10 for dangers).

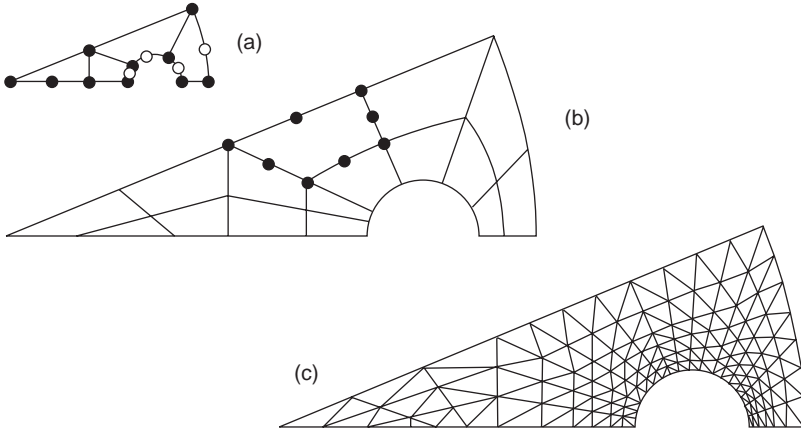


Fig. 9.15 Automatic mesh generation by parabolic isoparametric elements. (a) Specified mesh points. (b) Automatic subdivision into a small number of isoparametric elements. (c) Automatic subdivision into linear triangles.

efficient. However, elements of predetermined size and/or gradation cannot be easily generated.

The main drawback of the mapping and generation suggested is the fact that the originally circular boundaries in Fig. 9.15(a) are approximated by simple parabolae and a geometric error can be developed there. To overcome this difficulty another form of mapping, originally developed for the representation of complex motor-car body shapes, can be adopted for this purpose.²⁴ In this mapping blending functions interpolate the unknown u in such a way as to satisfy *exactly* its variations along the edges of a square ξ, η domain. If the coordinates x and y are used in a parametric expression of the type given in Eq. (9.1), then any complex shape can be mapped by a single element. In reference 24 the region of Fig. 9.15 is in fact so mapped and a mesh subdivision obtained directly without any geometric error on the boundary.

The blending processes are of considerable importance and have been used to construct some interesting element families²⁵ (which in fact include the standard serendipity elements as a subclass). To explain the process we shall show how a function with prescribed variations along the boundaries can be interpolated.

Consider a region $-1 \leq \xi, \eta \leq 1$, shown in Fig. 9.16, on the edges of which an arbitrary function ϕ is specified [i.e., $\phi(-1, \eta), \phi(1, \eta), \phi(\xi, -1), \phi(\xi, 1)$ are given]. The problem presented is that of interpolating a function $\phi(\xi, \eta)$ so that a smooth surface reproducing precisely the boundary values is obtained. Writing

$$\begin{aligned} N^1(\xi) &= \frac{1-\xi}{2} & N^2(\xi) &= \frac{1+\xi}{2} \\ N^1(\eta) &= \frac{1-\eta}{2} & N^2(\eta) &= \frac{1+\eta}{2} \end{aligned} \quad (9.45)$$

for our usual one-dimensional linear interpolating functions, we note that

$$P_\eta \phi \equiv N^1(\eta)\phi(\xi, -1) + N^2(\eta)\phi(\xi, 1) \quad (9.46)$$

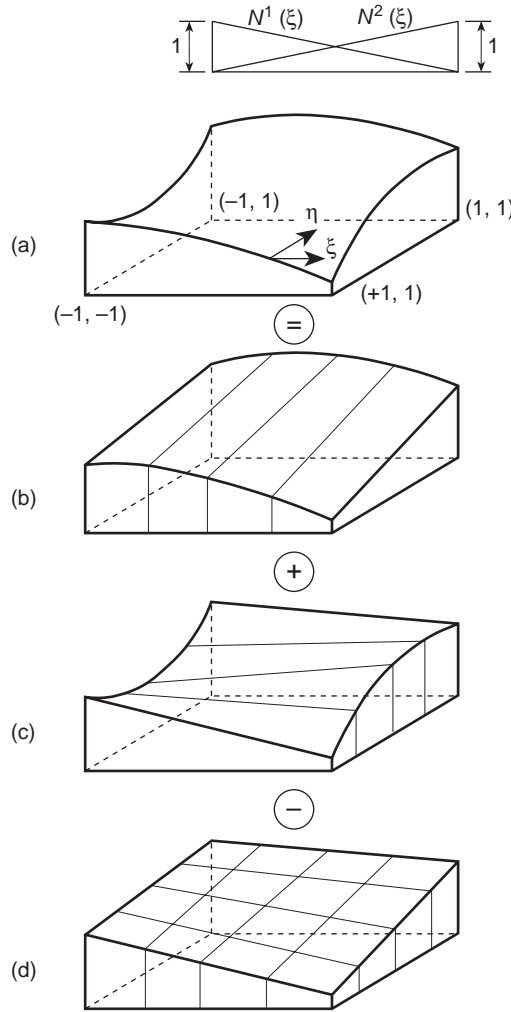


Fig. 9.16 Stages of construction of a blending interpolation (a), (b), (c), and (d).

interpolates linearly between the specified functions in the η direction, as shown in Fig. 9.16(b). Similarly,

$$P_{\xi}\phi \equiv N^1(\xi)\phi(\eta, -1) + N^2(\xi)\phi(\eta, 1) \quad (9.47)$$

interpolates linearly in the ξ direction [Fig. 9.16(c)]. Constructing a third function which is a standard linear, bilinear interpolation of the kind we have already encountered [Fig. 9.16(d)], i.e.,

$$\begin{aligned} P_{\xi}P_{\eta}\phi = & N^2(\xi)N^2(\eta)\phi(1, 1) + N^2(\xi)N^1(\eta)\phi(1, -1) \\ & + N^1(\xi)N^2(\eta)\phi(-1, 1) + N^1(\xi)N^1(\eta)\phi(-1, -1) \end{aligned} \quad (9.48)$$

we note by inspection that

$$\phi = P_\eta \phi + P_\xi \phi - P_\xi P_\eta \phi \quad (9.49)$$

is a smooth surface interpolating exactly the boundary functions.

Extension to functions with higher order blending is almost evident, and immediately the method of mapping the quadrilateral region $-1 \leq \xi, \eta \leq 1$ to any arbitrary shape is obvious.

Though the above mesh generation method derives from mapping and indeed has been widely applied in two and three dimensions, we shall see in the chapter devoted to adaptivity (Chapter 15) that the optimal solution or specification of *mesh density* or *size* should guide the mesh generation. We shall discuss this problem in that chapter to some extent, but the interested reader is directed to references 26, 27 or books that have appeared on the subject.^{28–31} The subject has now grown to such an extent that discussion in any detail is beyond the scope of this book. In the programs mentioned at the end of each volume of this book we shall refer to the GiD system which is available to readers.³²

9.13 Infinite domains and infinite elements

9.13.1 Introduction

In many problems of engineering and physics infinite or semi-infinite domains exist. A typical example from structural mechanics may, for instance, be that of three-dimensional (or axisymmetric) excavation, illustrated in Fig. 9.17. Here the problem is one of determining the deformations in a semi-infinite half-space due to the removal of loads with the specification of zero displacements at infinity. Similar problems abound in electromagnetics and fluid mechanics but the situation illustrated is typical. The question arises as to how such problems can be dealt with by a method of approximation in which elements of decreasing size are used in the modelling process. The first intuitive answer is the one illustrated in Fig. 9.17(a) where the infinite boundary condition is specified at a finite boundary placed at a *large distance* from the object. This, however, begs the question of what is a ‘large distance’ and obviously substantial errors may arise if this boundary is not placed far enough away. On the other hand, pushing this out excessively far necessitates the introduction of a large number of elements to model regions of relatively little interest to the analyst.

To overcome such ‘infinite’ difficulties many methods have been proposed. In some a sequence of nesting grids is used and a recurrence relation derived.^{33,34} In others a boundary-type exact solution is used and coupled to the finite element domain.^{35,36} However, without doubt, the most effective and efficient treatment is the use of ‘infinite elements’^{37–40} pioneered originally by Bettess.⁴¹ In this process the conventional, finite elements are coupled to elements of the type shown in Fig. 9.17(b) which model in a reasonable manner the material stretching to infinity.

The shape of such two-dimensional elements and their treatment is best accomplished by mapping^{39–41} these onto a bi-unit square (or a finite line in one dimension or cube in three dimensions). However, it is essential that the sequence of trial

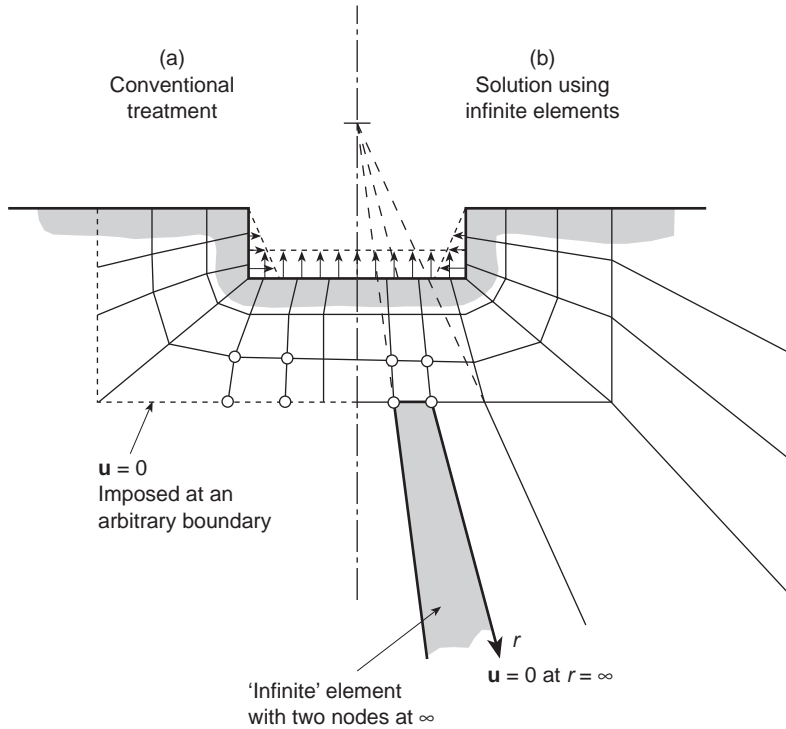


Fig. 9.17 A semi-infinite domain. Deformations of a foundation due to removal of load following an excavation. (a) Conventional treatment and (b) use of infinite elements.

functions introduced in the mapped domain be such that it is complete and capable of modelling the true behaviour as the radial distance r increases. Here it would be advantageous if the mapped shape functions could approximate a sequence of the decaying form

$$\frac{C_1}{r} + \frac{C_2}{r^2} + \frac{C_3}{r^3} + \dots \quad (9.50)$$

where C_i are arbitrary constants and r is the radial distance from the 'focus' of the problem.

In the next subsection we introduce a mapping function capable of doing just this.

9.13.2 The mapping function

Figure 9.18 illustrates the principles of generation of the derived mapping function.

We shall start with a one-dimensional mapping along a line CPQ coinciding with the x -direction. Consider the following function:

$$x = -\frac{\xi}{1-\xi}x_C + \left(1 + \frac{\xi}{1-\xi}\right)x_Q = \bar{N}_C x_C + \bar{N}_Q x_Q \quad (9.51a)$$

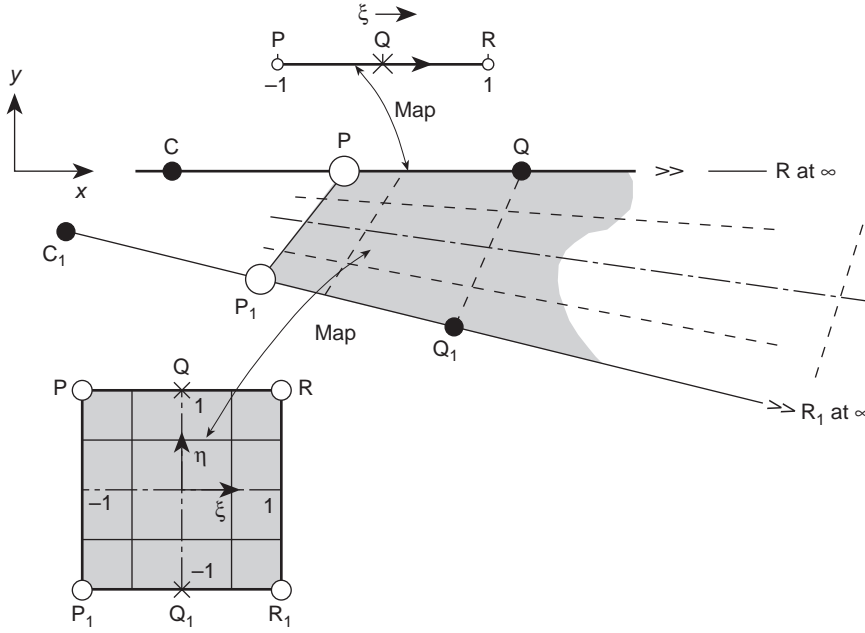


Fig. 9.18 Infinite line and element map. Linear η interpolation.

and we immediately observe that

$$\xi = -1 \quad \text{corresponds to } x = \frac{x_Q + x_C}{2} \equiv x_P$$

$$\xi = 0 \quad \text{corresponds to } x = x_Q$$

$$\xi = 1 \quad \text{corresponds to } x = \infty$$

where x_P is a point midway between Q and C .

Alternatively the above mapping could be written directly in terms of the Q and P coordinates by simple elimination of x_C . This gives, using our previous notation:

$$\begin{aligned} x &= N_Q x_Q + N_P x_P \\ &= \left(1 + \frac{2\xi}{1-\xi}\right) x_Q - \frac{2\xi}{1-\xi} x_P \end{aligned} \quad (9.51b)$$

Both forms give a mapping that is independent of the origin of the x -coordinate as

$$N_Q + N_P = 1 = \bar{N}_C + \bar{N}_Q \quad (9.52)$$

The significance of the point C is, however, of great importance. It represents the centre from which the ‘disturbance’ originates and, as we shall now show, allows the expansion of the form of Eq. (9.50) to be achieved on the assumption that r is measured from C . Thus

$$r = x - x_C \quad (9.53)$$

If, for instance, the unknown function u is approximated by a polynomial function using, say, hierarchical shape functions and giving

$$u = \alpha_0 + \alpha_1\xi + \alpha_2\xi^2 + \alpha_3\xi^3 + \dots \quad (9.54)$$

we can easily solve Eqs (9.51a) for ξ , obtaining

$$\xi = 1 - \frac{x_Q - x_C}{x - x_C} = 1 - \frac{x_Q - x_C}{r} \quad (9.55)$$

Substitution into Eq. (9.54) shows that a series of the form given by Eq. (9.50) is obtained with the linear shape function in ξ corresponding to $1/r$ terms, quadratic to $1/r^2$, etc.

In one dimension the objectives specified have thus been achieved and the element will yield convergence as the degree of the polynomial expansion, p , increases. Now a generalization to two or three dimensions is necessary. It is easy to see that this can be achieved by simple products of the one-dimensional infinite mapping with a 'standard' type of shape function in η (and ζ) directions in the manner indicated in Fig. 9.18.

Firstly we generalize the interpolation of Eqs (9.51) for any straight line in x, y, z space and write (for such a line as $C_1P_1Q_1$ in Fig. 9.18)

$$\begin{aligned} x &= -\frac{\xi}{1-\xi}x_{C_1} + \left(1 + \frac{\xi}{1-\xi}\right)x_{Q_1} \\ y &= -\frac{\xi}{1-\xi}y_{C_1} + \left(1 + \frac{\xi}{1-\xi}\right)y_{Q_1} \\ z &= -\frac{\xi}{1-\xi}z_{C_1} + \left(1 + \frac{\xi}{1-\xi}\right)z_{Q_1} \quad (\text{in three dimensions}) \end{aligned} \quad (9.56)$$

Secondly we complete the interpolation and map the whole $\xi\eta(\zeta)$ domain by adding a 'standard' interpolation in the $\eta(\zeta)$ directions. Thus for the linear interpolation shown we can write for elements $PP_1QQ_1RR_1$ of Fig. 9.18, as

$$\begin{aligned} x &= N_1(\eta) \left[-\frac{\xi}{1-\xi}x_C \left(1 + \frac{\xi}{1-\xi}\right)x_Q \right] \\ &\quad + N_0(\eta) \left(-\frac{\xi}{1-\xi}x_{C_1} + \frac{\xi}{1-\xi}x_{Q_1} \right), \quad \text{etc.} \end{aligned} \quad (9.57)$$

with

$$N_1(\eta) = \frac{1+\eta}{2} \quad N_0(\eta) = \frac{1-\eta}{2}$$

and map the points as shown.

In a similar manner we could use quadratic interpolations and map an element as shown in Fig. 9.19 by using quadratic functions in η .

Thus it is an easy matter to create infinite elements and join these to a standard element mesh as shown in Fig. 9.17(b). The reader will observe that in the generation of such element properties only the transformation jacobian matrix differs from standard forms, hence only this has to be altered in conventional programs.

The 'origin' or 'pole' of the coordinates C can be fixed arbitrarily for each radial line, as shown in Fig. 9.18. This will be done by taking account of the knowledge of the physical solution expected.

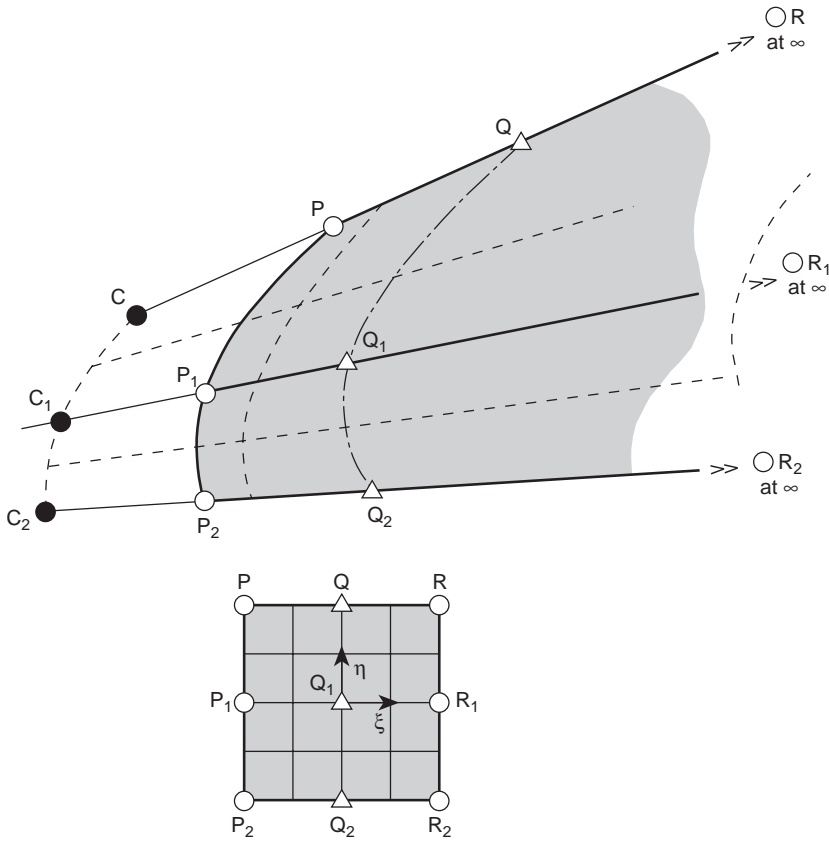


Fig. 9.19 Infinite element map. Quadratic η interpolation.

In Fig. 9.20 we show a solution of the Boussinesq problem (a point load on an elastic half-space). Here results of using a fixed displacement or infinite elements are compared and the big changes in the solution noted. In this example the pole of each element was taken at the load point for obvious reasons.⁴⁰

Figure 9.21 shows how similar infinite elements (of the linear kind) can give excellent results, even when combined with very few standard elements. In this example where a solution of the Laplace equation is used (see Chapter 7) for an irrotational fluid flow, the poles of the infinite elements are chosen at arbitrary points of the aerofoil centre-line.

In concluding this section it should be remarked that the use of infinite elements (as indeed of any other finite elements) must be tempered by background analytical knowledge and 'miracles' should not be expected. Thus the user should not expect, for instance, such excellent results as those shown in Fig. 9.20 for a plane elasticity problem for the displacements. It is 'well known' that in this case the displacements under any load which is not self-equilibrated will be infinite everywhere and the numbers obtained from the computation will not be, whereas for the three-dimensional case it is infinite only at a point load.

Extensive use of infinite elements is made in Volume 3 in the context of the solution of wave problems.

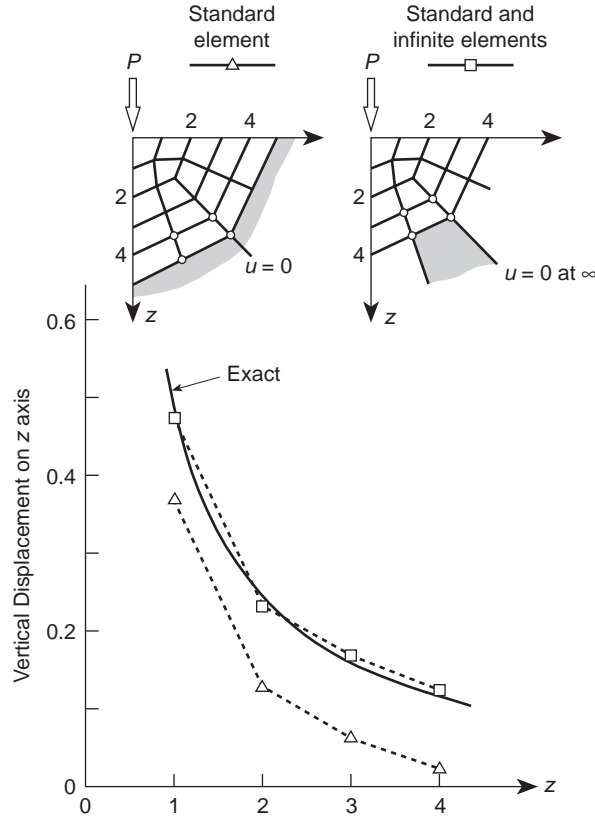


Fig. 9.20 A point load on an elastic half-space (Boussinesq problem). Standard linear elements and infinite line elements ($E = 1$, $\nu = 0.1$, $P = 1$).

9.14 Singular elements by mapping for fracture mechanics, etc.

In the study of fracture mechanics interest is often focused on the singularity point where quantities such as stress become (mathematically, but not physically) infinite. Near such singularities normal, polynomial-based, finite element approximations perform badly and attempts have frequently been made here to include special functions within an element which can model the analytically known singular function. References 42–69 give an extensive literature survey of the problem and finite element solution techniques. An alternative to the introduction of special functions within an element – which frequently poses problems of enforcing continuity requirements with adjacent, standard, elements – lies in the use of special mapping techniques.

An element of this kind, shown in Fig. 9.22(a), was introduced almost simultaneously by Henshell and Shaw⁶⁵ and Barsoum^{66,67} for quadrilaterals by a simple shift of the mid-side node in quadratic, isoparametric elements to the quarter point.

It can now be shown (and we leave this exercise to the curious reader) that along the element edges the derivatives $\partial u / \partial x$ (or strains) vary as $1/\sqrt{r}$ where r is the distance

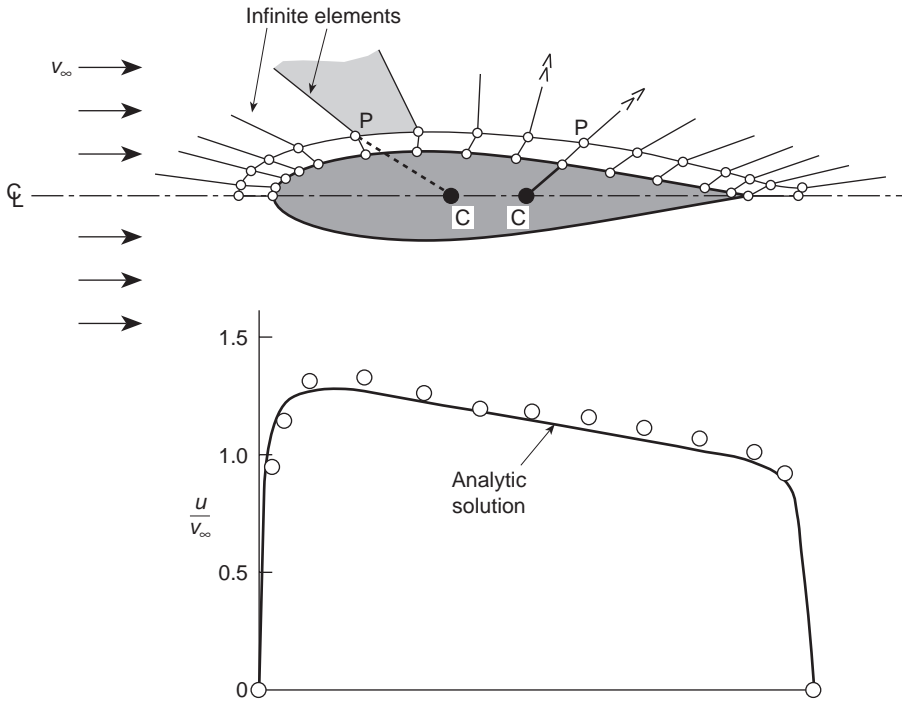


Fig. 9.21 Irrotational flow around a NACA 0018 wing section.³⁶ (a) Mesh of bilinear isoparametric and infinite elements. (b) Computed \circ and analytical — results for velocity parallel to surface.

from the corner node at which the singularity develops. Although good results are achievable with such elements the singularity is, in fact, not well modelled on lines other than element edges. A development suggested by Hibbitt⁶⁸ achieves a better result by using triangular second-order elements for this purpose [Fig. 9.22(b)].

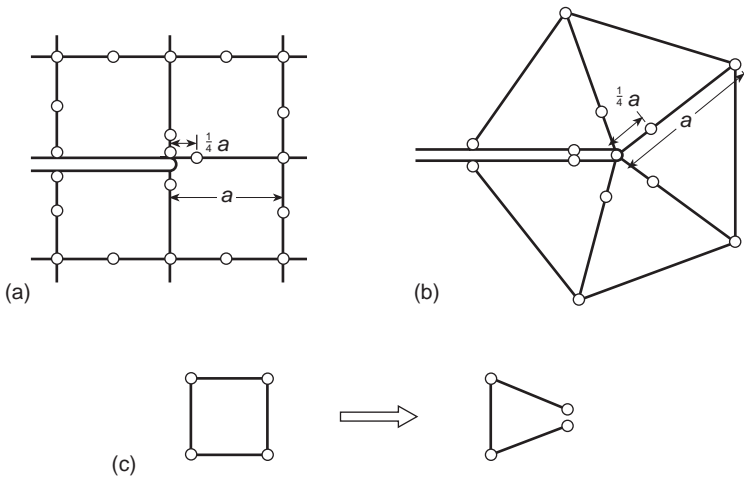


Fig. 9.22 Singular elements from degenerate isoparameters (a), (b), and (c).

Indeed, the use of distorted or degenerate isoparametrics is not confined to elastic singularities. Rice⁵⁶ shows that in the case of plasticity a shear strain singularity of $1/r$ type develops and Levy *et al.*⁴⁹ use an isoparametric, linear quadrilateral to generate such a singularity by the simple device of coalescing two nodes but treating these displacements independently. A variant of this is developed by Rice and Tracey.⁴⁵

The elements just described are evidently simple to implement without any changes in a standard finite element program. However, in Chapter 16 we introduce a method whereby any singularity (or other function) can be modelled directly. We believe the methods to be described there supercede the above described techniques.

9.15 A computational advantage of numerically integrated finite elements⁷⁰

One considerable gain that is possible in numerically integrated finite elements is the versatility that can be achieved in a single computer program.

It will be observed that for a *given class of problems* the general matrices are always of the same form [see the example of Eq. (9.8)] in terms of the shape function and its derivatives.

To proceed to evaluation of the element properties it is necessary first to *specify the shape function* and its derivatives and, second, to *specify the order of integration*.

The computation of element properties is thus composed of three distinct parts as shown in Fig. 9.23. For a *given class of problems* it is only necessary to change the prescription of the shape functions to achieve a variety of possible elements.

Conversely, the *same shape function* routines can be used in many different classes of problem, as is shown in Chapter 20.

Use of different elements, testing the efficiency of a new element in a given context, or extension of programs to deal with new situations can thus be readily achieved, and considerable algebra (with its inherent possibilities of mistakes) avoided.

The computer is thus placed in the position it deserves, i.e., of being the obedient slave capable of saving routine work.

The greatest practical advantage of the use of universal shape function routines is that they can be checked decisively for errors by a simple program with the patch test (viz. Chapter 10) playing the crucial role.

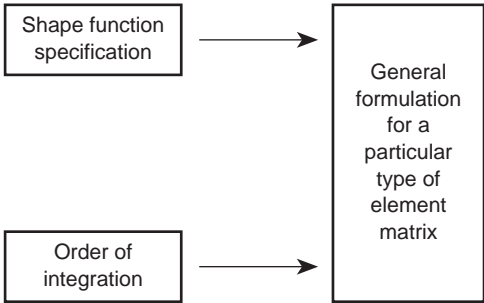


Fig. 9.23 Computation scheme for numerically integrated elements.

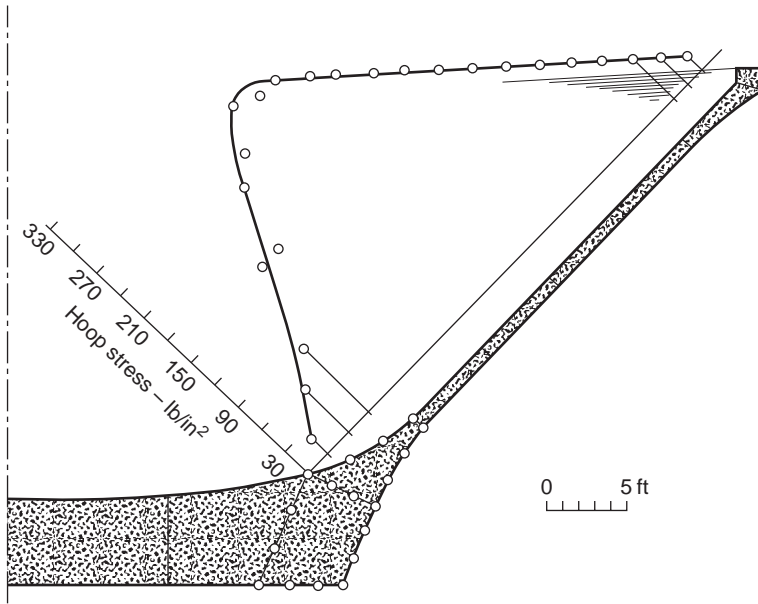


Fig. 9.25 Conical water tank.

9.16.3 A hemispherical dome (Fig. 9.26)

The possibilities of dealing with shells approached in the previous example are here further exploited to show how a limited number of elements can adequately solve a thin shell problem, with precisely the same program. This type of solution can be further improved upon from the economy viewpoint by making use of the well-known shell assumptions involving a linear variation of displacements across the thickness. Thus the number of degrees of freedom can be reduced. Methods of this kind will be dealt with in detail in the second volume of this text.

9.17 Three-dimensional stress analysis

In three-dimensional analysis, as was already hinted at in Chapter 6, the complex element presents a considerable economic advantage. Some typical examples are shown here in which the quadratic, serendipity-type formulation is used almost exclusively. In all problems integration using *three* Gauss points in each direction was used.

9.17.1 Rotating sphere (Fig. 9.27)

This example, in which the stresses due to centrifugal action are compared with exact

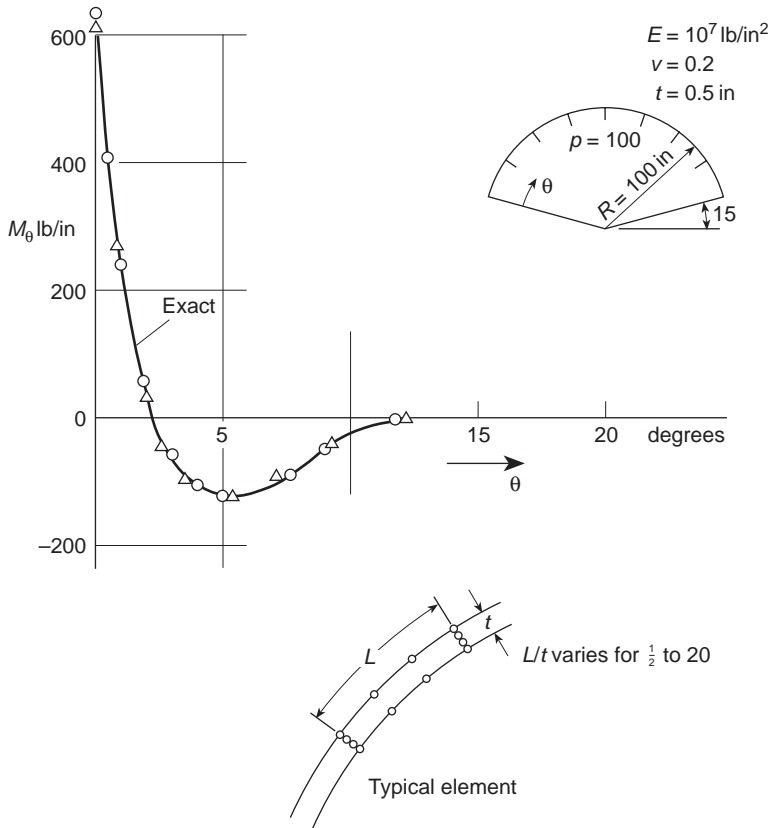


Fig. 9.26 *Encastré*, thin hemispherical shell. Solution with 15 and 24 cubic elements.

values, is perhaps a test on the efficiency of highly distorted elements. Seven elements are used here and results show good agreement with exact stresses.

9.17.2 Arch dam in rigid valley

This problem, perhaps a little unrealistic from the engineer's viewpoint, was the subject of a study carried out by a committee of the Institution of Civil Engineers and provided an excellent test for a convergence evaluation of three-dimensional analysis.⁷⁵ In Fig. 9.28 two subdivisions into quadratic and two into cubic elements are shown. In Fig. 9.29 the convergence of displacements in the centre-line section is shown, indicating that quite remarkable accuracy can be achieved with even one element.

The comparison of stresses in Fig. 9.30 is again quite remarkable, though showing a greater 'oscillation' with coarse subdivision. The finest subdivision results can be taken as 'exact' from checks by models and alternative methods of analysis.

The above test problems illustrate the general applicability and accuracy. Two further illustrations typical of real situations are included.

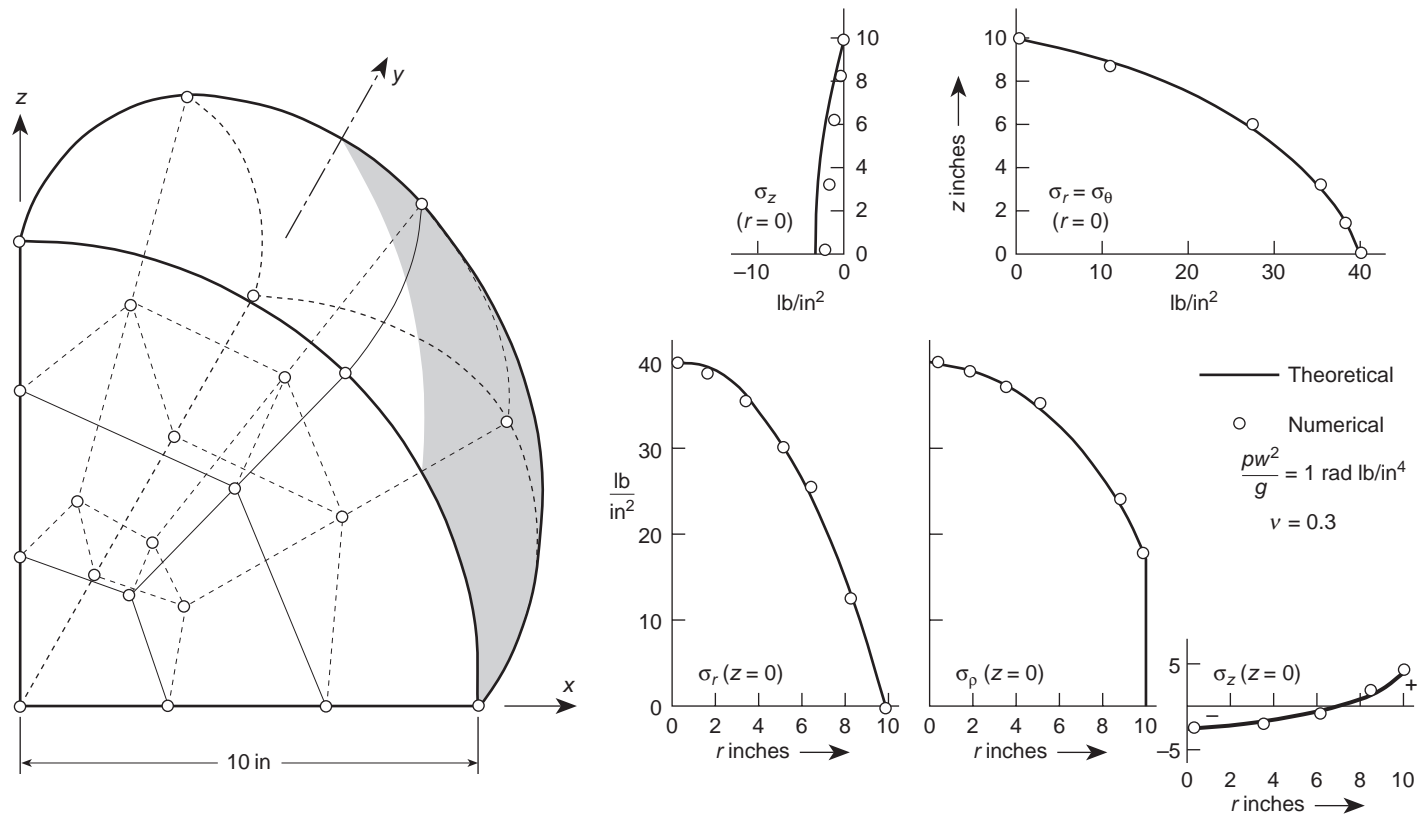


Fig. 9.27 A rotating sphere as a three-dimensional problem. Seven parabolic elements. Stresses along $z = 0$ and $r = 0$.

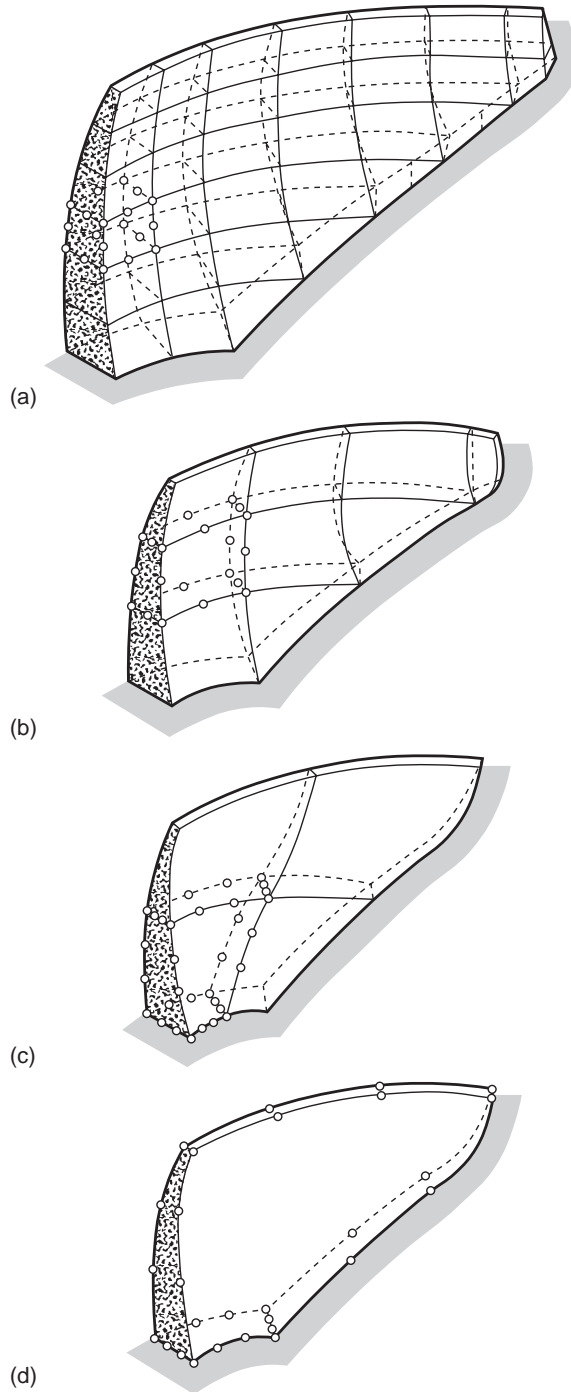


Fig. 9.28 Arch dam in a rigid valley – various element subdivisions.

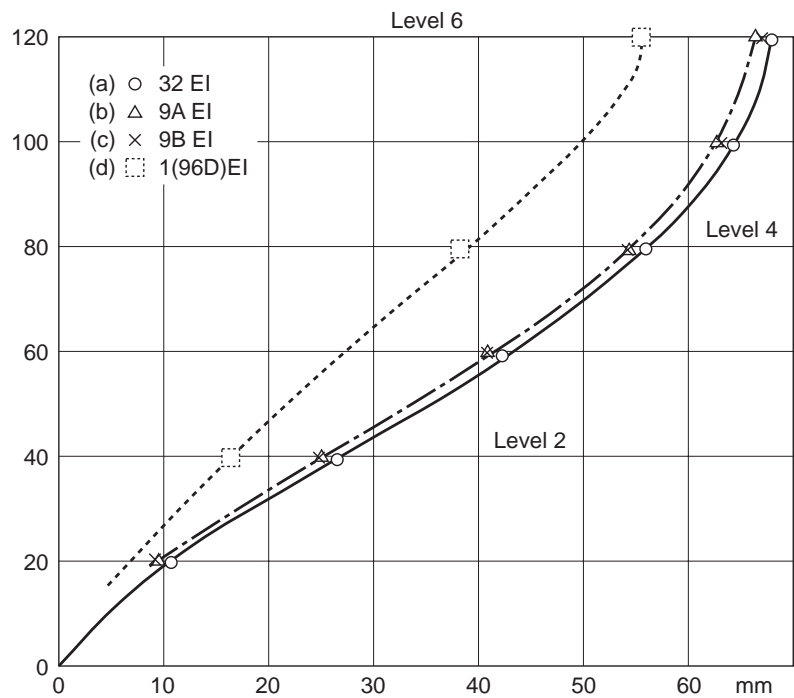


Fig. 9.29 Arch dam in a rigid valley – centre-line displacements.

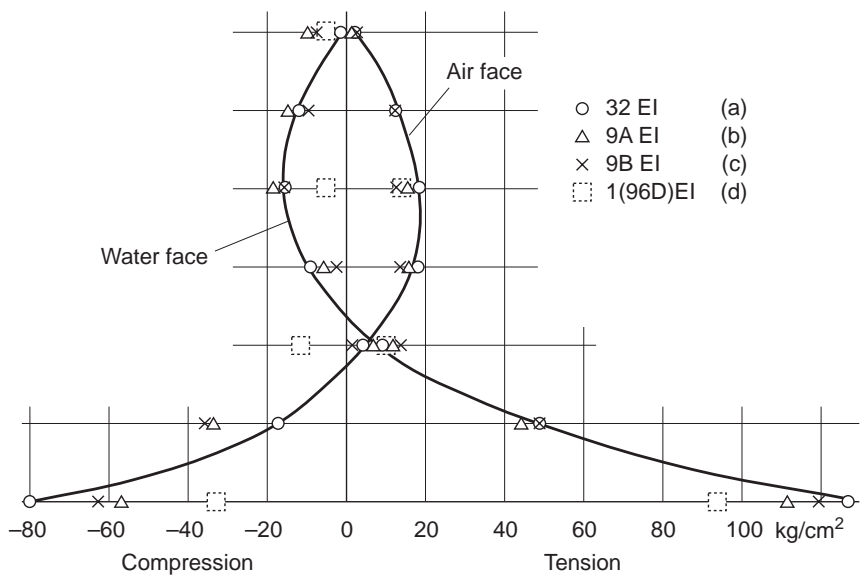


Fig. 9.30 Arch dam in a rigid valley – vertical stresses on centre-line.

9.17.3 Pressure vessel (Fig. 9.31): an analysis of a biomechanic problem (Fig. 9.32)

Both show subdivisions sufficient to obtain reasonable engineering accuracy. The pressure vessel, somewhat similar to the one indicated in Chapter 6, Fig. 6.7, shows the very considerable reduction of degrees of freedom possible with the use of more complex elements to obtain similar accuracy.

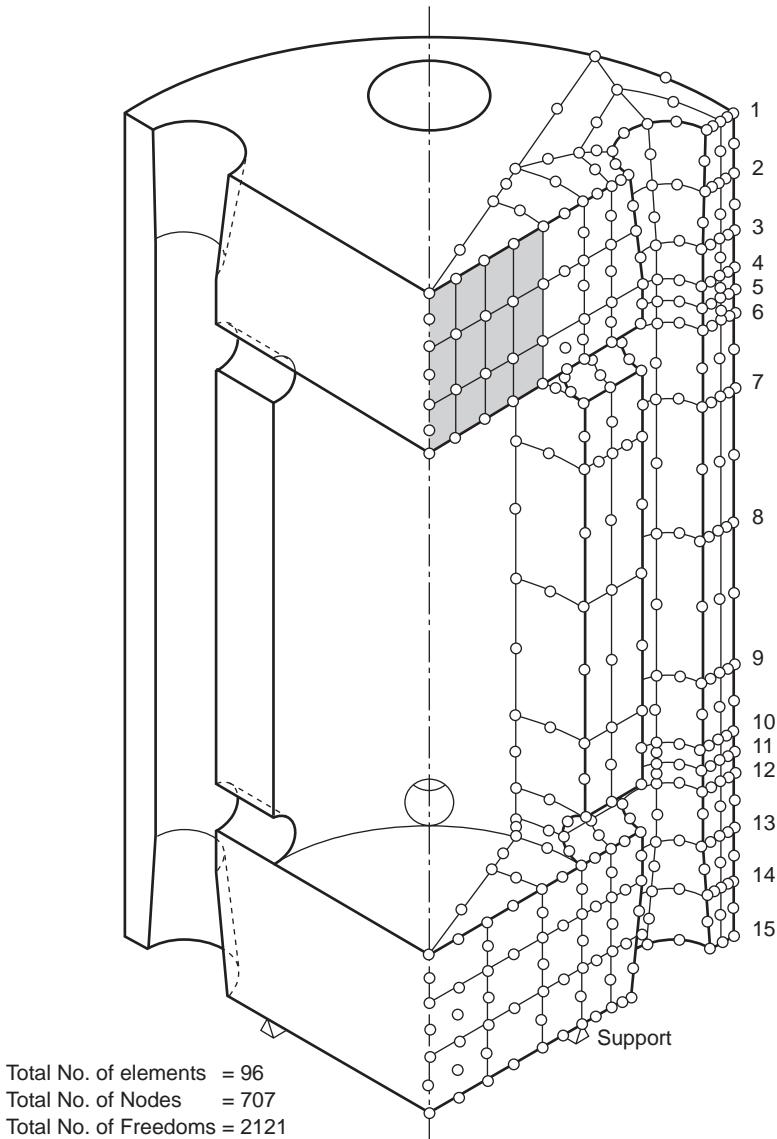


Fig. 9.31 Three-dimensional analysis of a pressure vessel.

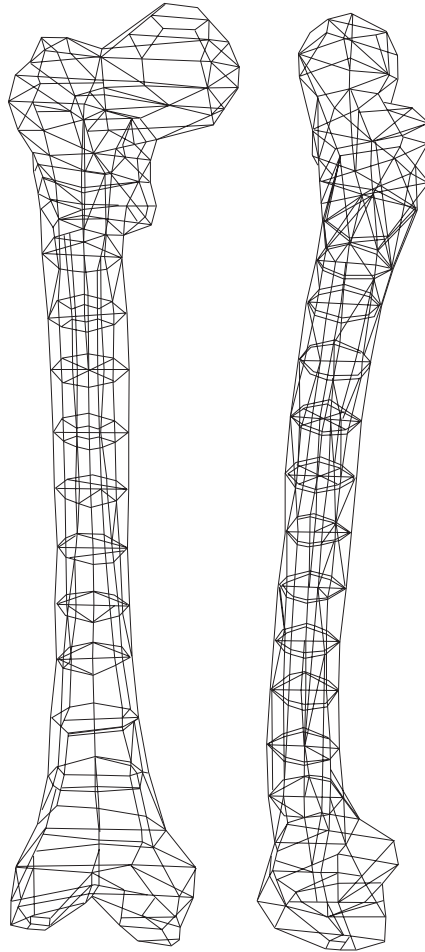


Fig. 9.32 A problem of biomechanics. Plot of linear element form only; curvature of elements omitted. Note degenerate element shapes.

The example of Fig. 9.32 shows a perspective view of the elements used. Such plots are not only helpful in visualization of the problem but also form an essential part of *data correctness checks* as any gross geometric error can be easily discovered.

The importance of avoiding data errors in complex three-dimensional problems should be obvious in view of their large usage of computer time. These, and indeed other,⁷⁶ checking methods must form an essential part of any computation system.

9.18 Symmetry and repeatability

In most of the problems shown, the advantage of symmetry in loading and geometry was taken when imposing the boundary conditions, thus reducing the whole problem to manageable proportions. The use of symmetry conditions is so well known to the

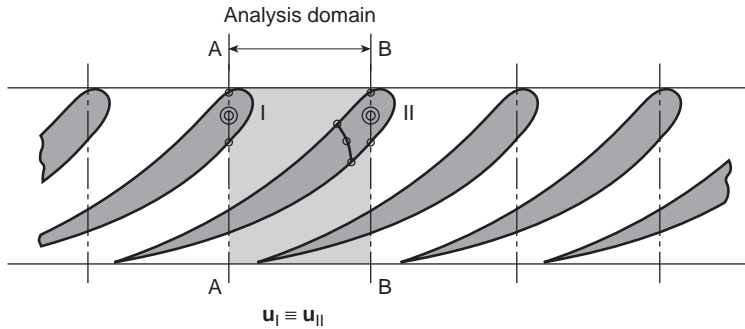


Fig. 9.33 Repeatability segments and analysis domain (shaded).

engineer and physicist that no statement needs to be made about it explicitly. Less known, however, appears to be the use of *repeatability*⁷⁸ when an identical structure (and) loading is continuously repeated, as shown in Fig. 9.33 for an infinite blade cascade. Here it is evident that a typical segment shown shaded behaves identically to the next one, and thus functions such as velocities and displacements at corresponding points of AA and BB are simply identified, i.e.,

$$u_I = u_{II}$$

This identification is made directly in a computer program.

Similar repeatability, in radial coordinates, occurs very frequently in problems involving turbine or pump impellers. Figure 9.34 shows a typical three-dimensional analysis of such a repeatable sector.

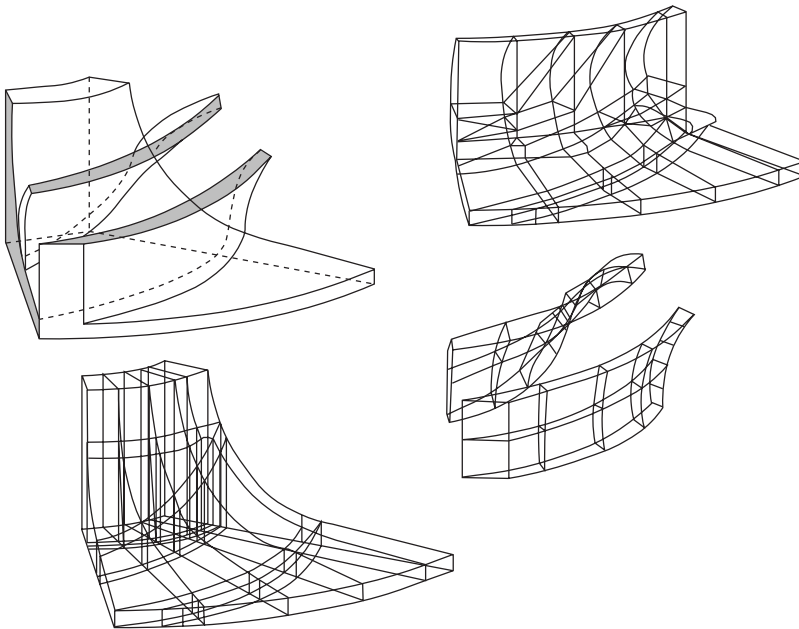


Fig. 9.34 Repeatable sector in analysis of an impeller.

References

1. I.C. Taig. *Structural analysis by the matrix displacement method*. Engl. Electric Aviation Report No. S017, 1961.
2. B.M. Irons. Numerical integration applied to finite element methods. *Conf. Use of Digital Computers in Struct. Eng.* Univ. of Newcastle, 1966.
3. B.M. Irons. Engineering application of numerical integration in stiffness method. *JAI AA*. **14**, 2035–7, 1966.
4. S.A. Coons. *Surfaces for computer aided design of space form*. MIT Project MAC, MAC-TR-41, 1967.
5. A.R. Forrest. *Curves and Surfaces for Computer Aided Design*. Computer Aided Design Group, Cambridge, England, 1968.
6. G. Strang and G.J. Fix. *An Analysis of the Finite Element Method*. pp. 156–63, Prentice-Hall, 1973.
7. E.L. Wachspress. High order curved finite elements. *Int. J. Num. Meth. Eng.* **17**, 735–45, 1981.
8. M. Crochet. Personal communication. 1988.
9. Nam-Sua Lee and K.-J. Bathe. Effects of element distortion on the performance of isoparametric elements. *Internat. J. Num. Meth. Eng.* **36**, 3553–76, 1993.
10. N. Abramowitz and I.A. Stegun. *Handbook of Mathematical Functions*. Dover, New York, 1965.
11. B.M. Irons. Quadrature rules for brick based finite elements. *Int. J. Num. Meth. Eng.* **3**, 293–4, 1971.
12. T.K. Hellen. Effective quadrature rules for quadratic solid isoparametric finite elements. *Int. J. Num. Meth. Eng.* **4**, 597–600, 1972.
13. Radau. *Journ. de Math.* **3**, 283, 1880.
14. R.G. Anderson, B.M. Irons, and O.C. Zienkiewicz. Vibration and stability of plates using finite elements. *Int. J. Solids Struct.* **4**, 1031–55, 1968.
15. P.C. Hammer, O.P. Marlowe, and A.H. Stroud. Numerical integration over simplexes and cones. *Math. Tables Aids Comp.* **10**, 130–7, 1956.
16. C.A. Felippa. *Refined finite element analysis of linear and non-linear two-dimensional structures*. Structures Materials Research Report No. 66–22, Oct. 1966, Univ. of California, Berkeley.
17. G.R. Cowper. Gaussian quadrature formulas for triangles. *Int. J. Num. Mech. Eng.* **7**, 405–8, 1973.
18. I. Fried. Accuracy and condition of curved (isoparametric) finite elements. *J. Sound Vibration*. **31**, 345–55, 1973.
19. I. Fried. Numerical integration in the finite element method. *Comp. Struc.* **4**, 921–32, 1974.
20. M. Zlamal. Curved elements in the finite element method. *SIAM J. Num. Anal.* **11**, 347–62, 1974.
21. D. Kosloff and G.A. Frasier. Treatment of hour glass patterns in low order finite element codes. *Int. J. Num. Anal. Meth. Geomechanics*. **2**, 57–72, 1978.
22. T. Belytschko and W.E. Bachrach. The efficient implementation of quadrilaterals with high coarse mesh accuracy. *Comp. Methods Appl. Mech and Engineering*. **54**, 276–301, 1986.
23. O.C. Zienkiewicz and D.V. Phillips. An automatic mesh generation scheme for plane and curved element domains. *Int. J. Num. Meth. Eng.* **3**, 519–28, 1971.
24. W.J. Gordon and C.A. Hall. Construction of curvilinear co-ordinate systems and application to mesh generation. *Int. J. Num. Meth. Eng.* **7**, 461–77, 1973.
25. W.J. Gordon and C.A. Hall. Transfinite element methods – blending-function interpolation over arbitrary curved element domains. *Numer. Math.* **21**, 109–29, 1973.

26. J. Peraire, M. Vahdati, K. Morgan, and O.C. Zienkiewicz. Adaptive remeshing for compressible flow computations. *J. Comp. Phys.* **72**, 449–66, 1987.
27. J. Peraire, K. Morgan, M. Vahdati, and O.C. Zienkiewicz. Finite element Euler computations in 3-d. *Internat. J. Num. Meth. Eng.* **26**, 2135–59, 1988.
28. P. Kaupp and S. Steinberg. *Fundamentals of Grid Generation*. CRC Press, 1993.
29. N.P. Weatherill, P.R. Eiseman, J. Hause, and J.P. Thompson. *Numerical Grid Generation in Fluid Dynamics and Related Fields*. Pineridge Press, Swansea, 1994.
30. P.L. George and H. Borouchaki. *Delaunay Triangulation and Meshing*. Hermes, Paris, 1998.
31. J.F. Thompson, B.K. Soni, and N.P. Weatherill, eds. *Handbook of Grid Generation*. CRC Press, January 1999.
32. GiD—The Personal Pre/Postprocessor, CIMNE, Barcelona, Spain, 1999.
33. R.W. Thatcher. On the finite element method for unbounded regions. *SIAM J. Numerical Analysis*. **15**, 3, pp. 466–76, June 1978.
34. P. Silvester, D.A. Lowther, C.J. Carpenter, and E.A. Wyatt. Exterior finite elements for 2-dimensional field problems with open boundaries. *Proc. IEE.* **123**, No. 12, December 1977.
35. S.F. Shen. An aerodynamicist looks at the finite element method, in *Finite Elements in Fluids* (eds R.H. Gallagher *et al.*). Vol. 2, pp. 179–204, Wiley, 1975.
36. O.C. Zienkiewicz, D.W. Kelly, and P. Bettess. The coupling of the finite element and boundary solution procedures. *Int. J. Num. Meth. Eng.* **11**, 355–75, 1977.
37. P. Bettess. Infinite elements. *Int. J. Num. Meth. Eng.* **11**, 53–64, 1977.
38. P. Bettess and O.C. Zienkiewicz. Diffraction and refraction of surface waves using finite and infinite elements. *Int. J. Num. Meth. Eng.* **11**, 1271–90, 1977.
39. G. Beer and J.L. Meek. Infinite domain elements. *Int. J. Num. Meth. Eng.* **17**, 43–52, 1981.
40. O.C. Zienkiewicz, C. Emson, and P. Bettess. A novel boundary infinite element. *Int. J. Num. Meth. Eng.* **19**, 393–404, 1983.
41. P. Bettess. *Infinite Elements*. Penshaw Press, 1992.
42. R.H. Gallagher. Survey and evaluation of the finite element method in fracture mechanics analysis, in *Proc. 1st Int. Conf. on Structural Mechanics in Reactor Technology*. Vol. 6, Part L, pp. 637–53, Berlin, 1971.
43. N. Levy, P.V. Marçal, and J.R. Rice. Progress in three-dimensional elastic–plastic stress analysis for fracture mechanics. *Nucl. Eng. Des.* **17**, 64–75, 1971.
44. J.J. Oglesby and O. Lomacky. An evaluation of finite element methods for the computation of elastic stress intensity factors. *J. Eng. Ind.* **95**, 177–83, 1973.
45. J.R. Rice and D.M. Tracey. Computational fracture mechanics, in *Numerical and Computer Methods in Structural Mechanics* (eds S.J. Fenves *et al.*). pp. 555–624, Academic Press, 1973.
46. A.A. Griffiths. The phenomena of flow and rupture in solids. *Phil. Trans. Roy. Soc. (London)*. **A221**, 163–98, Oct. 1920.
47. J.L. Swedlow. Elasto-plastic cracked plates in plane strain. *Int. J. Fract. Mech.* **4**, 33–44, March 1969.
48. T. Yokobori and A. Kamei. The size of the plastic zone at the tip of a crack in plane strain state by the finite element method. *Int. J. Fract. Mech.* **9**, 98–100, 1973.
49. N. Levy, P.V. Marçal, W.J. Ostergren, and J.R. Rice. Small scale yielding near a crack in plane strain: a finite element analysis. *Int. J. Fract. Mech.* **7**, 143–57, 1967.
50. J.R. Dixon and L.P. Pook. Stress intensity factors calculated generally by the finite element technique. *Nature*. **224**, 166, 1969.
51. J.R. Dixon and J.S. Strannigan. Determination of energy release rates and stress-intensity factors by the finite element method. *J. Strain Analysis*. **7**, 125–31, 1972.
52. V.B. Watwood. Finite element method for prediction of crack behavior. *Nucl. Eng. Des.* **II** (No. 2), 323–32, March 1970.

53. D.F. Mowbray. A note on the finite element method in linear fracture mechanics. *Eng. Fract. Mech.* **2**, 173–6, 1970.
54. D.M. Parks. A stiffness derivative finite element technique for determination of elastic crack tip stress intensity factors. *Int. J. Fract.* **10**, 487–502, 1974.
55. T.K. Hellen. On the method of virtual crack extensions. *Int. J. Num. Meth. Eng.* **9** (No. 1), 187–208, 1975.
56. J.R. Rice. A path-independent integral and the approximate analysis of strain concentration by notches and cracks. *J. Appl. Mech., Trans. Am. Soc. Mech. Eng.* **35**, 379–86, 1968.
57. P. Tong and T.H.H. Pian. On the convergence of the finite element method for problems with singularity. *Int. J. Solids Struct.* **9**, 313–21, 1972.
58. T.A. Cruse and W. Vanburen. Three dimensional elastic stress analysis of a fracture specimen with edge crack. *Int. J. Fract. Mech.* **7**, 1–15, 1971.
59. E. Byskov. The calculation of stress intensity factors using the finite element method with cracked elements. *Int. J. Fract. Mech.* **6**, 159–67, 1970.
60. P.F. Walsh. Numerical analysis in orthotropic linear fracture mechanics. *Inst. Eng. Australia. Civ. Eng., Trans.* **15**, 115–19, 1973.
61. P.F. Walsh. The computation of stress intensity factors by a special finite element technique. *Int. J. Solids Struct.* **7**, 1333–42, Oct. 1971.
62. A.K. Rao, I.S. Raju, and A. Murthy Krishna. A powerful hybrid method in finite element analysis. *Int. J. Num. Meth. Eng.* **3**, 389–403, 1971.
63. W.S. Blackburn. Calculation of stress intensity factors at crack tips using special finite elements, in *The Mathematics of Finite Elements* (ed. J.R. Whiteman), pp.327–36, Academic Press, 1973.
64. D.M. Tracey. Finite elements for determination of crack tip elastic stress intensity factors. *Eng. Fract. Mech.* **3**, 255–65, 1971.
65. R.D. Henshell and K.G. Shaw. Crack tip elements are unnecessary. *Int. J. Num. Meth. Eng.* **9**, 495–509, 1975.
66. R.S. Barsoum. On the use of isoparametric finite elements in linear fracture mechanics. *Int. J. Num. Meth. Eng.* **10**, 25–38, 1976.
67. R.S. Barsoum. Triangular quarter point elements as elastic and perfectly elastic crack tip elements. *Int. J. Num. Meth. Eng.* **11**, 85–98, 1977.
68. H.D. Hibbitt. Some properties of singular isoparametric elements. *Int. J. Num. Meth. Eng.* **11**, 180–4, 1977.
69. S.E. Benzley. Representation of singularities with isoparametric finite elements. *Int. J. Num. Meth. Eng.* **8** (No. 3), 537–45, 1974.
70. B.M. Irons. Economical computer techniques for numerically integrated finite elements. *Int. J. Num. Meth. Eng.* **1**, 201–3, 1969.
71. O.C. Zienkiewicz, B.M. Irons, J.G. Ergatoudis, S. Ahmad, and F.C. Scott. Isoparametric and associated element families for two and three dimensional analysis, in *Proc. Course on Finite Element Methods in Stress Analysis* (eds I. Holland and K. Bell). Trondheim Tech. University, 1969.
72. B.M. Irons and O.C. Zienkiewicz. The isoparametric finite element system – a new concept in finite element analysis. *Proc. Conf. Recent Advances in Stress Analysis*. Royal Aero Soc., 1968.
73. J.G. Ergatoudis, B.M. Irons, and O.C. Zienkiewicz. Curved, isoparametric, 'quadrilateral' elements for finite element analysis. *Int. J. Solids Struct.* **4**, 31–42, 1968.
74. J.G. Ergatoudis. *Isoparametric elements in two and three dimensional analysis*. Ph.D. thesis, University of Wales, Swansea, 1968.
75. J.G. Ergatoudis, B.M. Irons, and O.C. Zienkiewicz. Three dimensional analysis of arch dams and their foundations. *Symposium on Arch Dams*. Inst. Civ. Eng., London, 1968.
76. O.C. Zienkiewicz, B.M. Irons, J. Campbell, and F.C. Scott. Three dimensional stress analysis. *Int. Un. Th. Appl. Mech. Symp. on High Speed Computing in Elasticity*. Liège, 1970.

77. O.C. Zienkiewicz. Isoparametric and other numerically integrated elements, in *Numerical and Computer Methods in Structural Mechanics* (eds S.J. Fenves, N. Perrone, A.R. Robinson, and W.C. Schnobrich). pp. 13–41, Academic Press, 1973.
78. O.C. Zienkiewicz and F.C. Scott. On the principle of repeatability and its application in analysis of turbine and pump impellers. *Int. J. Num. Meth. Eng.* **9**, 445–52, 1972.